UNIVERSITÉ LAVAL

Investigating Haspin-dependent phosphorylation of histones during mitosis

Thèse

Ibrahim Alharbi

Doctorat en biologie cellulaire et moléculaire
Philosophiæ doctor (Ph. D.)

Québec, Canada

© Ibrahim Alharbi, 2020

Résumé

La protéine Haspine est une sérine / thréonine kinase mitotique conservée, connue pour fonctionner par la phosphorylation de l'histone H3 (H3pT3). Bien que H3T3 soit le seul substrat bien connu de Haspine, il se peut que H3pT3 ne suffise pas à expliquer toutes les fonctions de Haspine au cours de la mitose. Fait intéressant, l'homologie de la portion N-terminale de H3 avec la portion C-terminale de H2B suggère que la thréonine 119 de H2B (H2BT119) est un candidat potentiel fort pour être un substrat majeur de Haspine. Ainsi, l'objectif de ce projet était d'étudier la phosphorylation de H2BT119 dépendante de Haspine pendant la mitose. La phosphorylation de H2B recombinant sur la position T119 par Haspine a été confirmée par un dosage de kinase en utilisant la radioactivité. En outre, le signal H2BpT119 sur la protéine recombinante H2B a été détecté par un anticorps anti-H2BpT119, confirmant la phosphorylation de H2B dépendante de Haspine sur ce site dans le test de kinase in vitro. En outre, une augmentation de la taille moléculaire de H2B a été observée après le dosage de la kinase. Les résultats des expériences in vivo, incluant l'analyse par Western-blot d'extrait d'histones mitotiques et la microscopie à fluorescence avec l'anti-H2BpT119, suggèrent une phosphorylation de H2B au site T119, qui s'est également avérée dépendant de l'activité de Haspine. Cependant, en raison de la potentielle réactivité croisée de l'anti-H2BpT119 avec H3pT3, une forme marquée de H2B a été utilisée lors de l'étude du signal H2BpT119 au cours de la mitose. Le marquage augmente la taille moléculaire de H2B et aide à reconnaître H2BpT119 loin de H3pT3. Plusieurs systèmes de marquage ont été utilisés, mais toutes les tentatives ont échoué, en raison du faible niveau de H2B exogène. Cependant, les résultats de ce projet suggèrent que le signal H2BpT119 pendant la mitose pourrait révéler un nouveau mécanisme dépendant de Haspine pour la régulation de la ségrégation des chromosomes. Par conséquent, il reste important d'étudier cette marque d'histone au cours de la mitose.

Abstract

Haspin is a conserved mitotic serine/threonine kinase that is known to function through histone H3 phosphorylation (H3pT3). Despite this, H3T3 is the only well-known substrate for Haspin, H3pT3 may not be enough to explain all Haspin functions during mitosis. Interestingly, homology of H3 N-terminus with H2B C-terminus suggests that H2BT119 is a strong potential candidate to be a major substrate of Haspin. Thus, the aim was to investigate Haspin-dependent phosphorylation of H2BT119 during mitosis. Phosphorylation of recombinant H2B at T119 by Haspin was confirmed by a radioactivity-based kinase assay. Also, H2BpT119 signal on recombinant H2B was detected by an anti-H2BpT119 antibody, confirming Haspin-dependent phosphorylation of H2B at this site in the in vitro kinase assay. Also, an upshift of H2B was observed following the kinase assay. Results from in vivo experiments, including Western blot analysis of mitotic histone extract and immunofluorescence microscopy with the anti-H2BpT119, support phosphorylation of T119 in H2B, which also was found to depend on Haspin activity. However, due to the potential anti-H2BpT119 cross-reactivity with H3pT3, while exploring H2BpT119 signal during mitosis, tagged H2B was used. The tag increases H2B molecular size and helps to distinguish H2BpT119 from H3pT3. Several tagging systems was used, but all attempts failed, because of the low level of the exogenous tagged H2B. However, the results of this project suggest H2BpT119 signal during mitosis that may reveal a novel Haspin-dependent mechanism for chromosome segregation regulation. Therefore, it remains important to study this histone mark during mitosis.

Table of Contents

Table List

Figure List

Abbreviations

AAN: Acetonitrile

APC/C: Anaphase-promoting complex/cyclosome

ATP: Adenosine triphosphate

BGS: Bovine growth serum

BSA: Bovine serum albumin

BUB: Budding uninhibited by benzimidazole

CCAN: Constitutive centromere associated network

Cdc25a: Cell division cycle 25 homolog A

°C: Degree Celsius

CDK: Cyclin-dependent kinase

CENP: Centromere protein

CIN: Chromosomal instability

CPC: Chromosomal passenger complex

DNA: Deoxyribonucleic acid

dNTP: Deoxyribonucleotide triphosphate

DSBs: DNA double-strand breaks

DTT: Dithiothreitol

e.g.: For example

ECL: Enhanced chemiluminescence

EDTA: Ethylenediaminetetraacetic acid

FPLC: Fast protein liquid chromatography

GLEBS: Gle2- Binding Sequence

GSG: Germ cell-specific gene

GST: Glutathione S-transferase

GTP: Guanosine-5'-triphosphate

H: Hour

H1: Histone H1

H2A: Histone H2A

H2B: Histone H2B

H3: Histone H3

H4: Histone H4

Haspin: Haploid germ cell-specific nuclear protein kinase

HBIS: Haspin basic inhibitory segment

HCl: Hydrochloric acid

HPLC: High performance liquid chromatography

HR: Homologous recombination

5-IT: 5-Iodotubercidin

ICIS: Inner centromere Kin-I stimulator

IgG: Immunoglobulin G

INCENP Inner centromere protein

IPTG: Isopropyl β- d-1-thiogalactopyranoside

KCl: Potassium chloride

KLH: Keyhole limpet haemocyanin

KMN: Knl1, Mis12 and Ndc80

MAD: mitotic arrest defective.

MCAK: Mitotic centromere-associated kinesin

MCC: Mitotic checkpoint complex

MCM: Mini-chromosome maintenance complex

MgCl2: Magnesium chloride

MIM MAD2-interaction motif

MRN: MRE11-RAD50-NBN

MS: Mass spectrometry

NaCl: Sodium chloride

NHEJ: Non-homologous end-joining

OD: Optical density

ON: Over night

ORC: Origin recognition complex

PBS: Phosphate-buffered saline

PCR: Polymerase chain reaction

PLK1: Polo-like kinase1

PP1: Protein phosphatase1

PP2A: Protein phosphatase 2A

PRC2: Polycomb repressive complex 2

Pre-IC: Pre-initiation complex

Pre-RC: Pre-replication complex

PTM: Post-translational modification

PVDF: Polyvinylidene difluoride

Rb: Retinoblastoma protein

RT: Room temperature

RZZ: Rod–ZW10–Zwilch

S. pombe: *Schizosaccharomyces pombe*

S. cerevisiae: *Saccharomyces cerevisiae*

SAC: Spindle assembly checkpoint

SCF: Skp, Cullin, F-box containing complex

SDS-PAGE: Sodium dodecyl sulfate-polyacrylamide gel electrophoresis

Sec: Second

Sgo: Shugoshin

STLC: S-Trityl-L-cysteine

TBS: Tris-buffer saline

TCL: Total cell lysate

TFA: Trifluoroacetic acid

Top2: Topoisomerase II

TPR: Tetratricopeptide repeat

WAPL: Wings apart-like protein

WT: Wild-type

α: Alpha

β: Beta

βME: Beta-mercaptoethanol

ε: Epsilon

µg: Microgram

Acknowledgement

Thanks to Prof. Fatiha Chandad for supervising me for the completion of my PhD degree in her laboratory in the Faculty of dentistry at Université Laval. Thanks for all of the support and the guidance you provided me during my stay in your laboratory. Thanks for the suggestions, the advice, and the time you gave to me during my PhD studies.

Acknowledgements go to the members of the Groupe de Recherche en Écologie Buccale (GREB) in the Faculty of dentistry, who had kindly provided space and materials during my PhD. Acknowledgement to Chantal Garand and Alexandra Cote for the aid in the plasmid preparation. Acknowledgement to Chantal Garand, Guillaume Combes, Adeel Asghar, and Luciano Braga Gama for the aid in the lab work. Also, I would like to acknowledge anyone, otherwise mentioned in this thesis, who kindly provided directly or indirectly any support for this thesis.

For this long journey of graduate study, I would like to express a great thanks and nice words to people who have supported me. I am grateful to my family members for their kindness in supporting me.

I would like to thank Janie Raymond; we recently became parents of a handsome boy during the end of my PhD degree. I would like to say thanks for the good moments that we spent during my study and for the listening, the encouraging and all support. I would like to thank my parents, brothers and sisters for supports that they had provided me during my studies. I would like to thank all friends and colleagues for all of the help and the good moments. Thank you very much to everyone, who stayed close to me during my PhD.

Foreword

This thesis contains five chapters, including introduction, material and method, results, discussion, and general conclusion and perspectives. The introduction provides detailed information on the eukaryotic cell cycle phases and their regulations. All principles and aspects of chromosome segregation dynamics, regulation, and mis-regulation during mitosis are fully detailed to support and facilitate understanding this thesis. Also, at the end of the introduction chapter, the hypothesis and the aims of this thesis are explained with the context of the research work.

Briefly, this thesis was dedicated to study H2B phosphorylation at threonine 119 during mitosis. This is in order to identify a novel mitotic histone mark that might add more knowledge on the regulation of the chromosome segregation. During my thesis research work, I also participated in the publications listed below:

- Combes G, Barysz H, Garand C, Gama Braga L, Alharbi I, Thebault P, Murakami L, Bryne DP, Stankovic S, Eyers PA, Bolanos-Garcia VM, Earnshaw WC, Maciejowski J, Jallepalli PV, Elowe S. Mps1 Phosphorylates Its N-Terminal Extension to Relieve Autoinhibition and Activate the Spindle Assembly Checkpoint. Curr Biol. 2018;28(6):872-83 e5. Epub 2018/03/06. doi: 10.1016/j.cub.2018.02.002. PubMed PMID: 29502948; PMCID: PMC5863767.
- Combes G, Alharbi I, Braga LG, Elowe S. Playing polo during mitosis: PLK1 takes the lead. Oncogene. 2017;36(34):4819-27. Epub 2017/04/25. doi: 10.1038/onc.2017.113. PubMed PMID: 28436952.

To study H2B phosphorylation, several in vitro and in vivo experiments have been designed and performed. Indeed, a combination of biochemistry, cellular biology, molecular biology, and proteomics experiments were established in this thesis. The material and method are completely explained to allow the reader to easily understand the experimental approaches that were used in this research

project. The results obtained during my laboratory work for my PhD graduation are included in a separate chapter and fully explained. These results show the progress of the research project in regard of studying H2B phosphorylation during mitosis. Moreover, the interpretations of these results are explained in another chapter, in addition to a chapter for the conclusions and the perspectives of the presented study. Finally, the perspectives explain the possible ideas and approaches that can be used to move further in this research project.

Introduction

The planet earth is populated by diverse species, from the very tiny such as the bacterium to the giant such as the whale. The ability of growth and reproduce is fundamental for organisms to stay alive for a period of time and to keep the species for a long time. Living things, or so-called organisms, are all made of one (or more) cells with highly organized ordered-structures, which is enclosed by a membrane as a single cellular unit (*1*). The cell has an extraordinary capability to interact with the surrounding environment and to work as a chemical factory to use materials for feeding, and also to grow to divide itself into two identical daughter cells, reproducing later multiple copies of itself.

The cell is the basic unit of the organism and it possesses a hereditary material that passes through the offspring by reproduction or “perpetuation of life” (*2*). Cell reproduction comprises a distinctive series of well-regulated actions known as the cell cycle. This process includes replication of the chromosomes, which carry the genetic information, and the duplication of other cellular components of the progenitor cell and then their equal distribution to generate two identical copies. A set of signaling networks and complex proteins are involved in orchestrating the process and to ensure a healthy cell cycle, protecting the integrity of the genome and the proper transmission of the genetic information in the offspring (*3*). Through the cell cycle, the ancestral cell hands down the traits that the offspring must possess. Inheritance of the characteristics defines the sustainability of the living substances in comparison to the non-living substances. For instance, in crystallization, the growth or the production of the crystals, occurs by adding more molecules to the pre-existing crystals. In such case, there is no generation of copies from the original. Living substances possess extraordinary properties that need to be maintained and properly inherited from one generation to another by the reproduction.

Today, the planet earth is the home for approximately billions of species all of which use the cell cycle process for breeding, development, or repair (*4*). The cell cycle in some case can create an entire new organism, which occurs in the single-celled species (*5*). During the development of the multicellular organisms, the cell cycle is required for production of cells that make communities to build up the different tissues (*6*). While in the tissue, the cell cycle is necessary to replace the lost or dead cells due to external damaging factors or aging (*7*). Despite, the diversity of the species, cell reproduction follows similar major steps, including the duplication and the division of the cellular components (*8*). The process can be simple in a binary fission pattern as in prokaryotic organisms (*8*) or highly complicated cell cycle as in the multicellular eukaryotic organisms (*9*).

Chapter 1

1 Cell Cycle

1.1 Interphase

Chromosomes must undergo the faithful fate of genetic information transmission throughout the cell cycle (Figure 1-1). Chromosomes first duplicate during the synthesis phase (S phase), then separate during the mitotic phase (M phase). The transition from M phase to S phase is normally separated by an interval step called gap 1 phase (G1 phase) (*10*). As well, there is another interval before entering mitosis called gap 2 phase (G2 phase) (*10*). During both gaps, the cell takes advantage of these interval times to grow and prepare itself for the division (*11, 12*). Together, G1 and G2 phases, in addition to S phase, represent the first stage of the cell cycle that is known as interphase (Figure 1-1).

1.1.1 G1 phase

Commitment to another cell cycle after division is determined during G1 (*13*). The decision whether the cell will continue to replicate again or to enter the quiescence state (or so-called G0) is robustly regulated by the phosphorylation and expression of a group of well-known proteins such as cyclins, cycling-dependent kinases (CDKs), and retinoblastoma protein (Rb) (*14*). The quiescent cell in G0 state can enter again into early G1 upon stimulation by appropriate growth signals, thus indicating that the transition between the early G1 and G0 is reversible (*15*) (Figure 1-2). During the early G1, cell metabolism rate and size dramatically elevate, then the cell passes the restriction point (G1/S checkpoint) to the late G1, during which there is an additional growth factor-independent checkpoint prior to S phase (*13*).

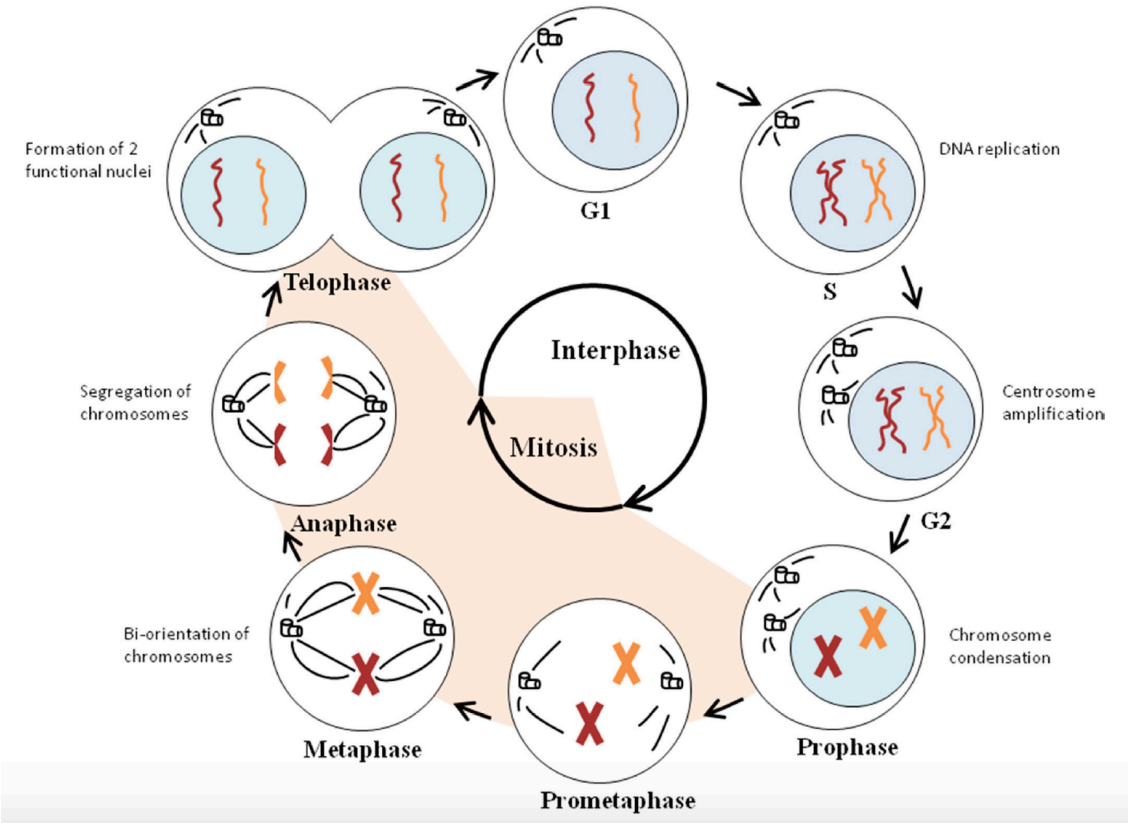

Figure 1-1: A summary of the cell cycle. From the top, clockwise; the cell cycle starts with interphase (G1, S, and G2), during which the cell grows and duplicates chromosomes, and the centrosome, which organizes the microtubules that separate chromosomes during mitosis in cells where they exist. Also, the cell organizes the duplicated chromosomes as sister chromatids, preparing them for the segregation. In the last stage of interphase (G2), the duplicated centrosomes begin to separate from each other to the opposite poles of the cell. Then, the cell starts the division process, which includes distributing chromosomes equally (mitosis) and physical separation of the nascent daughter cells (cytokinesis). Mitosis begins with prophase, during which the sister chromatids are condensed to facilitate their interaction with microtubules and segregation. In prometaphase, the nuclear envelope is completely removed, and the microtubules begin to interact with the sister chromatids. In metaphase, all sister chromatids must align at the cell equator before their segregation. During anaphase, the microtubules pull the separated chromosomes away from each other to the opposite poles of the cells, which is followed by nuclear membrane reformation in telophase and separation of the cells during cytokinesis to produce two identical daughter cells (adapted from (*16*)). G1; Gap1, S; Synthesis phase, G2; Gap2.

After passing the restriction point, removal of the growth factors will not reverse cell cycle to exit into G0, and therefore, the cell will be committed to completing the cell cycle unless arrested by other checkpoints (*11, 14, 15*). The G1/S transition checkpoint is conserved from mammals to yeast (*13*). Similar to the mammalian restriction point, START is the commitment point of the cell cycle in the dividing yeast (*17*), but this checkpoint is sensitive to the nutrient availability rather than growth factors (*10, 17*).

1.1.2 S phase

DNA replication is a challenging process that produces intact and identical copies of the genetic material in a timely-frame fashion during S phase. Duplication of chromosomes begins with building the pre-replication complex (pre-RC) on the origins of replication on DNA prior to S phase transition (*18*). Assembly of pre-RC starts with binding the origin recognition complex (ORC) protein to the replication origins, subsequently, ORC recruits cdc6, and chromatin licensing and DNA replication factor 1 (cdt1) (*18*). Then, this leads to recruiting and loading the heterohexameric mini-chromosome maintenance complex2-7 (MCM2-7), which is a replicative helicase that unwinds the DNA during S phase in an ATP-dependent manner (*18*). Establishing the pre-RC in the origins of replication enables the origins to be licensed for replication (*19*). The pre-RC remains inactive until it becomes activated by the CDK kinases and additional factors to convert the pre-RC into a replication fork upon S phase entry (*18, 20*). Initiation of DNA synthesis requires recruiting additional factors to constitute the pre-initiation complex (pre-IC) in the origins, leading to conversion of MCM2-7 to an active helicase to unwind the DNA (*21*). Once the replication is initiated, DNA polymerases (α, δ, and ε) are recruited to establish the replicon (*22-24*).

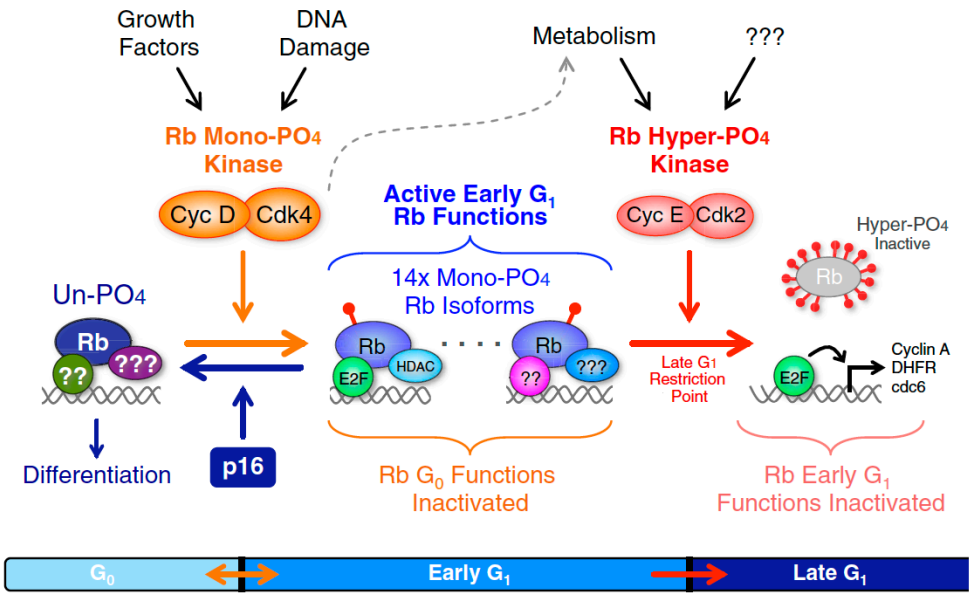

Figure 1-2: G1 checkpoint signaling. Retinoblastoma (Rb) is a tumor suppressor protein that works as an inhibitor of cell cycle progression and a positive regulator of cellular differentiation. Activation of Cyclin D-CDK4 complex in response to the external factors leads to Rb hypophosphorylation and inactivation of Rb G0 function. At this stage, removal the growth factors may lead to cell cycle exit to G0 (orange arrow). Also, expression of p16, which is a tumor suppressor protein, can decelerate the cell cycle by inhibiting cyclin D-CDK4 complex. Rb hypophosphorylation induces Cyclin E expression, which interacts with CDK2 and catalyzes Rb hyperphosphorylation, leading to E2F dissociation from Rb and irreversible passage through the restriction point (red arrow). E2F promotes expression of genes such as Cyclin A, DHFR, and cdc6 that are necessary for G1 progression and G1/S transition (adapted from (*25*)). PO_4; Phosphate group, DHFR; Dihydrofolate reductase, Cdc6; Cell division cycle 6.

1.1.3 G2 phase

The G2 phase provides an appropriate and excellent time for the cell to grow and to validate that nothing went wrong (no DNA damage) following a successful chromosomes replication, as well as the preparative signaling initiation of chromosome segregation (onset of mitosis) and cell division (*26*). DNA double-strand breaks (DSBs) are virtually repaired by the non-homologous end-joining (NHEJ) pathway throughout mammalian cell cycle (*27*). NHEJ is the dominant repair mechanism, during which the ends of the broken DNA strands are brought

head-to-head and then tied up (*28*). However, after DNA replication, DSBs can be healed by additional pathway called homologous recombination (HR) repair (*29*). In HR, a homologous intact DNA template is used for DNA synthesis at the lesion site followed by complementary-dependent repair and ligation. Thus, the repair mechanism is restricted to the replicated chromosomes (*29, 30*).

Also, CDK1 activity plays important roles in G2 and it drives a significant lead into the mitotic entry (*31, 32*). CDK1 in complex with cyclin B promotes activation of several proteins (e.g. Aurora A and PLK1) to promote G2/M transition and mitosis progression, driving crucial functions, including centrosome separation, chromosome condensation, and nuclear membrane break down to initiate chromosome separation during mitosis (*31, 33, 34*). Moreover, Wee1 and Myt1 catalyze inhibitory phosphorylation at threonine 14 and tyrosine 15 of CDK1 during G2 (*35, 36*). These kinases are DNA structure checkpoint proteins that sense the incomplete DNA replication and/or Damage (*37*). Cyclin B-CDK1 activation occurs at the late G2 by Cdc25C, which is a phosphatase that has dual specificity that counteracts Wee1 and Myt1-depedent phosphorylation of CDK1 (*35, 36*). This is considered as a final checkpoint before leaving interphase to mitosis. In agreement, CDK1 inhibition by chemical drugs (e.g. RO-3306) induces cell cycle arrest at G2/M that can be reversed by removing the inhibitor (*38*).

1.2 Mitosis

Mitosis is the process of genetic material division or chromosome segregation. The genetic material is packaged and organized in thread-like structure called chromosomes in the nucleus. Each individual chromosome is composed of a long-linear DNA molecule that is wrapped and tightly coiled by proteins to form a highly compacted structure. This DNA-protein complex is called chromatin, and its basic structural unit is the nucleosome. The proteins that interact with the DNA can be dived into two major groups, namely the histones and the non-histone proteins (*1*). Histones are basic proteins rich in positively charged amino acids. They are the

primary contributors of nucleosome assembly and contribute to chromosome dynamic organization. The single nucleosome core particle is composed of a complex of histone octamer proteins, including two histones H2B-H2A dimers and H3-H4 tetramer (*1*). The eight molecules are wrapped by 147 nucleotide pairs long of double-stranded DNA molecule, forming one single nucleosome particle (*39*). The particles of the nucleosomes are connected with each other through DNA-linker (varies from 20 to 80 nucleotides long) (*39, 40*). In addition to these fours histones, histone H1 (also called the linker histone) interacts with both the DNA-linker and nucleosome to stabilize the chromatin (*39, 41*).

Chromatin exists in two distinctive types; a highly condensed form minority called heterochromatin and less condensed one called euchromatin, the latter represents all of the rest chromatin population. The heterochromatin forms specialized condensed regions known as centromere at the center and telomere at the arm (*42*). In each pair of chromosomes, the centromere makes a primary constriction point, which provides a platform for the assembly of the kinetochore protein complexes that mediate the interaction with microtubules and the separation of the chromosomes during mitosis (*42*). The centromere also divides the chromosome into two areas; the short arm (also called p arm) and the long arm (q arm) (*43*). The centromeric heterochromatin also contains particular histone variant that mediates kinetochore assembly (detailed later). Moreover, several events are occurring along the chromosome either on the centromere/arms during mitosis, including proteins recruitment or histone modifications to regulate the chromosome segregation.

1.2.1 Early mitosis

1.2.1.1 Prophase

Upon mitotic entry, the duplicated chromosomes begin to condense and appear more visibly-distinct during prophase (*44, 45*) (Figure 1-3). Establishing sister chromatid cohesion begins during DNA replication in S phase (*46, 47*). The duplicated chromosomes are structured as a sister pairs through the complexing of

cohesin subunits (including Smc1, Smc3, Scc1/Rad21, and SA1/SA2 in vertebrates) along each two chromosomes (*48, 49*).

In prophase, the cohesion begins to be removed from chromosome arms by PLK1-depdent phosphorylation (*50*). PLK1 phosphorylates SA1/SA2, leading to destabilization of the cohesin complex and induces their disassociation from the chromosome arms (*51, 52*). Cohesion remains protected at the centromere region due to Sgo1-dependent recruitment of protein phosphatase 2A (PP2A), which counteracts cohesin phosphorylation by PLK1 (*53*).

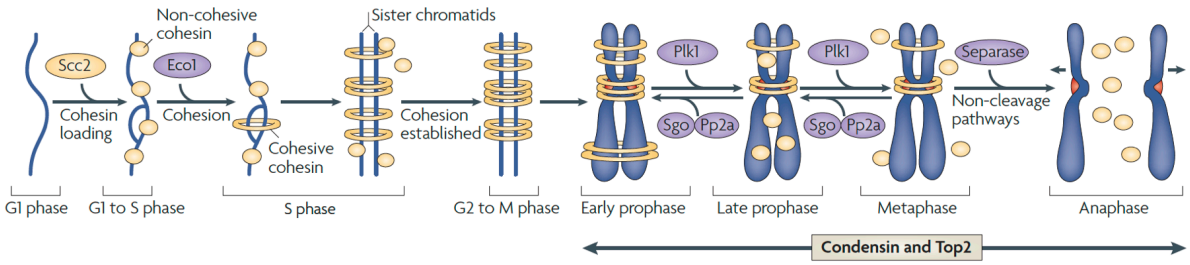

Figure 1-3: Cohesin complex loading and removal during the cell cycle. During S phase, on the left, cohesin rings are formed around the duplicated chromosomes to hold them together until their separation in mitosis. Following mitotic entry, on the right, sister chromatid cohesion is controlled by two factors; cohesin and Top2. Both play an integral role in determining chromosome structure, and are responsible for the chromosomes "X-shape". These activities include winding and unwinding by Top2 and maintenance of sister chromatid cohesion at centromeres. In vertebrates, cohesion is eliminated gradually during mitosis by PLK1 phosphorylation activity, which induces cohesion removal from the arms, but this removal is opposed at the centromere by the PP2A de-phosphorylation activity. Upon mitotic exit, separase cleaves cohesion, allowing the chromosomes to be completely separated (adapted from (*50*)).

The dynamic structure of the condensed chromosome is also mediated by DNA Topoisomerase II (Top2) activity to resolve the physically interlocked (catenated) DNA to form the X shaped chromosomes (*50, 54*) (Figure 1-3). Top2 in ATP-dependent manner transiently and continuously cuts the double stranded DNA molecules, then re-ligates the breaks to arrange and create the topological

architectures of the mitotic chromosomes (*50, 54, 55*). Top2 activity is essential for proper chromosome segregation as its inhibition by drugs or depletion by RNAi leads to segregation defects in anaphase (*56-59*).

Another event that occurs in prophase is the beginning of mitotic spindle formation in the cell cytoplasm (*60, 61*). The mitotic spindle is made up of microtubules, which are polarized protein subunits that assemble together to form a bipolar cylindrical hollow fiber (*62*) (Figure 1-9). Microtubules are highly active and undergo growth and shrinkage during spindle formation (*62*) (Figure 1-4). Several proteins bind to the side and the end of the microtubules and help the establishment of the spindle and movement of the chromosomes during the separation (*9*).

The spindle originates from the centrosomes, or the spindle pole bodies in budding and fission yeast, which starts to separate and move toward the opposite poles of the cell during prophase (*61, 63*). Microtubule fibers have two ends, a minus-end located in the centrosome, and the another plus-end headed outward until it reaches the chromosome and the cell membrane, or it meets the plus-end of the opposite pole and form polar microtubules at the midzone (*64*). Microtubules cannot capture the chromosome during prophase due to the presence of the nuclear membrane, which begins to break in prophase (*65*). However, the broken fragments of the nuclear membrane undergo a complete removal from the way of the microtubules in the subsequent stage, known as “open mitosis” starting from prometaphase (*66*).

1.2.1.2 Prometaphase and metaphase

Successful and accurate chromosome separation crucially relies on the steady attachment of the microtubule with the sister chromatid during prometaphase and metaphase (*9, 67*). In prometaphase, microtubules begin to reach and form interactions with a specialized protein-complex structure called kinetochores, which are localized at the centromere region of chromosomes (*9, 68*) (Figure 1-1 and

Figure 1-5). The centromere is a distinctive and specialized chromatin domain that contains a particular histone H3 variant named centromere protein A (CENP-A) (*68*) (Figure 1-5). CENP-A functions as a major landmark and anchor for loading several proteins to the centromere region in order to promote kinetochore assembly (*68, 69*). The constitutive centromere associated network (CCAN) protein complex, particularly CENP-C and CENP-N of the inner kinetochore region, interact directly with CENP-A to establish the region for kinetochore assembly (*42, 69-71*) (Figure 1-5).

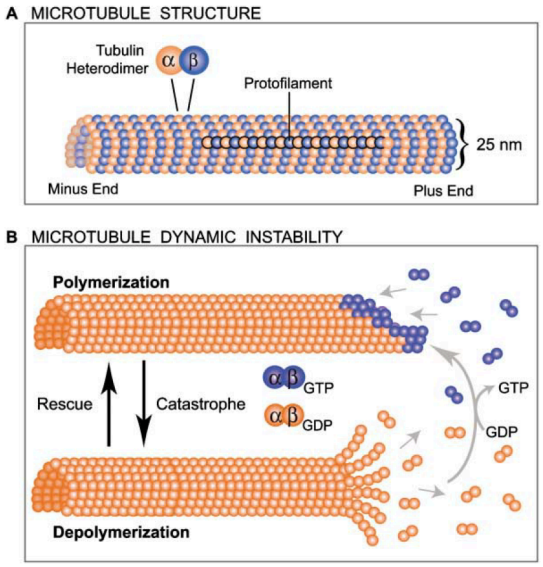

Figure 1-4: Microtubule components and formation. A. Microtubule bundles are the major components from which the mitotic spindle is built. The assembly of α/β tubulin heterodimers occurs head (minus-end) to tail (plus-end) from linear protofilaments, 13 of which align in parallel orientation to make up a hollow cylindrical microtubule lattice. **B.** Microtubules exhibit a dynamic instability, including polymerization (growth) and depolymerization (shrinkage). The tubulin subunits are added to the lattice by orienting β tubulin toward the plus-end and α tubulin toward the minus-end. This addition stimulates the GTPase activity of β tubulin and leads to the hydrolysis of tubulin-bound GTP to GDP. The GDP tubulin rapidly disassociates from the microtubule lattice, leading to shrinkage (catastrophe/depolymerization). This status is rescued by adding new GTP-bound tubulin subunits, resulting in a rapid growth at plus-end (polymerization) (adapted from (*64*)).

In addition to CENP-A, other inner kinetochore proteins, including, CENP-T, -S, -X and -W have been found to make a nucleosome-like complex and interact with the chromosome, presumably essential in forming the kinetochore (*69, 72*) (Figure 1-5). Moreover, CENP-T connects the centromere chromatin and the inner kinetochore protein complexes with the outer kinetochore structure. The outer kinetochore is composed of microtubule-binding proteins such as the KMN network (including Knl1, Mis12 and Ndc80) (*72, 73*) (Figure 1-5). Unlike the inner kinetochore components that mostly exist at centromeres throughout the cell cycle, the majority of outer kinetochore proteins are recruited only during mitosis (*9, 42*). The outer kinetochore not only provides a platform for microtubule binding, it also mediates the recruitment of the checkpoint signaling proteins that monitor microtubule-kinetochore attachment (*74*).

Kinetochore initially interact with the lateral surface, or so-called lattice, of the microtubule to secure its binding with the mitotic spindle (*75*) (Figure 1-6) . Numerous outer kinetochore proteins, including CENP-E, CENP-F, dynein, Rod–ZW10–Zwilch (RZZ) complex are believed to expand and form an area named the corona (*76-78*). At the tip of the kinetochore, the corona structure mediates the anchoring of the microtubule lattice (*79*). The lateral attachment must switch to the end-on kinetochore-microtubule attachment (Figure 1-5 and Figure 1-6), which is important during mitosis to ensure equal and accurate chromosome segregation (*79*).

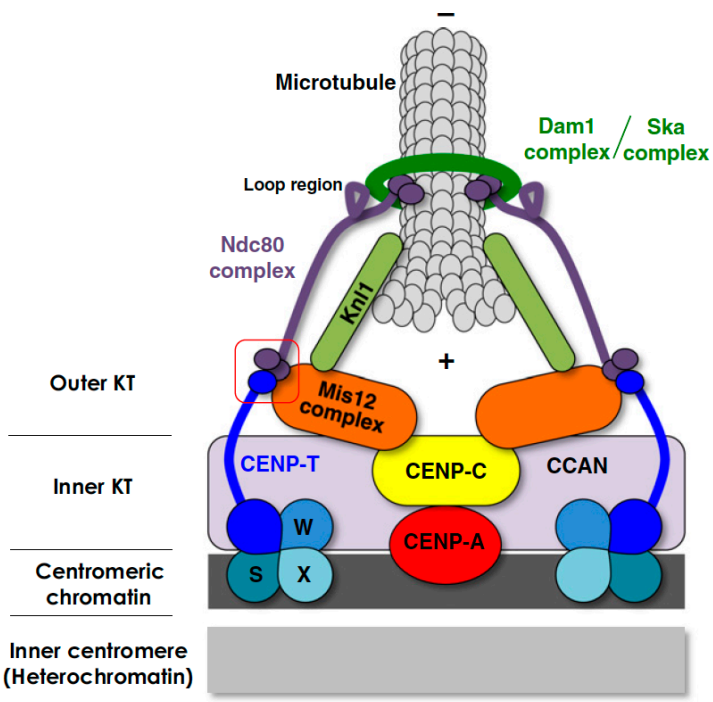

Figure 1-5: Kinetochore structure and attachment to microtubules. Kinetochore building blocks localize at specialized chromatin structure that is assembled with CENP-A (a histone H3-like protein) instead of the canonical histone H3. Inner kinetochore assembly starts early during the cell cycle in G1, then serves as platform for outer kinetochore proteins recruitment in mitosis. CENP-C and CENP-T mediate the association of the inner kinetochore protein with centromeres and with the outer kinetochore region. During mitosis, the plus-end of the microtubule interacts with the outer kinetochore proteins (including Knl1, Mis12 and Ndc80). Additional proteins are recruited such as the Ska complex to regulate end-on microtubule attachment (adapted from (*68*)).

Generation of the end-on attachment occurs upon embedding the emanating plus-end of the microtubule within the kinetochore (*75, 80*). The mature end on capture of the microtubule is mediated by KMN network complexes by forming interaction with CENP-E (mitotic kinesin) and stabilized by other factors, including Astrin-Ska1 complex (*81, 82*). Furthermore, to achieve lateral to end-on conversion, a phosphorylation/de-phosphorylation (by Aurora B/PP2A) gradient is created on KMN network components at the anchoring surface to monitor and correct the attachment (*83, 84*) (detail in section 1.3.2). The end-on kinetochore-microtubule attachment remains under high tension until a steady bi-polar (bi-

orientated) attachment with microtubules initiating at the two poles occurs (*85, 86*). As soon as all kinetochores become attached to the microtubules, the mitotic spindle directs the chromosome to align at the cell equator during metaphase to wait their separation and therefore mitotic exit. Prometaphase and metaphase provide a sufficient time for the mitotic checkpoint to ensure a correct and complete attachment between the kinetochores and the microtubules (*87*) (more detail will be discussed later).

1.2.2 Late mitosis

Mitotic exit events terminate the series of events initiated upon mitotic entry that rely on CDK1-dependent phosphorylation (*88*). Indeed, the onset of mitotic exit is triggered by attenuating CDK1 kinase activity (*88, 89*). This occurs upon establishing a proper and stable kinetochore-microtubule attachment (*88, 89*) (Figure 1-7). Such attachment brings satisfaction of the mitotic checkpoint and the activation of ubiquitination-dependent proteolysis of several regulatory proteins (*73, 90*) (Figure 1-7). The anaphase-promoting complex/cyclosome (APC/C) is the key E3 ubiquitin ligase that induces the degradation of specific mitotic substrates by the 26S proteasome (*90, 91*). APC/C is in complex with cdc20 (cell division cycle 20) (or cdc20p in yeast) and CDH1 (or hct1) which control the ligase activity and the selection of the targeted proteins (*90, 92*). Prior to mitosis, APC/C is kept inhibited by emi1, which interferes with APC/C-cdc20 interaction, allowing accumulation of cyclin B-CDK1 to promote cell cycle progression (*93, 94*). However, upon mitotic entry, CDK1 phosphorylates emi1 to induce its ubiquitination and degradation by Skp, Cullin, F-box containing complex (SCF) E3 ligase activity, thus resulting in APC/C activation (*95*). In addition to that, APC/C activity is regulated by PLK1/CDK1-dependent phosphorylation and de-phosphorylation by phosphatases during mitosis to ensure substrate selection (*96*). This provides an excellent co-regulation and feedback mechanism, thus ensuring a stepwise and timed transition of cell cycle phases.

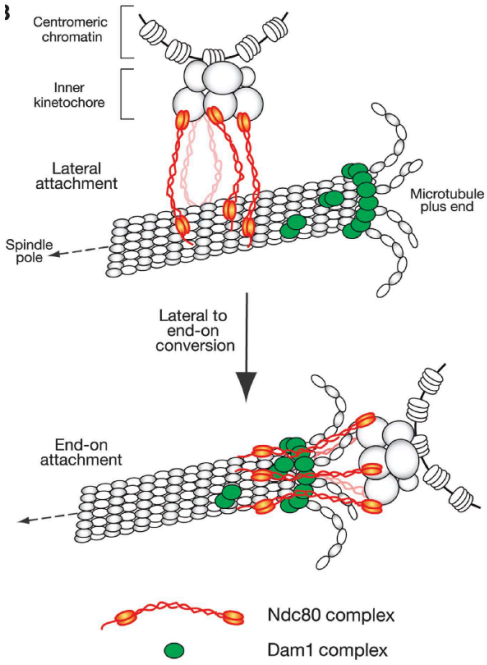

Figure 1-6: Lateral to end-on kinetochore-microtubule attachment. The expanded area of the outer kinetochore provides an interaction surface for the microtubule lattice, forming a lateral attachment. Thereafter, the Ndc80 complex (a KMN network component) facilities and mediates microtubule embedding in the kinetochore to generate end-on attachment. The mature end-on attachment is then regulated and stabilized by the Ska complex to tightly maintain the microtubule plus-end interaction with the kinetochore (adapted from (*75*)).

To initiate chromosome separation, APC/C-cdc20 also induces the degradation of securin, which is an inhibitor of proteolytic separase activity (156, 161,163). In anaphase, the active separase catalyzes cohesin ring structure disassociation by cleavage of Scc1 subunit of the cohesin complex, allowing poleward dragging of the separated chromosomes (Figure 1-7) (164). In telophase, APC/C-cdh1 complex also induces the proteolytic degradation of several mitosis regulatory proteins (163). Approximately 170 proteins (including several kinases) are degraded following the onset of mitotic exit onset, promoting chromosome de-condensation, mitotic spindle assembly termination, and nuclear envelope reformation (166).

1.2.3 Meiosis

Mitosis is a feature of the somatic cell, which leads to the production of two diploid cells (e.g. in humans each cell with 23 pairs of chromosomes). In meiosis, germ cells undergo two divisions, with a single DNA replication (*97*). Hence, meiosis decreases the number of chromosomes to half. For instance, four haploid individuals, eggs (in female) or sperm cells (in male) are produced in humans, each with 23 chromosomes in the meiotic division (*97*). Furthermore, meiosis generates cells with non-identical genetic material due to the DNA exchange during the division (*98, 99*).

Chromosome recombination occurs during meiosis-I, particularly in prophase-I, by forming a physical interaction between sets of two sister chromatids (*97*). This permits chiasmata generation to exchange the genetic materials between the chromosomes. In meiosis-I, sister chromatid cohesion at the centromere remains, but is removed from the arms, to allow only the segregation of the homologous chromosomes (*100, 101*) (Figure 1-8). The division during meiosis-I produces two cells that enter another round of (meiosis-II) without passing another interphase (*97*). During meiosis-II, in particular anaphase-II, there is also no centromeric-cohesion protection during sister chromatids segregation (*99, 100*). Therefore, at the end, four haploid individuals are generated from the meiotic division.

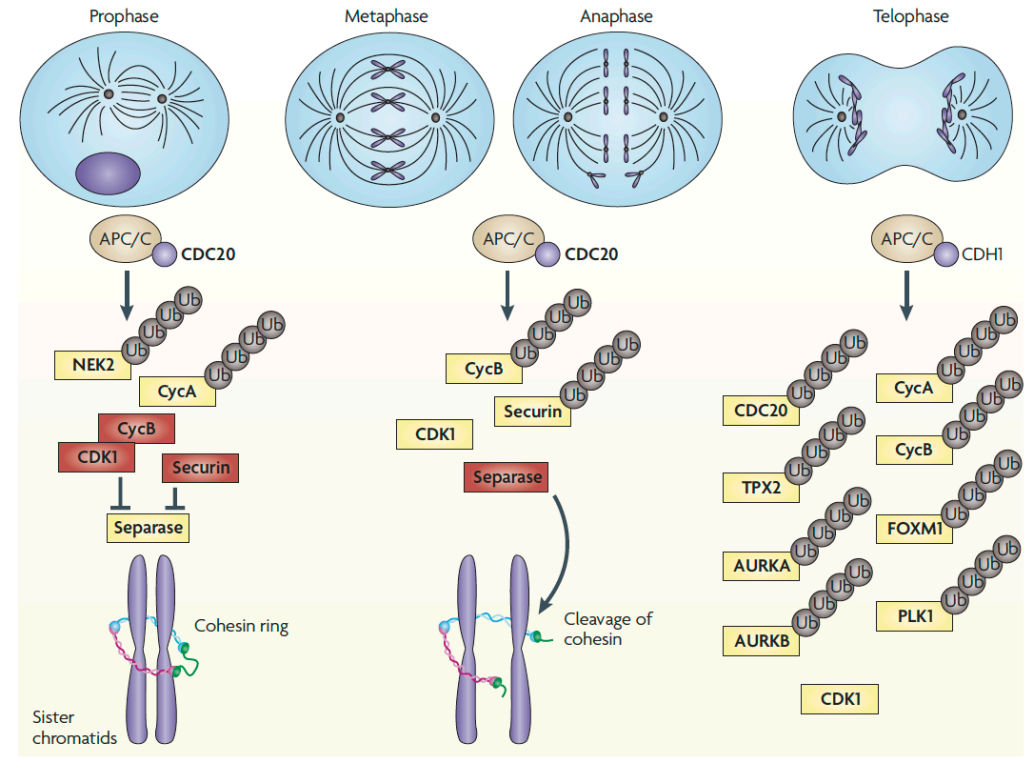

Figure 1-7: The onset of mitotic exit and chromosome segregation. Sister chromatids remain attached to each other due to cohesion activity and the activation of mitotic checkpoint. In anaphase, CDK1-dependent phosphorylation promotes APC/C-cdc20 complex-mediated ubiquitination of cyclin B and securing. This inhibits CDK1 activity, which a key kinase regulator of early mitotic progression and regulation, and also results in activation of separase to degrade the cohesin SCC1 subunit. On other hand, the major mitotic phosphatases (PP1 and PP2A) are re-localized on the centromere and the kinetochore to catalyze dephosphorylation of several substrates to enforce the mitotic exit. Some of the mitotic kinases (e.g. Aurora B) also localize to the midzone to promote cytokinesis and nuclear membrane reformation in anaphase and telophase. However, APC/C-cdh1 continues the ubiquitin-dependent degradation of most of the mitotic regulatory proteins to ensure mitotic exit and the transition to G1 (adapted from (*102*)).

Meiotic division includes mono-orientated chromosome movement during meiosis-I that leads to the separation of the homologous chromosomes rather than separating the sister chromatids from each other, as in mitosis or meiosis-II (*103, 104*). This requires the sister chromatid to be attached to only one pole during

anaphase-I (*100, 103, 104*) (Figure 1-13). Also, this movement needs extraordinary protection of centromeric cohesion between sister chromatids. In *S. cerevisiae*, Spo13 and the monopolin subunit (specifically Mam1) regulate centromeric-cohesion protection and also promote their mono-orientation during meiosis-I, respectively (*103*) (Figure 1-8). Spo13 induces securin re-accumulation, thus inhibiting cohesin degradation by separase (*103*). Moreover, Spo13 induces Mam1 targeting to the kinetochore to enforce monopolar attachment to microtubules (attachment from one pole) of the sister chromatid, resulting in mono-orientation movement (*103, 104*). The mechanism is conserved throughout different species. Centromeric cohesion protection and sister chromatid mono-orientation are both mediated by Moa1 in *S. pombe* and Meikin in mammals instead of Spo13 and Mam1 (*105, 106*) (Figure 1-8). Importantly, knock out/ knock down of these regulatory proteins in either species cause pre-mature cohesion defect and chromosome mis-segregation, thus aneuploidy.

1.2.3.1 Birth defects

Birth defects are believed to be result of maternal age-associated aneuploidy (*107, 108*). Down syndrome (also called trisomy 21) is an example of a birth defect where the patient of this disease born with three copies of chromosome 21, which leads to serious development delays and defects. Chromosome segregation regulation in meiosis during spermatogenesis and oogenesis may provide an insight into understanding maternal aneuploidy. The event of meiosis-I is distinctively regulated at the centromere by special meiotic proteins (e.g. Meikin in mammals). The main goal of the mechanism is to ensure sister chromatid cohesion and mono-orientation. Indeed, premature cohesion loss, lagging chromosomes, and mis-segregation are observed following knockout/down Meikin in mouse oocytes and spermatocytes (*106*). Importantly, deleting the Meikin gene causes infertility in the male and female mice. Understanding and preventing birth defect diseases could be achieved by studying the sources of aneuploidy during meiosis.

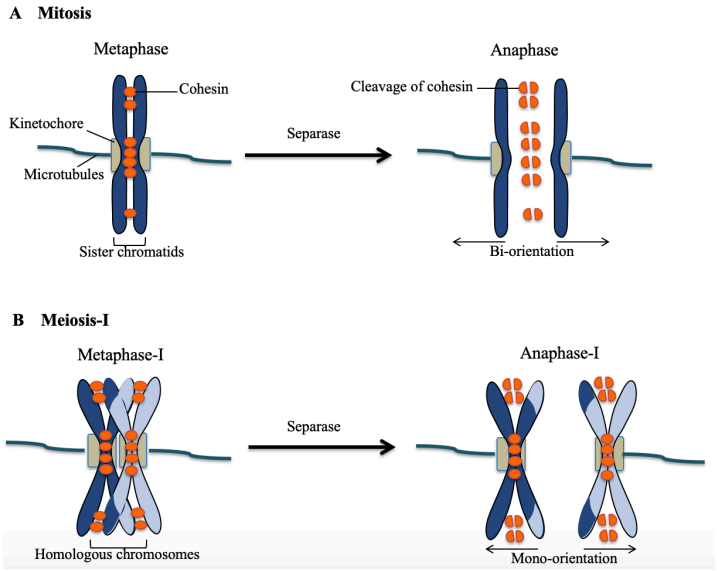

Figure 1-8: Illustration of chromosome mono-orientation movement during meiosis-I. A. In mitosis, the separated chromosomes are moved poleward by the microtubules, resulting in a bi-oriented movement. **B.** In meiosis-I, regulatory proteins (e.g. Meikin in mammals) promote centromere cohesion protection and microtubule interaction with only one kinetochore in each sister chromatid, resulting in mono-orientation. Different chromosome colors (light and dark blue) in (**B**) indicates chromosome recombination (adapted from (*106*)).

1.3 Chromosome segregation regulation

Maintaining an equal diploid chromosome number during cell division is ensured by tightly regulated chromosome segregation events. Chromosome mis-segregation is one of the major causes of aneuploidy (abnormal number of chromosomes) which leads to chromosomal instability (CIN) (*109, 110*). Indeed, a majority of human solid tumors are aneuploid and exhibit a high rate of CIN, which is described as continuous gain and loss of the whole or segments of a chromosome (*110, 111*). Chromosome mis-segregation can occur during mitosis due to several reasons such as kinetochore-microtubule mis-attachment and/or pre-mature cohesion loss (*112*). Such inaccurate chromosome segregation incidence may induce the loss of chromosome capture by mitotic spindle or may

cause an aberrant sister-chromatid movement in anaphase (*111, 112*) (Figure 1-9). Generally, p53 activation is trigged to induce cell cycle arrest and apoptosis of the aneuploid cells to remove any nondiploid cells in the normal tissue (*113*). However, to avoid reaching that stage, regulatory pathways are monitoring and controlling proper kinetochore-microtubule attachment. Also, centromeric cohesion protection and degradation are monitored during the transition in mitosis to prevent chromosome mis-segregation (*102*).

1.3.1 Mitotic checkpoint signaling

The ubiquitous heart of the protective regulatory machine that ensures achieving proper chromosome segregation is the spindle assembly checkpoint (SAC). The SAC, also named mitotic checkpoint, or metaphase checkpoint, prevents the progression to anaphase until full, stable, and proper kinetochore-microtubule attachment is achieved (*114, 115*). It is also known as “a wait anaphase signal” due to its critical role in arresting the cells prior to the mitotic exit when there is an error during chromosome congression at the metaphase plate (*115*). The SAC machinery detects and senses unattached kinetochores as in the case of monotelic attachment (*42*) (Figure 1-9-B and 10-A). Moreover, SAC also detects the improperly attached kinetochores with the microtubules, for instance, the syntelic attachments (*42, 116*) (Figure 1-9-C). The components of the SAC accumulate at the kinetochore region to establish a protein complex during the early mitosis (*115*). The objective of SAC is to ensure generation of the amphitelic bipolar attachment (Figure 1-9-A), where the separated chromosomes will later in anaphase be dragged poleward in a bi-oriented manner by the microtubules emanating from the two centrosomes of the cell (*42*). Indeed, establishing a rigid amphitelic attachment diminishes the strength of the SAC (*117*). Therefore, the SAC plays major role as sensory or guard to prevent aneuploidy to be initiated during cell division and protect genetic identity and equality in the daughter cells (*118*).

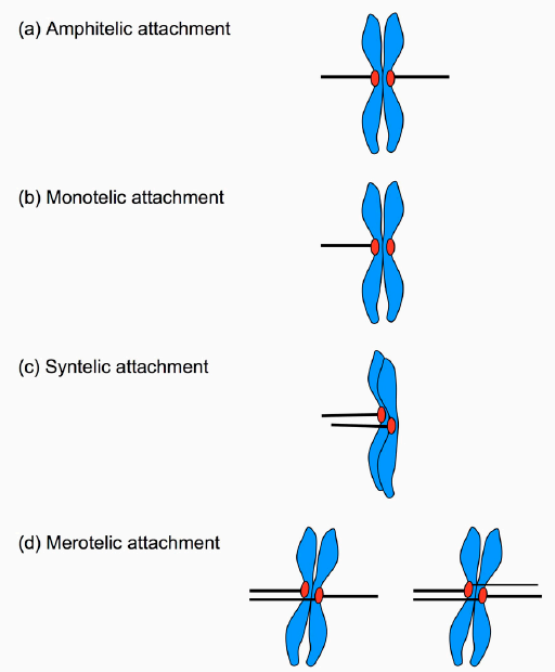

Figure 1-9: Kinetochore-microtubule misattachment. A. Amphitelic bipolar attachment occurs upon interaction of each kinetochore with the microtubules from both poles, resulting in normal bi-oriented movement in anaphase. **B.** Monotelic attachment, in which only one kinetochore is attached with the microtubule from one pole. This kind of attachment leads to mono-orientated movement that is a feature of meiosis-I. However, monotelic attachment in mitosis and meiosis-II is held in check by mitotic checkpoint to prevent aneuploidy. **C.** In syntelic attachment, both kinetochores are attached to microtubules from the same pole, and are also subject to the same regulation described in (**B**). **D.** In merotelic attachments, one kinetochore became attached with the microtubules from both poles. This generates high tension and escapes the mitotic checkpoint and normally produces lagging chromosomes in anaphase. Also, centrosome amplification may occur due to a high rate of CIN causing kinetochore attachment with microtubules from multipolar spindle (adapted from (*119*)).

1.3.1.1 SAC protein complex components

Almost three decades ago, since some of SAC proteins were first identified as mitotic regulatory factors. A genetic screen in *S. cerevisiae* led to the discovery of genes that their mutagenesis causes mitotic cells to escape arrest in presence of benzimidazole (also called benomyl), which is a microtubule assembly poisoning chemical. The Hoyt research team (*120*) found that some budding yeast (*S.*

cerevisiae) mutants could not arrest after benzimidazole treatment and formed extra buds. They therefore coined the term BUB for budding uninhibited by benzimidazole. During their genetic screening, they identified the BUB genes that include BUB1, BUB2, and BUB3 to be the responsible genes for that phenotype in the budding yeast mutants. Around the same time, Li and Murray (*121*) found that some yeast mutants exhibit a rapid division and short mitosis following treatment with benzimidazole. They termed the mutants MAD, for mitotic arrest defective. They also identified the implicated genes, which are MAD1, MAD2, and MAD3 (BUBR1 in humans).

SAC components comprise of several proteins that are recruited to regulate SAC activation and deactivation during the response to the defects in the kinetochore-microtubule attachment (*122*). These proteins include wide range of structural subunits and catalytic factors such as kinases and phosphatases. SAC components are evolutionary conserved in eukaryotes from yeast to man (*123*). These components use the kinetochore as a platform to assemble in prometaphase to monitor the attachment status (*122*). The KMN network is the main binding complex for the SAC components to establish a sensing machine (Figure 1-10-B) (186, 192). In agreement, KMN network mediates microtubules interaction with the kinetochores. Thus, it is a feasible place for the SAC function and feedback regulation (*73*).

1.3.1.2 SAC assembly

During early mitosis the unattached kinetochores allow the formation of the SAC effector complex, which is also known as the mitotic checkpoint complex (MCC) (*124, 125*). This effector complex consists of BUB3, BUBR1, MAD2 and cdc20 that localizes near or at the kinetochore (*124, 125*) (Figure 1-10-D). Some of these proteins exist in an inactive conformational status and thus able to create different pools/fractions and also requires forming dimers to establish the complex (*126*). There are two models to explain the steps and manner of MCC assembly.

MAD2 is known to exist in two different conformations and locations, an inactive one in the cytosol (open O-MAD2) and another during SAC activation at the kinetochore in the closed conformation (C-MAD2) (*127-129*). MAD2 adopts a closed conformation at the kinetochore by interacting with MAD1, which leads to formation of a stable fraction of C-MAD2 at the kinetochore during early mitosis (*128-130*). Otherwise, MAD2 has an open conformation (O-MAD2) that remains in the cytosol as mobile fraction (*128-130*). C-MAD2-MAD1 is recruited to the kinetochore by RZZ complex at the expanded corona (*131*). Also, C-MAD2-MAD1 dimer interacts with the cytosolic O-MAD2, which then induces its conformational change into C-MAD2, which is a cdc20 inhibitory conformation (*128, 132*).

MAD2 contains HORMA domain in the C-terminus that when it is in the closed conformation forms a safety belt-like structure and wraps around the MAD2-interaction motif (MIM) of Cdc20 and also mediates the dimerization with MAD1 (*133, 134*). HORMA domain folding is regulated by the triple A (AAA) ATPase Trip13 and p31comet to facilitate association and disassociation of MAD2 (*135, 136*). Upon interaction of Cdc20, which is both part of MCC and also the target subunit for SAC, this converted cytosolic pool of C-MAD2 is then released to the MCC complex (*137-139*). This was one of the paradigms that is called the "template model" to explain the stepwise assembly of some of the SAC/MCC proteins (*140, 141*). However, it does not provide a broaden explanation for the assembly of the all SAC/MCC components.

Another paradigm is the "two-step model", which gives more insights into the basis of the kinetochore-dependent and independent mechanisms during the SAC/MCC assembly (*140, 141*). This model sheds the light on the existence of the MCC (BUB3, BUBR1, MAD2 and cdc20) in a stoichiometric complex (*126, 142*) (Figure 1-10-D). The MCC complex was initially purified from mitotic HeLa cells and was found to be more potent (3000-fold) in inhibiting APC/C-cdc20 than the MAD2 alone (*143*). Moreover, unlike MAD2 kinetochore-dependent activation as in the template model, the MCC complex was found active even during interphase,

when the kinetochore has not yet reached complete maturation (*143-145*). The kinetochore was thus proposed to only provide a recruitment station rather than be an activation requirement of the SAC effector (*141, 146*). Evidence based on SAC protein depletion indicates that Mad1, Bub1, or Bub3 knock down individually did not have a significant effect on mitotic periodicity; only BubR1 or Mad2 depletion accelerates mitosis exit (*147, 148*). This supports the notion that SAC effectors can be either dependent or independent of kinetochores, and also indicates other possible mechanisms are involved in SAC recruitment and amplification at the kinetochore.

1.3.1.3 SAC recruitment, function and regulation

The goal of the SAC is to prevent chromosome mis-segregation during mitosis, and its activity is most obvious prior to the onset of mitotic exit. The unattached or even incorrectly attached kinetochore initiates SAC proteins recruitment and signal amplification at the kinetochore (*116*). This occurs due to Aurora B activity, which peaks at the centromere in the absence of the microtubules or in the presence of incorrect microtubule interactions with kinetochores (*149*). Aurora B phosphorylates the microtubule-binding domain of Hec1 to recruit Mps1 kinase, which in turn phosphorylates the Knl1 protein (Spc7 in yeast) at the Met-Glu-Leu-Thr (MELT) motifs (*85, 150, 151*) (Figure 1-10-B). Phospho-MELT creates docking sites for Bub3 pools that form dimers with BubR1 and Bub1, and thus mediates recruitment of C-MAD2-MAD1, O-Mad2, and Cdc20 to form the MCC (*150-152*) (Figure 1-10-C). Both Aurora B and Mps1 kinases are crucial for SAC effector recruitment and strength during mitosis. Depletion of either kinase by RNAi, or its chemical inhibition by drugs such as ZM447439 (for Aurora B) or reversine (for Mps1) abrogates SAC-dependent arrest and alters mitotic timing (*153-156*). Indeed, to abolish the synergistic effect of Aurora B inhibition or Hec1 knockdown, tethering Mps1 with Mis12, a protein that is long-lived at kinetochores during mitosis enforces Mps1 localization at the kinetochore and importantly, rescues SAC effector recruitment and function (*153-156*).

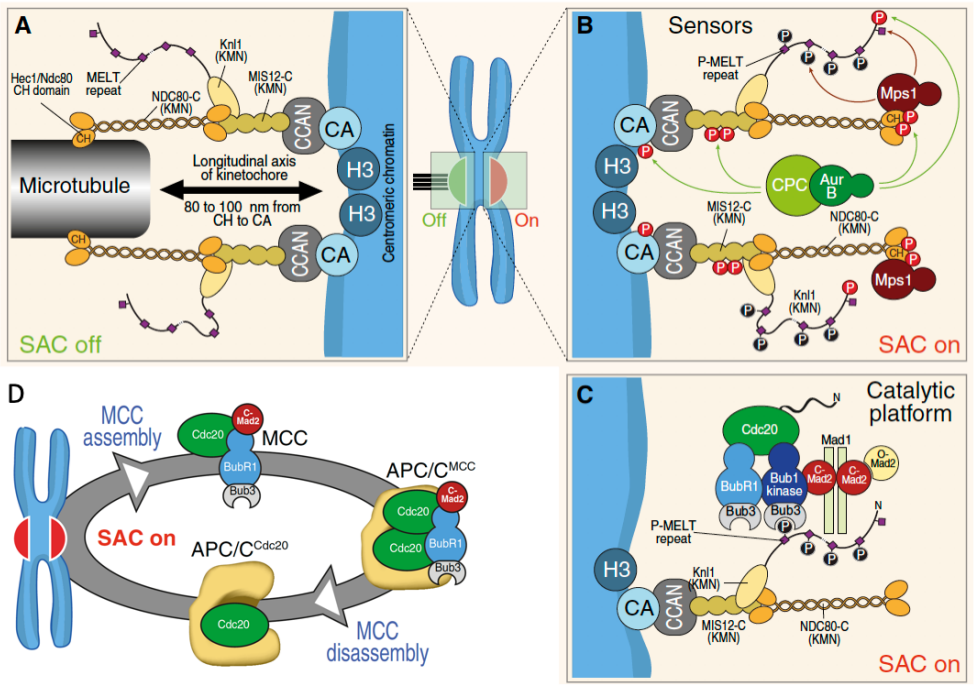

Figure 1-10: SAC assembly, function, and regulation. A. Kinetochore-microtubule attachment brings the satisfaction of mitotic checkpoint signaling. However, presence of unattached kinetochore or weak and inaccurate attachment activates the spindle assembly checkpoint (SAC). **B.** The incomplete or defective attachment allows Aurora B to reach and phosphorylate several proteins at the kinetochore. These phosphorylations recruit the SAC kinase Mps1, the latter phosphorylates Knl1 to create binding region for SAC effector (MCC complex). **C.** In a stoichiometric complex, 2 molecules of Bub3 forms a complex with BubR1 and Bub1 to recruit C-MAD2-MAD1, which then brings O-MAD2. Bub3-BubR1 and C-MAD2 in complex with Cdc20 form the MCC and interact with phoshpho-Knl1 to bind at the kinetochore. Bub1 has been found to have a more structural role in stabilizing the recruitment of BubR1 and MAD2. **D.** The assembled MCC interacts with APC/C-Cdc20 complex to inhibit its activity, thus the MCC prevents degradation of Cyclin B and securing allowing to maintenance of the mitotic state (adapted from (*122*)). CA, CENP-A.

The downstream target of SAC is the APC/C-Cdc20 complex, the activity of which is blocked mitotic progression to allow for sufficient time to correct attachment errors between kinetochores and microtubules (Figure 1-10-D). The MCC acts as an inhibitory factor for the APC/C-Cdc20, keeping it inactive before

anaphase (*122*). Mechanistically, the KEN1 box and the tetratricopeptide repeat (TPR) of BubR1 N-terminal domain bind to C-Mad2 and Cdc20 (*157*). The safety belt-like structure of MAD2 HORMA domain wraps around MIM of Cdc20 that is part of MCC (*134*). BubR1 also forms interactions with Bub3 through its GLEBS sequence (*158*). Then, the KEN2 box of BubR1 interacts with the Cdc20 that is in complex with APC/C, with which also Bub3 presumably interacts, converting MCC (containing one Cdc20 subunit) into MCC (containing two Cdc20 subunits) (*159, 160*). This results in sequestering Cdc20-dependent substrate recognition activity, rendering the APC/C incapable of targeting mitotic proteins (e.g. securin and Cyclin B) for degradation, thereby inducing arrest at metaphase (*161*). Therefore, Cdc20 appears to have dual functions, it is, on the one hand, important for APC/C to recognize the substrates and, on the other, it acts as a pseudo-substrate inhibitor. Furthermore, although this may explain the different paradigms for SAC/MCC activity, they all rely on sequestering the different pools of Cdc20, and robustness of the SAC requires complete MCC assembly and targeting to the kinetochore.

1.3.1.4 SAC silencing

The spatiotemporal function of SAC is regulated by phosphorylation events that are catalyzed by Aurora B and Mps1. Consequently, an opposing dephosphorylation plays a significant role in SAC activity silencing and termination. To that regard, SAC components negatively feedback themselves by recruiting and regulating phosphatases. Protein phosphatase1 (PP1) is well known in counteracting Mps1-dependent phosphorylation of Knl1 that is required for SAC recruitment (*146*). The N-terminus segments of KNL1 itself, including the Serine-Isoleucine-Leucine-Lysine (SILK) motif and the Arginine-Valine-Serine-Proline (RVSF) motif recruit the protein phosphatase1 (PP1) (*162, 163*). During the early mitosis, Aurora B phosphorylates Knl1 at the PP1-binding motif and prevents the interaction of the phosphatase (*163, 164*). However, in a phosphorylation-dependent manner, the kinetochore loaded MCC, particularly BubR1 recruits PP2A-B56, which in turn removes the phosphorylation in the PP1-binding domain

in Knl1 (*165*). Therefore, the SAC signal eventually induces its extinction from the kinetochore region.

The physical interaction of the microtubule with the kinetochore decreases the distance between Aurora B and Mps1 and their kinetochore substrates (Figure 1-11). With beginning of dephosphorylation events by PP1 and PP2A, SAC robustness is diminished. Kinetochore-microtubule interaction dynamics are also involved in switching the SAC on/off at the kinetochore. Furthermore, removal of SAC can be accomplished by a process known as “stripping”, in which the dynein, which is a motor protein that moves cargo along microtubules, moves the C-Mad2-Mad1 and RZZ complex poleward (*146*). A recent study also indicates that the microtubule-associated Ska1 complex also recruits PP1, thus promoting dephosphorylation of kinetochore substrates to abolish SAC activity (*166*) (Figure 1-11).

MCC disassembly also occurs upon termination of SAC activity. The Mad2 binding partner, p31comet, appears to have a potent activity for SAC silencing (*135*). It was believed earlier that p31comet binds to C-Mad2-Mad1 and inhibits O-Mad2 conversion to C-Mad2 (*167*). However, p31comet was later found to not have a significant effect on O-Mad2 kinetochore recruitment (*135*). The p31comet-dependent SAC silencing pathway is most likely dependent on an interaction with C-Mad2 to reduce MCC formation. Another study has suggested sequential MCC disassembly (*168*); first, p31comet interacts with Mad2 and CDK1 phosphorylates Cdc20, leading to disassociation of Mad2-Cdc20 from Bub3-BubR1. Second, the triple A (AAA) ATPase Trip13 activity and p31comet mediate Mad2-Cdc20 disassembly by converting C-Mad2 into O-Mad2.

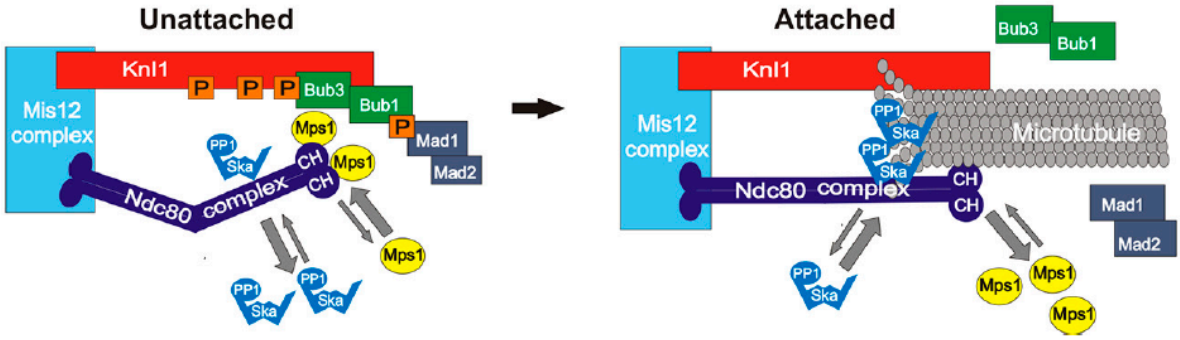

Figure 1-11: SAC silencing upon kinetochore-microtubule attachment. On the unattached kinetochore, the SAC is recruited to abrogate APC/C-Cdc20 activity in order to arrest the cell at metaphase until the attachments occur, left. Upon kinetochore-microtubule attachment, microtubule physically induces SAC silencing by sequestering the mitotic kinases (Aurora B and Mps1) preventing MCC recruitment. Also, recruitment of PP1 by Knl1 or the Ska complex can lead to dephosphorylation events, removing the docking sites that recruit SAC components (adapted from ***(166)***).

1.3.1.5 SAC protein deregulation in cancer

Many of the regulatory proteins of the chromosome segregation process are deregulated in numerous cancer types. Overexpression of Mad2 was observed in oral squamous cell carcinoma (*169*), while BubR1 was observed in breast and esophageal squamous cell cancers (*170, 171*). In gastric cancer, Bub3, Bub1, and BubR1 were also found to be overexpressed (*172*). The mRNA and protein expression of all of the SAC proteins, including Mad1, Mad2, Bub1, BubR1, Bub3, and Cdc20 were analyzed in 12 breast cancer cell lines and their levels were significantly elevated (*173*). Controversially, Mad2 shows low expression in ovarian cancer cells and testicular germ cell tumors (*174*). Moreover, SAC efficiency was tested in the low-Mad2 ovarian cancer cell lines through treating the cells by microtubule depolymerization drugs (nocodazole or colcemid) in order to arrest them at mitosis (*174*). These cell lines were found to overcome mitotic arrest and go through cell division after drugs treatment. Indeed, similar phenotype was obtained following microinjection of Mad2 antibody into HeLa cells and treatment with nocodazole. To validate the effect of Mad2 low expression, the exposure to

the microtubule drugs were tested after establishing an inducible Mad2 expression system in the ovarian cancer cell lines, which was found to reinstate the effect SAC and promote mitotic arrest (*174*). However, understanding the deregulation of gene expression of SAC proteins in the different cancer types is still not fully clarified. Similarly, Aurora B is deregulated in many cancer cells, but a defined link with the cancer development is not understood (*175*). Mainly, more comprehensive studies are required to understand the effect of overexpression versus the low expression of the genes on mitotic regulation and progress, and whether genetic mutations are implicated.

1.3.2 Attachment correction

Chromosome mis-segregation also can be prevented by correction of the inaccurate attachment between the kinetochore and the microtubule. The correction process generates unattached kinetochores to activate the SAC in order to arrest the cell to give enough time for achieving proper attachment (*176*). Importantly, attachment correction provides a great strategy in sensing the inaccurate attachments that the SAC itself cannot detect. The SAC effectively arrests cells in the presence of unattached kinetochores or upon detecting syntelic attachments, which need correction (*42*). However, the SAC is insensitive to merotelic attachments, where the kinetochore interacts with the microtubules emanating from the two poles (*42, 177*). Merotelic attachment is often observed as early as prometaphase during mitosis (*178*). The kinetochore merotelically attached with the microtubule is a primary cause of CIN, which is one of the major characteristics of tumors (*179*). This kind of attachment thus must be removed to allow generating the bipolar amphitelic attachment.

The error correction pathway is controlled by Aurora B kinase activity, which localizes at the centromere region and monitors the status of the kinetochore-microtubule attachment (*161, 180*) (Figure 1-12). Aurora B generates a phosphorylation gradient at the kinetochore to repair the erroneous attachments, thus ensuring the bipolar attachment and the bi-orientated movement of chromosomes during anaphase (*161, 180*). The targeted kinetochore-substrates of

Aurora B include proteins located at both proximal and distal distances from the centromere. This allows Aurora B to target two distinctive regions; inter-kinetochore (or inner kinetochore proteins) and intra- kinetochore (or outer kinetochore proteins) (*181*).

Aurora B activity is controlled by the kinetochore status such as unattached or properly/improperly attached (e.g. amphitelically or merotelically) kinetochores (*182, 183*). On the unattached kinetochore, in this case there is no tension produced by the microtubule and the phosphorylation gradient will be high, because Aurora B can reach its substrates (*182-185*). Bipolar amphitelic attachments, on the other hand, produce high tension due to forces the kinetochore poleward (*182-184*). In such case the microtubule physically blocks Aurora B from reaching the substrates and displaces them from the zone of Aurora B activity (*182-184*). In anaphase, upon the separation of the sister kinetochore, Aurora B is localized at the midzone to promote cytokinesis (*186*). Thus, the microtubule moves the targeted substrates away from the phosphorylation gradient of Aurora B to terminate the attachment correction pathway. Importantly, improper attachment generates only low tension, thus Aurora B can phosphorylate several substrates at both inter and intra-kinetochore to destabilize and remove the attachment to activate the SAC, allowing correction before anaphase (*182, 183, 185*) (Figure 1-12).

1.3.2.1 Intra-kinetochore substrates

Among Aurora B's best-known substrates at the intra-kinetochore are KMN network proteins complexes (Knl1, Mis12 (Dsn1, Mis12, Nsl1, and Nnf1), and Ndc80 (Spc24, Spc25, Nuf2, and Ndc80)) that indeed cooperatively mediate the kinetochore and the microtubule interaction, relying predominantly on electrostatic interactions (*68, 72, 73, 187*). For that, the calponin homology (CH) domains in the N-terminus tail of the Ndc80 subunit (or Hec1 in human) possesses several positively charged amino acids (15 residues) that provide a receptor for the negatively charged C-terminus of α and β tubulin subunits (*187-189*). However,

Aurora B phosphorylates Ndc80 subunit (Hec1) and reduces its microtubule binding affinity (*187, 190, 191*) (Figure 1-12). Moreover, Aurora B, as discussed in SAC silencing, phosphorylates Knl1 to oppose PP1 recruitment, mostly to protect its targeted functional substrates (Figure 1-11 and 12). In contrast, Mis12 phosphorylation by Aurora B plays role in kinetochore assembly (see next section).

The kinesin-related protein MCAK (mitotic centromere-associated kinesin) and Kinesin-like protein KIF2A, which are microtubule depolymerases, are also apparently important Aurora B substrates in the error correction pathway (*192*). Through in vitro kinase assays and mass spectrometry mapping, several residues have been recognized to be Aurora B substrate in MCAK, three of which were found crucial for MCAK function and localization (*193-195*). Aurora B phosphorylates MCAK at the threonine 95 (T95) to promote the association of the latter to the chromosome arm during the early mitosis (*195*). However, the phosphorylation of MCAK at serine 196 (S196) induces its disassociation from the arm and pS110 promotes the re-localization to the centromere (*194, 195*). Phosphorylation at S196 inhibits the depolymerase activity of MCAK and injecting antibody against pS196 of MCAK in PtK2 cells alters mitotic timing and causes segregation defects (*194, 195*). The inhibitory Aurora B-dependent phosphorylation of MCAK can be abolished by the inner centromere Kin-I stimulator (ICIS), which interacts with MCAK (also with KIF2A) and activates its depolymerase activity at the centromere during mitosis (*196*).

1.3.2.2 Inter-kinetochore substrates

Aurora B activity on the inter-kinetochore substrates presumably regulates kinetochore assembly during mitosis. Dsn1 (Mis12 subunit in KMN) contains two serine residues (S100 and S109), which were identified as major target sites for Aurora B and it seems to play role in kinetochore assembly (*197, 198*). Indeed, phosphorylation of Dsn1 by Aurora B seems to contribute in KMN interaction with the inner kinetochore proteins, in particular CENP-C (*197*). The expression of phosphomimetic-Dsn1 mutant (S100 and S109) induces restoring KMN network

even in interphase, although Dsn1 phosphorylation is not essentially required during mitosis (*87, 197*). Therefore, Aurora B's role in kinetochore assembly may be restricted only to stabilization and re- reconstitution in response to activation of the error correction pathway, but this still needs to be validated in term of the acquired phenotypes due to the loss of Dsn1 phosphorylation by Aurora B.

Controversially, a recent study has revealed that Cnp3 (CENP-C equivalent in *S. pombe*) and Knl1 phosphorylation by Ark1 (Aurora B equivalent in *S. pombe*) destabilizes KMN interaction with the microtubule for error correction (*199*). Furthermore, in budding yeast, the function of Ipl1 (Aurora B equivalent in *S. cerevisiae*) in error correction can be centromere-dependent as in humans or independent (*200*). Thus, Aurora B functional model for the error correction pathway is not evolutionary conserved. More detail on Aurora B localization and recruitment will be discussed in the coming sections.

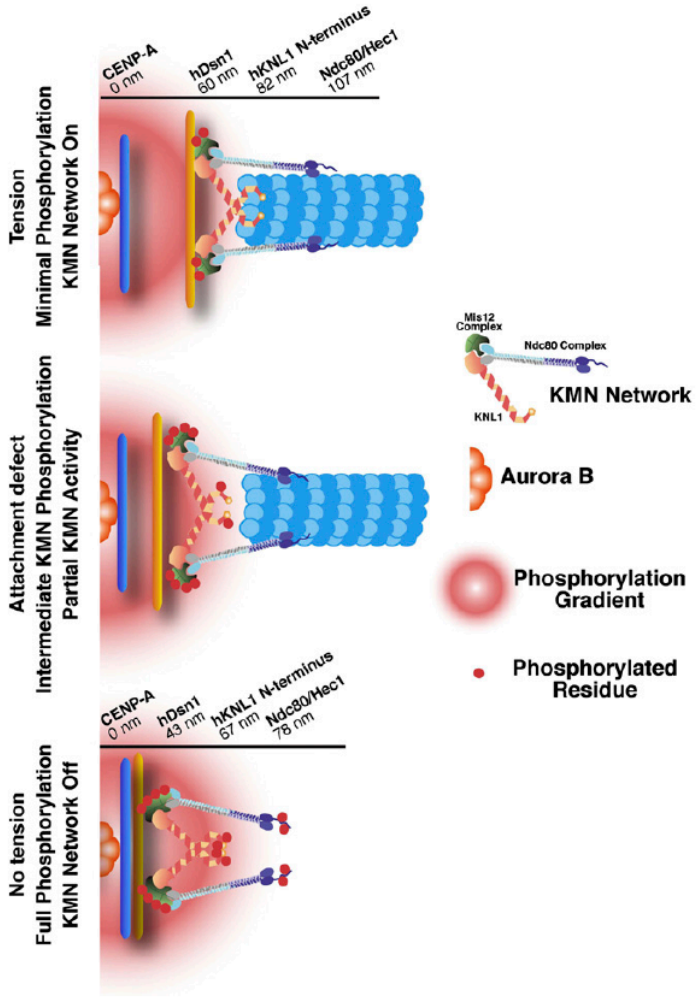

Figure 1-12: KMN network phosphorylation by Aurora B during mitosis. Aurora B localizes at the centromere region and generates a phosphorylation gradient to regulate the error correction pathway. Top, the proper interaction of the microtubule with the kinetochore produces high tension due to kinetochore stretch. This limits Aurora B access to its substrates through their displacement. For example, under high tension, the microtubule action can lead to stretching the distance between CENP-A and Mis12 to 100 nm at the kinetochore region (*201*). Middle, presence of inaccurate/weak interaction produces low tension and allows Aurora B to phosphorylate the KMN complex and reduce microtubule affinity toward the kinetochore. Under such low tension, the distance between CENP-A and Mis12 is reduced to around 45 nm in humans (*80*). However, the persistent presence of the misattachment leads to generation of unattached kinetochores (bottom) and activates the SAC until the proper attachment occur (adapted from (*87*)).

1.4 Histone modification and mitosis

Histones (H2B, H2A, H3, and H4) are small proteins, about 102-135 long amino acids, which bind to the DNA to constitute the chromatin (*202*) (Figure 1-13). Approximately, the positively charged amino acids (lysine and arginine) make up more than one fifth of each histone (*1*). All of the core histones share a structurally conserved motif around 70 amino acids, known as the histone fold or the globular domain (*39*). The histone fold composed of three α helices that are linked by two short loops and is responsible for octamer assembly (*39*). The DNA wraps around the octamer, and then the enriched positively charged amino acid content of the histones neutralizes the negative charge of the phosphate group in the DNA during nucleosome core particle formation. Each of the core histones also contain flexible domains at the N-terminal and the C-terminal that form tails (*202*) (Figure 1-13). The tail domains of the histones represent the regions extended out from the DNA-histone complex. Tail domain size varies between the histones from long e.g. 40 amino acids in N-terminal of H3 and short e.g. ~20 amino acids in H2A/H2B C-termini (*203-205*). While the tails of histones can interact with nucleosomal DNA, they also contribute to the interaction between nucleosomes to pack them together, a process regulated by certain modifications (e.g. acetylation) (*206*).

The tail domains of all core histones in the nucleosome are subject to an extraordinary variety of reversible covalent modifications in an event known as post translational modification (PTM) (*207*) (Figure 1-13). This occurs by introducing functional group into the modifiable amino acid residues in the histones such as lysing (K), arginine (R), threonine (T), and serine (S). The modification includes mostly small chemical groups in case of acetylation, methylation, and phosphorylation, but it also could be a large group in case of ubiquitination, which is a small protein made up from 76 amino acids (*208*). PTMs play an essential role in regulation of several cellular processes, including gene expression, proliferation, and DNA damage (*209, 210*). During mitosis, histone PTMs undergo numerous drastic changes e.g. H3K9ac at the active promoter subjects a decrease for gene expression silencing (*209, 210*). On other hand, histone phosphorylation shows a

robust increase such as H2ApT120 and H3pT3, which are both important functional modifications that ensure proper chromosome segregation (*209*).

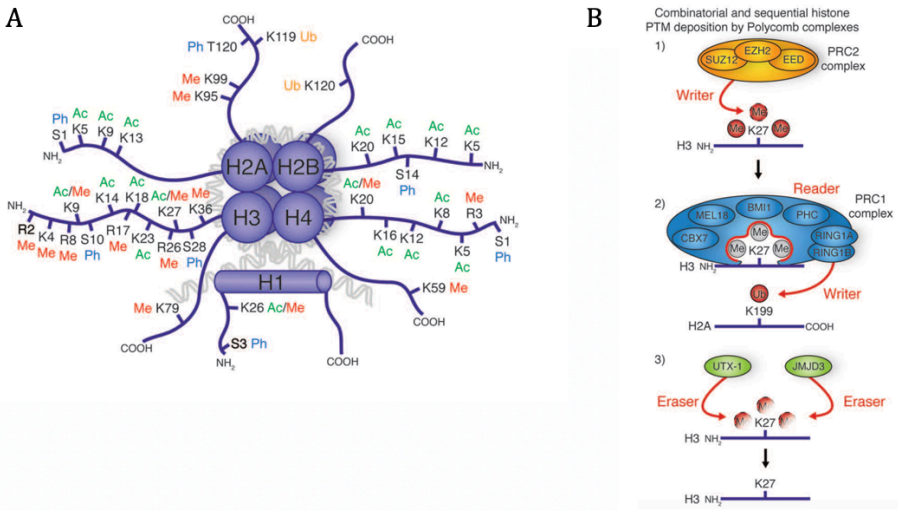

Figure 1-13: Nucleosome structure and histone PTM. A. The nucleosome is assembled from eight core histone molecules (two of each H2B, H2A, H3, and H4) forming an octameric complex that then becomes wrapped by 147 nucleotides pairs of double-stranded DNA. Histone H1 is a fifth protein that interacts with the nucleosome or with the linker DNA to stabilize the formed chromatin beads in a string-like structure. Some of the canonical core histones have several variants that may differ by a few residues (canonical H3 and H3.1) or at many positions (e.g. majority of H3 and CENP-A; centromere-specific variant). In the tail domain of each core histone, several modifications can occur to regulate the chromatin dynamics and/or perform certain physiological functions. Among these modifications are lysine and arginine methylation and acetylation that can be mono, di, or tri moieties. Also, other types of modifications, include serine and threonine phosphorylation have also been identified. **B.** Histone modification is reversible, which can be catalyzed by a specific enzyme (writer) to anchor a particular chemical group covalently with the amino acid residue and then removed by another enzyme (eraser), thus making it reversible. For example, the methyltransferase activity (writer) of PRC2 (polycomb repressive complex 2) tri-methylates lysine 27 in histone H3 (H3K27me3). The PRC1 complex interacts (reader) with H3K27me3 and translates it into biological function. Removal of H3K27me3 is catalyzed by the demethylase activity (eraser) of UTX-1 or JMJD3 (adapted from (*207*)).

1.4.1 Bub1 and H2ApT120

1.4.1.1 Bub1 protein kinase

Bub1 is an evolutionary conserved mitotic multifunctional serine/threonine protein kinase. It was first identified during a genetic screening in the budding yeast and functionally defined as a gene involved in the spindle checkpoint signaling during mitosis (discussed above). Bub1 structure includes several functional motifs and domains (*211*). The N-terminus contains a triple tandem repeat of 34 amino acids called the tetratrico peptide repeat (TPR) domain (residues 1-150), which interacts with Knl1 for kinetochore localization (*211-213*). Following the TPR domain, a short-conserved motif about 40 amino acids (in human BUB1 residues from 240 to 280), called the Gle2- Binding Sequence (GLEBS) and involved in BubR1 and Bub3 recruitment, thus it is also known as Bub3-binding domain (B3BD) (*214, 215*). Proceeding downstream, residues 458–476 is the conserved motif1 (CD1) that is involved in Mad1 loading (*215, 216*). Further, two motifs called KEN boxes (each contains three amino acids of Lys-Glu-Asn at residues 535–537 and 625–627), which recruits Cdc20 (*214, 215, 217*). Finally, at the C-terminus (residues 784-1085) the kinase domain is located (*214*).

During the early mitosis, Bub1 is recruited to the kinetochore, where it facilitates the loading of several proteins such as CENP-E, CENP-F, and the SAC proteins (Mad1, Mad2, Cdc20, Bub3, and BubR1) (*211, 215, 218*). Remarkably, Bub1 kinase activity is not required for the recruitment or the function of these kinetochore proteins (*216, 219-221*). An earlier study has showed that the expression of exogenous Bub1-lacking the kinase domain can rescue SAC protein recruitment in cells in which the endogens Bub1 is depleted (*216*). While, another recent study has indicated that inhibiting Bub1 by specific chemical drug (BAY-320 or BAY-524) slightly affects the SAC activity during mitosis (*221*). However, Bub1 kinase domain plays a crucial functional role during mitosis by phosphorylating (histone mark writer) threonine 120 of H2A (H2AT120 or H2AS121 in yeast) (*222*). Through H2AT120, Bub1 creates an important mitotic landmark for recruitment of the protector proteins of centromeric cohesion (*222, 223*).

1.4.1.2 Shugoshin (Sgo) recruitment

Shugoshin is a Japanese word that means the ‘‘guardian spirit’’ to point out the role of this protein in centromere cohesion protection during meiosis (*224*). Shugoshin (Sgo) was also first identified through a genetic screening in fission yeast (*224, 225*). It was functionally characterized as a protein that protects cohesion (contains Rec8 subunit instead of Scc1/Rad21) at the centromere from the disassociation during meiosis-I in yeast and also in D. melanogaster (by Sgo equivalent MEI-S332) (*224-227*). In human, two orthologs of Sgo gene exist, and are known as human Sgo (hSgo 1/2) or Shugoshin-like 1/2 (SGOL1/2), and both function during meiosis and mitosis for cohesion protection (*53, 228, 229*). Earlier, it was observed that Sgo1 depletion by RNAi leads to cohesion and segregation defects during mitosis in human cells (*228, 230*). This phenotype was rescued by expression of an exogenous non-phosphorylatable SA2 subunit of the cohesin ring complex (*230*). Then, to describe the molecular mechanism of Sgo1, a combination of immunoprecipitation and tandem mass spectrometry (LC–MS/MS) was implemented to identify the binding partners of Sgo1 during mitosis (*53*). Accordingly, PP2A subunits were the major interacting proteins that include the catalytic phosphatase subunit (PP2A-C). Plus, two other subunits, including the scaffold A subunit (PP2A-A), which recruits regulatory B subunit (B56) to regulate phosphatase affinity and recruitment.

Sgo1 localizes along the chromosome during prophase, but it re-localizes and concentrates at the centromere region in prometaphase (*228, 231, 232*). The major function of Sgo1 is PP2A-B56 recruitment to the chromosome to counteract the PLK1-induced dissociation of cohesin subunits (see prophase section) (*50*). Indeed, PP2A in vitro can dephosphorylate C-terminal phosphopeptide of SA2, which in vivo is phosphorylated by PLK1 to induce cohesin removal from the chromosome arm during prophase (*50, 53*). In vivo experiments in yeasts and vertebrates have validated that PP2A-B56 recruitment by Sgo1 counteracts PLK1 activity against cohesin in the centromere (*53, 230-232*). Moreover, PP2A-B56 also was found to remove CDK1-dependent phosphorylation of Sororin, the latter then

can interact with the cohesin subunits to antagonize wings apart-like protein (WAPL), which is a cohesion destabilizing factor (*233*).

Sgo1 (histone mark reader) is recruited to the centromere region during mitosis mainly through Bub1-dependent phosphorylation of H2AT120 (*222, 223*). This histone mark appears from prophase and persists until it completely disappears in late anaphase (*222, 223*). The inhibition of Bub1 activity by BAY-320 or BAY-524, or even depletion by RNAi causes H2ApT120 loss and a significant decrease in Sgo1 localization at the centromere (*221*). Furthermore, H2ApT120 loss leads to ectopic cohesion, which is a particular phenotype, in which the constriction point is lost at the centromere and the chromosome arm remains unsolved (*221, 222*). This ectopic cohesion is presumably due to the re-localization and the distribution of Sgo1 along the chromosome (*53, 222, 232*). Taken together, recruitment of Sgo1 to the mitotic chromosome is a challenging topic to understand, because Bub1 localization is restricted to the kinetochore, hence how Sgo1 localizes at the arm? Moreover, a small portion of Sgo1 still can localize at the kinetochore upon Bub1 depletion by RNAi (*221*). Recent study in human cell found that CDK1-dependent phosphorylation of Sgo1 at T346 promotes its interaction directly with the cohesin during mitosis (*233*). Thus, this presumably can recruit Sgo1 to the arm through an interaction with the cohesion. Additionally, CDK1 phosphorylation of Borealin can promote Sgo1 recruitment to the kinetochore (more detail next section) (*234*). Nevertheless, despite existence of other pathways for Sgo1 recruitment, Bub1 through H2ApT120 contributes to the kinetochore recruitment of a large population and is responsible for the efficient localization of Sgo1 to the kinetochore during mitosis.

1.4.2 Haspin and H3pT3

1.4.2.1 Haspin protein kinase

Haspin was discovered by the Tanaka research team through genetic screening of subtracted cDNA library constructed from adult mice testes (*235, 236*). The principle of this kind of screen is to prepare cDNA clones from mRNAs of a specific cell/tissue type and then validate their presence in another cell/tissue type (*237*). To do so, Tanaka and his colleagues generated two cDNA libraries: one from total RNAs extracted from adult mice testis containing germ cells and another from mutant mice testis lacking these specific cells (*235, 236*). In their screening, they identified a novel protein that has a serine/threonine kinase activity, is solely expressed in haploid germ cells and localizes in the nucleus. Thus, they named this protein Haspin for **ha**ploid germ cell-**s**pecific nuclear **p**rote**in** kinase. Also, the gene encoding Haspin is called GSG for **g**erm cell-**s**pecific **g**ene-2 (GSG-2), which is localized to chromosome 11 in mouse and 17 in human. Structurally, Haspin contains atypical and unique protein kinase domain (*238, 239*) (Figure 1-14). Further analysis by Higgins and colleagues who were the first to characterize Haspin mitotic functions, indicated that Haspin also ubiquitously expresses in other tissue types and proliferating cancerous cells, but the robust expression is exclusive to the spermatid cells (*240-242*). Haspin orthologs have been also found in most of the eukaryotic lineages such as plant, vertebrates, and nematodes (*241, 242*). Moreover, Haspin has two equivalents/homologs in budding yeast, including ALK1 and ALK2 (*243*). While, Hrk1 is the Haspin equivalent in fission yeast (*223*). All homologs appear to have an active serine/threonine kinase domain; However, both Haspin and Haspin-like proteins have a divergent kinase domain sequence comparing to the canonical eukaryotic protein kinases (*244*).

Immunofluorescence microscopy studies have revealed Haspin localization, which appears exclusively in the nucleus in the interphase cell (*236, 245*). During mitosis, Haspin was observed at the centrosomes from metaphase until telophase, during which it also observed with the spindle at the midzone (*245*). In addition to that, Haspin localizes in the centromere region and it has also been observed at

the chromosome arms, but at significantly lower levels (*245*). It was earlier concluded that Haspin has major function during cell cycle, because inducing Haspin overexpression in somatic cell causes cell cycle arrest (*236, 245*). Moreover, through an in vitro Haspin kinase assay with nucleosome or recombinant histones, it was discovered that Haspin catalyzes histone H3 threonine 3 (H3T3) phosphorylation, and that was validated in vivo as well (*245*). With the use of RNAi against Haspin or through utilizing 5-Iodotubericidin (5-IT) (Haspin inhibitor), more detail was revealed about the functional aspects of this protein kinase during mitosis (*245, 246*).

1.4.2.2 Cohesion protection

One of the important functions of Haspin during mitosis is maintaining the sister chromatid cohesion. Premature sister chromatid separation due to cohesion defect prior to anaphase was observed following depletion of Haspin in HeLa cells (*247*). Cohesion defect was also observed in Haspin-knockout HeLa cells (*248*). Two recent studies have shown that Haspin interaction with cohesion is crucial for cohesin ring-structure stability during mitosis (*249, 250*). It has been found that Haspin through specific residues (14-RTYGA-17) in its N-terminal domain interacts with Pds5B, which is a protein that stabilizes the cohesin complex. This interaction prevents WAPL (the cohesion destabilizer) from binding to Pds5B, thus Haspin binding results in cohesion protection. Furthermore, Haspin phosphorylates T8 in the YSR motif of the WAPL N-terminus to antagonize the interaction of the latter with Pds5B in order to protect the cohesion during mitosis. However, cohesion protection does not explain all mitotic functions that are attributed to Haspin kinase activity, because Haspin inhibition also causes impaired kinetochore performance and chromosome mis-segregation (*246*). In addition to that, cohesion protection by Haspin is more structural than catalytic (*246*).

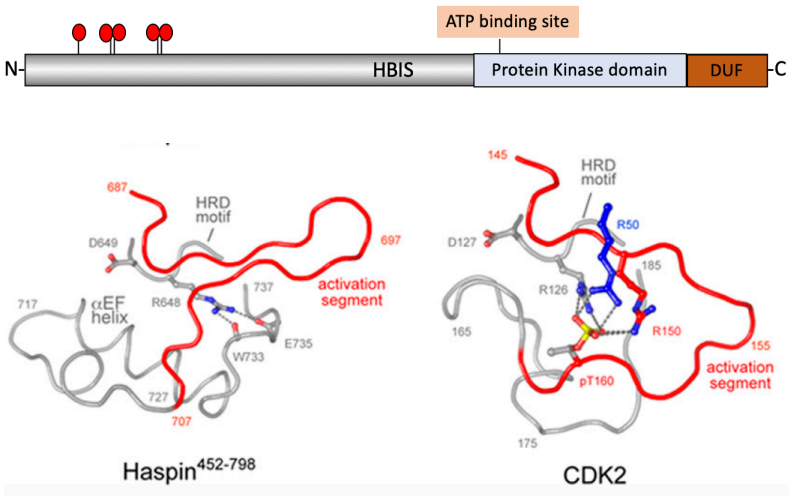

Figure 1-14: Haspin protein kinase structure. Haspin (798 amino acids, 88 kDa) is an enzyme that catalyzes the transfer of a gamma phosphate group from a donor molecule (ATP) to a serine/threonine residue on a specific protein. Top, protein domains illustration, in the N-terminus region, Haspin contains several serine/ threonine residues phosphorylation of which by CDK1, PLK1, and Aurora B are required for Haspin activation during mitosis. Haspin also can auto-phosphorylate itself for activation. Also, at the end of the N-terminus, Haspin contains a highly conversed motif that is enriched in positively charged amino acids (391-394 His-Lys-Lys-Lys), and is known as the Haspin basic inhibitory segment (HBIS) (337). The kinase domain is located in the C-terminus, and lacks the conserved ATP binding motifs (Asp-Phe-Gly and Ala-Pro-Glu of the activation segment) and contains instead another motif (Asp-Tyr-Thr). Thus, Haspin is an atypical kinase that contains a divergent sequence from the major eukaryotic protein kinases. Haspin also contains a domain of unknown function (DUF). Bottom, Kinase activation loop illustration, in most of eukaryotic protein kinases (e.g. CDK2 on the right) phosphorylation at the activation segment (e.g. pT160 in CDK2) is required to keep the active conformation of the kinase by interacting with the His-Arg-Asp (HRD) motif. While (on the left), the phosphorylation is not required for Haspin activation and the HRD motif forms Hydrogen bonds with other residues, including Trp-733 and Glu-735 (adapted from (*238*)).

1.4.2.3 H3T3 phosphorylation

Haspin is an important histone mark writer in mitosis, during which it phosphorylates H3T3 (*240*). The level of H3pT3 signal robustly increases in mitosis, starting from prophase until anaphase (*240*). The signal appears along the

chromosome, including the arm and the centromere in prophase (*240*). During mitotic progression, H3pT3 arm signal decreases in prometaphase and the most predominant and intense signal begins to concentrate at the centromere region (*240*). This occurs due to the loss of cohesion at the chromosome arm due to PLK1-dependent phosphorylation of cohesin subunit SA1/2 (*50*) (see previous sections). Thus, Haspin relocalizes and concentrates at the centromere upon cohesin dissociation from chromosome arms. At the centromere, Haspin is also mainly recruited by a direct interaction with the cohesin as has been demonstrated in yeast and human cells (*223*), persisting until anaphase, during which separase degrades the cohesin complex (*90*). However, a study in egg extracts of *Xenopus laevis* has revealed an additional mechanism for Haspin centromere recruitment (*251*). Accordingly, the SUMO-E3 ligase PIASy catalyzes TOP2A C-terminal domain SUMOylation at lysine 660, which promotes Haspin interaction and centromeric recruitment during mitosis. Nevertheless, it is important to mention that this mechanism has not been validated in human cells.

1.4.2.4 Haspin activation

Outside of mitosis, Haspin kinase domain remains in a partially active conformation and the catalytic function exists, but at a very low efficiency (*252*). Remarkably, Haspin possess an autoinhibition mechanism that is abolished by sequential phosphorylation events upon mitotic entry. Haspin contains within its structure an evolutionary conversed inhibitory segment called HBIS at the end of the N-terminal region, also located right next to the kinase domain (*252*) (Figure 1-15 and 1-16). The HBIS segment contains four positively charged amino acids, suggesting capacity to form an electrostatic interaction with the negatively charged amino acids in the kinase domain (*252*). This mechanism has been validated in vitro by kinase assay. Accordingly, incubating Haspin with a peptide containing HBIS in presence of ATP and GST-H3 N-terminal tail (1-45) leads to a significant decrease in Haspin activity compared to the control (*252*). Moreover, it was found that the presence of the HBIS increased Michaelis-Menten constant (km) of H3pT3, indicating initially low affinity toward H3T3 site. Moreover, deleting HBIS

residues reinstates the activity of Haspin outside of mitosis in vivo in human cell and *Xenopus laevis*.

Two studies (one by Funabiki team (*252*) and another by Higgins team (*253*)) revealed the activation mode of Haspin during mitosis. The activation relies on the phosphorylation of the Haspin N-terminus by several mitotic kinases, including CDK1, PLK1, Aurora B, and Haspin itself (auto-phosphorylation) (Figure 1-15). The event is triggered by CDK1 at the G2/M transition, during which it phosphorylates the Polo-binding box at specific residues in Haspin N-terminus (T128 in human and T206 in Xenopus). This promotes PLK1 interaction with Haspin N-terminal domain to prime more phosphorylation events on several residues upon the mitotic entry. These PLK1-dependent phosphorylation events induce Haspin conformational changes by forming interactions with the HBIS to neutralize its inhibitory effect. During mitotic progression, Aurora B and presumably Haspin itself catalyze additional phosphorylation events to keep the active conformation (Figure 1-15).

By monitoring H3pT3 in human cell, differential effects of losing the haspin phosphorylation sites were observed. For instance, depleting the endogens Haspin by RNAi and expressing exogenous Haspin mutants (T128A, or mutating PLK1 target sites to alanine) did not lead to a complete loss of H3pT3 in mitotic human cells. Moreover, it was found that treating RPE1 cells by BI2536 or GSK461364A (PLK1 inhibitors) leads to a complete loss of H3pT3 in prophase, but not in prometaphase and Aurora B inhibition (by Hesperadin or ZM447439) causes the opposite effects. This thus indicates the stepwise and sequential activation of Haspin during mitosis.

1.4.2.5 CPC recruitment

CPC recruitment at the centromere region is also one of the major functions of Haspin kinase activity during mitosis (*254*). The CPC is a protein complex that through Aurora B kinase subunit plays several functions as extensively described in the previous section on the mitotic checkpoint signaling. This includes SAC

protein recruitment and regulation of the error correction pathway of microtubule-kinetochore attachment. Here, the discussion in this section will be restricted to Aurora B recruitment as part of the CPC. Also, in another section Aurora B histone marks will be discussed to illustrate the regulation of recruitment of this kinase during mitosis.

CPC components are composed of two parts: structural (Survivin, Borealin (also called Dasra), and INCENP) responsible for centromere localization of the complex and another catalytic (Aurora B) subunit responsible for its downstream signaling (*234*) (Figure 1-15). Targeting the components of CPC to the different locations on the chromosome is important during mitotic progression. Importantly, the centromere region is the most distinctive dynamic area that is regulated by multiple activities of Aurora B kinase activity during chromosome segregation. Haspin through priming H3pT3 mark in the chromatin creates an anchoring site for the CPC component (*234, 254*). Indeed, H3pT3 functions as a direct centromeric adaptor for Survivin, which interacts with this mark through its BIR domain in the N-terminus (*255, 256*). Through studying the crystal structure of human Survivin in complex with H3pT3 peptide (ARpTK), particular residues in the Survivin BIR domain include K62, E65, and H80 were identified to be the responsible amino acids for the interaction (*256*). Moreover, the importance of these residues has been validated in vivo; mutating them into alanine causes an impaired Aurora B localization at the centromere in HeLa cell.

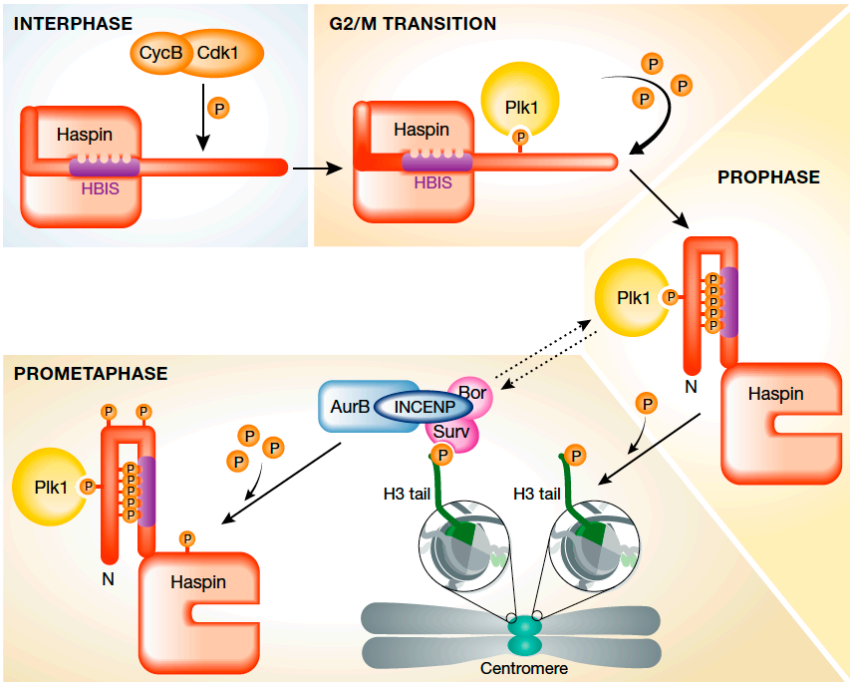

Figure 1-15: Haspin activation and chromosomal passenger complex recruitment during mitosis. Briefly, Haspin is inactive outside of mitosis due to the interaction of HBIS segment by the kinase domain. Sequential phosphorylation events occur on the Haspin N-terminus (catalyzed by CDK1, PLK1, and Aurora B) during cell cycle progression, resulting in Haspin activation in mitosis. Haspin phosphorylates H3T3 to recruit the chromosomal passenger complex (Survivin, Borealin, Inner centromere protein (INCENP), and Aurora B) (adapted from (*254*)).

By forming hydrophobic bonds and non-covalent salt bridges, Borealin and INCENP bind to the C-terminal helix of Survivin to establish a triple helical bundle (*257*). Aurora B then interacts with the highly conserved IN-BOX at the C-terminus in the INCENP (*258*). Indeed, Aurora B and INCENP can form an active complex; however, they need the other components of CPC for targeting to the centromere (*180, 259*). In agreement with this, a common phenotype associated with inhibiting Haspin by 5-IT (*246, 260*), microinjection of H3pT3 antibody (*261*), or Haspin RNAi (*261*) is reduced Aurora B signal under the IF microscope. This in turn also negatively affects Aurora B functions, including MCAK and BubR1 targeting to the centromere, the error correction pathway, and SAC activation (*246, 260*).

By monitoring U2OS cells by live imaging to examine the timing of mitosis, 5-IT treatment was found to accelerate mitotic exit due to poor SAC maintenance (*246, 260*). This occurred even in the presence of nocodazole. Restoring normal centromere function after 5-IT treatment can occur by forcing Aurora B targeting to the centromere (*246, 260*). Indeed, transfecting INCENP that is fused with CENP-B (centromere protein) can counteract H3pT3 loss (*246, 260*). Therefore, Haspin-dependent H3pT3 mark through Aurora B is important for proper chromosome alignment and healthy mitotic checkpoint signaling.

1.4.2.6 CPC-Sgo1 network

Efficient kinetochore functions rely on establishing sufficient and effective recruitment of CPC-Sgo1 complexes, which cooperate and feedback to each other (*68, 234*) (Figure 1-16). The key is the earlier targeting of CPC by H3me2/3K9 to the centromere. This allows Aurora B to reach its substrates that include KMN network in order to recruit Bub1 at the outer kinetochore (*262-264*). Bub1 by phosphorylating H2AT120 recruits Sgo1-PP2A-B56 (*223*). PP2A, by contracting PLK1-dependent removal of cohesion induces Haspin recruitment to the centromere region through the cohesin subunits (*223, 249*). Thereafter, Haspin through H3pT3 keeps CPC at the centromere during the mitotic progression (*234*). The CPC is also physically interacting with Sgo1 through Borealin, occurring after phosphorylating the latter by CDK1 (*265*). Moreover, CPC protects the network by phosphorylating Repo-Man at S893, resulting in its disassociation from the chromatin (*266*). This hinders Repo-Man-PP1 complex from reaching and dephosphorylating H3pT3 to terminate the network recruitment. Indeed, inhibiting Aurora B, Bub1, or Haspin in human cells by chemical drugs such as ZM447439, BAY-320, or 5-IT respectively, affects CPC-Sgo1 network as whole (*221, 252, 266*).

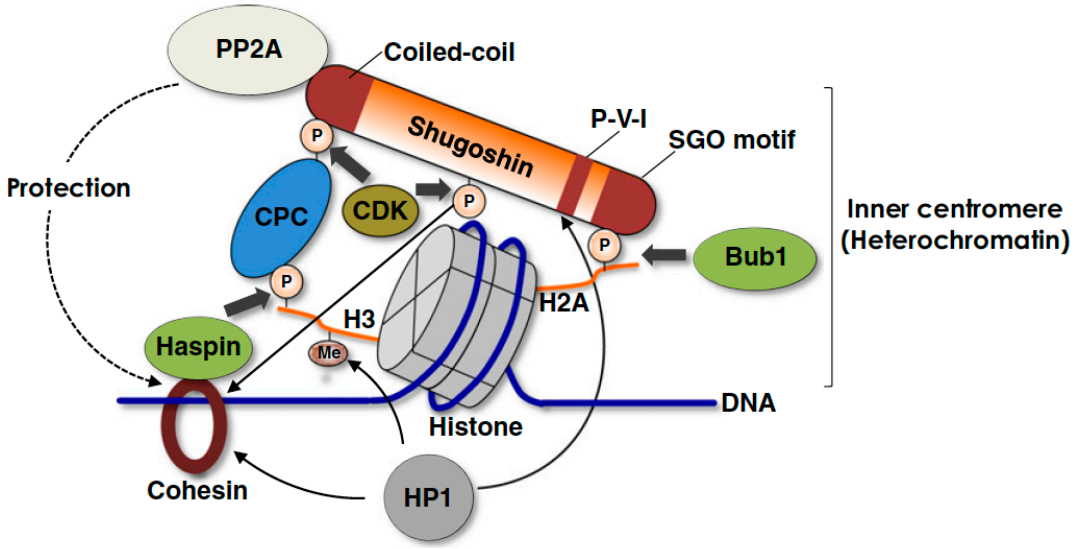

Figure 1-16: Summary of CPC-Sgo-1 network. In brief, Bub1 phosphorylates H2AT120 to recruit Sgo-1, which in turns recruit PP2A to protect the cohesion. Haspin phosphorylates H3T3 to recruit the CPC that functions through Aurora B (adapted from (*68*)).

1.4.2.7 Histone modification by Aurora B

Aurora B catalyzes phosphorylation of the H3 N-terminus, including H3S10 and H3S28 (*209*). It also phosphorylates CENP-A S7; CENP-A being a specific variant of H3 at the centromere (*209*). H3S10 phosphorylation is an important countermark against the H3 di or trimethylation at Lys-9 (H3me2K9 or H3me3K9) reader Heterochromatin protein-1 (HP-1) during G2/M transition as well as during early mitosis (*264*). On other hand, understanding H3pS10 and H3me2/3K9 marks mitotic regulation can provide better insight on the regulation or the crosstalk between mitotic histone modifications. HP-1 indeed can recruit CPC components, including Borealin, (INCENP), and Aurora B, forming an active complex on the chromosome arm and the centromere. In agreement, Aurora B activity appears early in late G2 (*262, 264*). However, Aurora B phosphorylation of H3S10 antagonizes HP-1 recruitment and promotes its displacement from the chromatin (*264*). This allows CPC localization and recruitment at the centromere by H3pT3, which requires Survivin as indicated above. Remarkably, H3pS10 signal appears before H3pT3 and mainly functions to provide feedback regulation for proper CPC

recruitment. Most importantly, treating cells with ZM447439 (Aurora B inhibitor) leads to a decrease in both H3pS10 and H3pT3 signal at the centromere, and also causes INCENP re-localization on the chromosome arm (*263*).

1.5 Hypothesis and aims

1.5.1 Hypothesis

Haspin's best-known and most extensively studied substrate is H3T3, which has been validated by in vitro kinase assay and also in vivo by phospho-specific antibodies. Additionally, Haspin was found to catalyze phosphorylation of WAPL at T8 in the N-terminus. Comparably, Haspin recruits Aurora B, which has several substrates in the chromatin; however, Haspin itself has only one known target site in the chromatin. Thus, it is still important to characterize other substrates for Haspin in the centromere. This, on the one hand, will improve our understanding of Haspin kinase activity on the chromatin and, on the other hand, it may reveal a novel mechanism that prevents chromosome instability and protects genome integrity during mitosis.

Identifying a novel candidate substrate in the histones was based on the previous studies on Haspin kinase (*267*). The most preferred recognition motif (consensus) for Haspin kinase activity has been identified in a large-scale proteomic study. This was accomplished by preforming a Haspin kinase assay on peptide library, in which a fixed serine or threonine residue served as a phosphoacceptor. A short consensus sequence (A/V-R-**T**/**S**-K-(X; any amino acid except D/E)) was identified and matched the amino acids around H3T3.

Based on Haspin consensus motif, are there other sites on histones? Interestingly, this consensus sequence matches with H2B N-terminus and C-terminus; two sites have been identified T19 and T119. These sites are equal to T20 and T120 when counting the first methionine in the protein sequence of H2B. A notable exception is the presence of a positively charged amino acid (R) prior to the targeted S/T. Strikingly, sequence around H2BT119 in the C-terminus shows

an interesting homology with the sequence around T3 in the N-terminus of H3. This suggests that H2BT119 may be a candidate Haspin substrate.

1.5.2 Aims

The goal of this research project is to determine whether T119 of Histone H2B is a Haspin substrate. Thus, set of aims were designed to answer two main questions:

Q1: Can Haspin phosphorylate this site?

Q2: Does H2BpT119 signal exist in vivo and is it linked to mitosis?

To answer these questions, a number of aims were envisioned:

Aim-1: In vitro validation of H2BT119 phosphorylation by Haspin.

Aim-2: In vivo analysis of H2BT119 phosphorylation during mitosis.

Aim-3: Validation of the specificity of the H2BpT119 signal detected in vivo.

Chapter 2

2 Material and method

This chapter is dedicated to describing the materials and the methods that were used for performing the experiments of the presented thesis. Combinations of cellular and molecular biology, proteomics and biochemistry-based approaches were used to investigate Haspin-dependent phosphorylation of H2BT119. In particular, the experiments were created to study H2BT119 phosphorylation in vitro and in vivo during mitosis and to determine Haspin involvement in catalyzing the phosphorylation.

To conduct the first aim, PCR-based mutagenesis reactions were performed to generate mutation in the histone and the GST-Haspin plasmids to produce protein version that can be used as negative control. Recombinant histones and GST-Haspin WT and mutants were produced in competent bacteria and purified by chromatography-based approaches. The purified proteins were then used to perform the in vitro kinase assays. To investigate H2BT119 phosphorylation signal in vivo during mitosis as proposed in the second aim, a polyclonal phospho-specific antibody against H2BpT119 was produced in rabbit and purified by affinity chromatography. This antibody was used to detect the H2BT119 phosphorylation signal in vivo by Western blotting and IF microscopy in HeLa and RPE1 cells. Moreover, additional experiments were designed to circumvent certain issues, including phospho-H2B upshift and the anti-H2BpT119 cross-reactivity with H3pT3. Therefore, the third aim was based on performing experiments to validate H2BT119 phosphorylation signal in vivo. To do so, PCR cloning was used to generate tagged-H2B plasmids for transient expression or generating stable cell lines. Finally, histone purification-coupled with mass spectrometry was used as an independent approach.

2.1 Single site mutagenesis

Primers for mutagenesis were designed according to a particular strategy explained in a previous published protocol, with some modifications (*268*). Each primer pair consisted of two sequences that were non-overlapping at 3' end and complementary at the 5' end. The size of the two regions were designed to make the melting temperature of the complementary sequence 5 to 10°C lower than the non-overlapping sequence. The desired mutation was placed generally in the complementary sequence (Table 2-1).

PCR were performed with Phusion High-Fidelity DNA Polymerase (BioLabs, New England). Reaction contained 1x Phusion HF Buffer, 0.2 mM dNTPs, 0.5 µM primers (for each forward and reverse) (IDT Technologies, United States), ~100 ng Plasmid DNA, 1 unit Phusion DNA Polymerase, and Nuclease-Free Water. Cycling instruction were 1 cycle for initial denaturation at 98°C for 30 sec, 25 cycles for denaturation at 98°C for 5 sec, annealing at 72°C for 30 sec, and extension at 72°C for 15 sec/kb. Final extension at 72°C for 5 min for 1 cycle and parental DNA was degraded by adding Dpn-I for 1 h at 37°C. Mutagenesis was confirmed by DNA sequencing at Plateforme de Séquençage et de Génotypage des Génomes of the CHU de Quebec Research Center, Quebec, Canada.

2.2 Recombinant GST-Haspin production and purification

pGEX-6P-3 plasmid (from Andrea Musacchio) containing GST-Haspin kinase domain was transformed into BL21(DE3) competent bacteria and plated on an ampicillin LB agar for selection. A single colony was picked and cultured in 5 ml of LB-treated ampicillin overnight (ON) at 37°C in an orbital shaker (12620-948 VWR, United States). The pre-culture bacteria were transferred to 200 ml of LB-ampicillin and incubated at 37°C in the orbital shaker until optical density (OD) values at 595 nm of 0.7-0.9 were reached. Protein production was induced by 0.5 mM IPTG treatment (MP Biomedical) and culturing at 30°C in the orbital shaker for 4 h. The cultured bacteria were collected and centrifuged at 7700 x g for 10 min at 4°C, then the pellet was washed once with 1x PBS and snap frozen and stored at -

80°C. The pellet was suspended in the lysis buffer (20 mM Hepes pH 7.5, 120 mM NaCl, 10% Glycerol, 2 mM EDTA, 10 mM NaF, 20 mM β-Glycerophosphate, 0.1 mM Na-Vanadate, 10 mM Na-pyrophosphate, 1 µg/ml Leupeptin, 1 µg/ml Aprotinin, and 1 mM AEBSF).

The lysate was sonicated (3 rounds each 30 secs at 10% amplitude with 0.5 sec ON/OFF pulse and pausing 1 min on ice). After sonication, 0.5% NP40 was added to the lysate, which then was incubated on ice for 30 min. Lysate was centrifuged at 13000 rpm at 4°C for 10 min. Glutathione-Sepharose beads were washed twice by the lysis buffer and incubated with the cleared lysate ON at 4°C with rotation. Beads were washed once with lysis buffer, twice with lysis buffer containing 180 mM NaCl, and once with 1x TBS buffer. GST-Haspin was eluted by 50 mM glutathione (pH 8) in 1x TBS buffer ON at 4°C with rotation. The eluate was dialyzed into 1x TBS buffer ON at 4°C with stirring and 10% glycerol was added to the final product.

2.3 Recombinant histones production and purification

pET15b-Histone plasmids (from Amélie Fradet-Turcotte) was transformed and cultured as described above. Protein production was induced at 0.6 OD by 0.4 mM IPTG treatment (MP Biomedical) and culturing at 37°C and shaking at 250 rpm for 3 h. The pellet was collected and resuspended in the wash buffer (50 mM Tris pH 7.5, 100 mM NaCl, 1 mM ETDA, 1 mM benzamidine, and 5 mM β-mercaptoethanol (βME)), then snap frozen in liquid N_2 and stored at -80°C. Inclusion bodies were prepared by thawing the pellet in warm water and refreezing in liquid N_2 for one round.

Cell wall lysis was catalyzed by adding 1 mg/ml lysozyme and nutating (swaying) for 30 min at 4°C. Lysates were sonicated as described above and the pellet was collected by centrifugation at 12 000 x g for 20 min at 4°C. Pellets were resuspended in wash buffer containing 1% Triton-X100 and washed once. Pellets were resuspended in the wash buffer without Triton-X100 and washed once. Pellet

was dissolved in 260 µl DMSO for 30 min at RT and minced with spatula. Inclusion bodies unfolding were performed by incubating the pellets with the unfolding buffer (7 M Guanidine-HCl, 20 mM Tris-HCl pH 7.5, and 5 mM DTT) and rotating at RT for 1 h. Supernatants were collected by centrifugation at 23 000 x g for 10 min at 20°C. Pellets were rinsed again with the unfolding buffer and centrifuged to collect the supernatant. The supernatants were combined and dialyzed in Urea dialysis buffer (7 M Urea, 1 mM EDTA, 10 mM Tris-HCL pH 8, 100 mM NaCl, and 5 mM βME) for 3 h and ON at 4°C.

HiTrap SP HP column was equilibrated with water and wash buffer (7 M Urea, and 20 mM Tris-HCl pH 8) at 2 ml/min rate in peristaltic pump. Supernatants were loaded on the column at 1.5 ml/min and washed with wash buffer. The column was attached to FPLC (Bio-Rad) and elution was performed with the elution buffer (7 M Urea, 20 mM Tris-HCl pH 8, and 1 M NaCl) with a linear gradient (25 column volume) from 0-100%. Eluted histone peaks were confirmed on SDS-PAGE with Coomassie blue staining. Fractions containing histone was combined and dialyzed into water with 2 mM βME, then aliquoted and stored at -80°C.

2.4 Kinase assay

Kinase assays were performed by incubating 0.5 µg purified GST-Haspin with 0.5 µg purified recombinant histone in the master mix reaction buffer (50 mM Tris-HCl pH 7.6, 10 mM MgCl2, 150 mM NaCl, 1 mM EDTA, 1 mM DTT, and 250 µM ATP). The radioactivity-based assay was supplemented with 5 µCi [^{32}P]ATP. The reaction was incubated for 30 min or 1 h with agitation at 30°C. Adding SDS-PAGE loading buffer and heating at 95°C for 5 min was used to stop the reaction. The samples were subjected to Western blotting when non-radioactive ATP was used or subjected to SDS-PAGE in case radiolabeled ATP was used. Here, gels were stained by Coomassie blue and dried on Whatman paper and visualized by autoradiography.

For Kinase assay on peptide arrays, membranes with the indicated peptides covalently bound were wet with ethanol and rehydrated with the master mix reaction buffer for 1h. The membrane was blocked by 0.5 mg/ml BSA in the reaction buffer with no ATP ON at RT. Kinase reaction with performed by incubating the membrane with 10 nM GST-Haspin in the reaction buffer containing BSA 0.2 mg/ml and 50 µCi [^{32}P]ATP for 3 h with shaking at 30°C. Membranes were washed 10 times each for 15 min with 1 M NaCl, 3 times each 5 min with water, 3 times each 15 min with 5% H_3PO_4, 3 times each 5 min with water, and finally 2 times each 2 min with ethanol. Signals were visualized by autoradiography in the case of radiolabeled ATP or by Western blotting with the appropriate antibodies in case of non-radiolabeled ATP.

2.5 Plasmid cloning

Plasmids containing 3xFlag-2xStrep-H2B were prepared as follow (performed by Chantal Grand and Alexandra Cote, Research center CHUL, CHUQ, Quebec). PCR amplification (Table 2-1) of AAVS1 Puro FS v2 plasmid (plasmid given by Yannick Doyon) containing 3xFlag-2xStrep was performed with Phusion High-Fidelity DNA Polymerase (BioLabs, New England). Reaction contains 1x Phusion HF Buffer, 0.2 mM dNTPs, 0.5 µM primers (forward and reverse) (IDT Technologies), 2 units Phusion DNA Polymerase, 10 ng DNA plasmid, and 15 µl mQ H_2O. Cycling was done as follows: 1 cycle for initial denaturation at 98°C for 1 min, 35 cycles for denaturation at 98°C for 20 sec, annealing at 64°C for 30 sec, extension at 72°C for 1 min. Final extension at 72°C for 10 min for 1 cycle. PCR product was run on 2% agarose gel in 1x TAE buffer at 100-120 volt for 15 min. The gel was visualized by UV light and the plasmid band was cut by using a clean scalpel. The DNA was purified by from the agarose gel by EZ-10 Spin column DNA gel extraction kit. The AAVS1 and pCDNA 3-1 H2B-mCherry (WT and T119A) plasmids were digested by using BamHI and XbaI. PCR reactions generally contain 1x CutSmart buffer (NEB), 3 µg DNA plasmid, 30 units BamHI (NEB), 30 units XbaI, and mQ H_2O autoclaved to complete volume up to 30 µl. Plasmids were digested for 1 h at 37 ° C in the thermal cycler. Digests were run on 1% agarose

gel and the bands of interest were purified as described above. Ligation was done as follow: 7 µl of insert (3xFlag-2xStrep) at the C-terminus of H2B, 1 µl of vector (pCDNA 3-1-H2B), 1 µl T4 ligation buffer, and 1 µl T4 DNA ligase, then incubation ON at 16°C.

Single Flag-H2B plasmid was prepared as follow. Flag sequence was inserted into pcDNA4 TO Puro plasmid and amplified (Table 2-1) by PCR reaction that was performed as described above. The PCR product was run on agarose gel and purified as described above. AAVS1 Puro FS v2 plasmid (3xFlag-2xStrep-H2B) (insert) and pcDNA4 TO Puro plasmid (vector) were digested by KpnI (NEB) and ApaI (NEB) for 1 h at 37°C and 25°C, respectively. The products were run on gel and purified for the ligation. The ligation of 27.33 ng insert (H2B) and 50 ng vector (pcDNA4 TO Puro 1xFlag- at the N-terminus of H2B) was performed as described above.

Table 2-1: Primers and plasmids used for the project.

Parental plasmid	Protein/Tag	Mutagenesis/ Amplification	Oligo's
pET15b	6xHis-hH2B	T119A	F:5'AGGCTGTCGCCAAGTATACAAGCTGAGGATCCG'3 R:5'ACTTGGCGACAGCCTTGGTACCTTCGGACACTG'3
pET15b	Xenopus H3	T3A	F:5'CCGTGCCAAGCAGACCGCCCGTAAATCCACCGG'3 R:5'GGTCTGCTTGGCACGGGCCATGGTATATCTCCTTCTTAAAGTTAA'3
pCDNA 3-1	H2B-mCherry	T119A	F: 5'GCAGTTGCCAAGTACACTAGCTCTAAGGATCCACCG'3 R: 5'AGTGTACTTGGCAACTGCCTTAGTGCCCTCGGACA'3
AAVS1 Puro	3xFlag-2xStrep	Amplification	F:5'TATTTATGCAGAGGCCGAGG'3 R:5'CCTCGGCCTCTGCATAAATA'3
pcDNA4 TO Puro	1xFlag	Amplification	F:5'gacgaGGTACCATGgactacaaagacgatgacg acaagGCACCTGAACCCTCTAAGTCTG'3 R:5'GTTaccAAGTACACTAGCTCTAAGTAGGGGCCCggaag3'

2.6 Cell culture and transfection

Cell lines (from the laboratory Sabine Elowe, CHUL Research center, CHUQc-UL, Quebec) were grown in DMEM/high glucose media (Hyclone) supplemented with 10% bovine growth serum (BGS) (GE Life Sciences/PAA Laboratories) and 1% penicillin/streptomycin (Hyclone) at 37°C with 5% CO_2. The culture media of the HeLa TREx cells was supplemented with 10 µg/µl blasticidin (GIBCO, life technologies). The culture media of the HeLa S3 cells that stably expresses Flag-H2B was supplemented with 2 µg/µl puromycin. Cell cycle arrest at interphase (G1/early S) was done by adding 2 mM thymidine (Acros Organics) for 16 h to 60-70% confluent cells. Treatment of 60-70% confluent cells with 330 nM nocodazole (Sigma) for 16 h was generally used to induce mitotic arrest.

Drug treatments were done as follows, MG132 (Calbiochem, United States) was used at 2 µM for 2 h. Okadaic acid (Santa Cruz Biotechnology), which is an inhibitor of PP1 and PP2a/b phosphatases, was used at 500 nM for 60 min and 5-Iodotubercidin (5-IT) was used at 10 µM for 90 min, unless otherwise mentioned. Transient plasmid transfection was carried out with TrasnIT-LT1 (Mirus) reagent following the manufacturer's manual. Briefly, pcDNA3.1 plasmid containing tagged H2B was added to a pre-warmed opti-MEM I reduced-serum medium. Then, Trans IT-LT1 reagent was added, mixed well, and incubated for 20 min at room temperature (RT). The mixture was added to the cell drop-wise to different areas of the cultured cells at confluence $\geq$ 80% and incubated for 48 h.

2.7 Cell lysis

To collect attached cell (arrested at interphase), the media was removed, and the cells were washed two times by 1 x PBS, then cells were harvested by a scraper in 1 x PBS. Mitotic cells were harvested by shake-off, the media was removed, and the cells were gently washed by 1 x PBS, then cells were harvested by a mechanical agitating in 1 x PBS. Harvested cells were centrifuged at 360 x g for 10 min at 4°C to collect the pellets. Cells were lysed by using histone purification mini kit (Active Motif, catalog No. 40026) (*269*), acid-solubility based

extraction (*270*), according to the manufacturer's manual with some modifications. To obtain a highly enriched extract, 1 volume collected pellets was incubated with 5 volumes lysis buffer in presence of phosphatase and protease inhibitor cocktail (5 mM NaF, 20 mM β-glycerophosphate, 0.1 mM Sodium vanadate, 10 mM Na-pyrophosphate, 1 µg Leupeptin, 1 µg Aprotinin, and 1 mM AEBSF (PEFABLOC). Cell lysis was carried out at 4°C with rotation for 30 min, or to reach an efficient histone extraction for 3 h. Then, the lysates were centrifuge at maximum speed for 10 min at 4°C. The supernatants were kept and neutralized to pH 8 with the 5x neutralization buffer. Protein concentration in the total cell lysate (TCL) was quantified by BCA protein assay kit (Fisher, United States) according to the manufacturer's manual or Bradford assay (Bio-Rad).

2.8 Antibody purification

Phosphopeptide covering T119 in H2B C-terminus tail was covalently conjugated to Keyhole limpet haemocyanin (KLH), which is a protein carrier to induce the immunization in the rabbit. After injection of this conjugated complex in the rabbit the serum was collected to purify the antibody. Polyclonal H2BpT119 antibody was purified by Protein A-Sepharose to obtain the pool of IgG and peptide affinity to obtain the final purified pool. To do so, 10 ml of serum containing H2BpT119 antibodies was centrifuged at 2580 x g for 20 min at 4°C. Resin was prepared by taking washing 5 ml of 50% Protein A-Sepharose slurry in 5 ml of 1x PBS, which was then centrifuged at 10322 x g for 3 min to remove the washing PBS. The serum was incubated with the pre-washed Protein A-Sepharose resin for 1 h with rotation at 4°C. The antibody-coupled resin was packed in disposable plastic chromatography column and follow-through was collected for further analysis. The packed resin was washed with 1x PBS (up to 50 ml) and then with 15 ml of 1 x PBS containing 1 M NaCl. Elution was performed with 0.2 M Glycine buffer pH 2.8 (up to 10 ml) and 1 ml fractions were collected with eppendorfs containing 0.2 ml of 1 M Tris-HCl buffer pH 8 for neutralization. Fractions at 20 µl were run on SDS-PAGE to check the purification process. Ten IgG containing fractions were pooled together and dialyzed in 1 x PBS buffer ON at 4°C.

Peptide affinity purification was done by SulfoLink coupling resin and sulfhydryl-containing phosphopeptide of H2B C-terminus covering T119, precisely the same version that was used for the immunization and the production. The SulfoLink resin contains iodoacetyl group, which reacts with the free sulfhydryl of the peptide. To generate available sulfhydryl groups for coupling with the resin, 2 mg of phosphopeptide was dissolved in 12 ml total volume of coupling buffer (50 mM Tris-HCl pH 8.5, 5 mM EDTA). Then, 10 µl of the suspended peptide was taken to measure the coupling efficiency (T0). Then, 25 mM TCEP (reducing agent) was added to the suspended peptide and combined with 2 ml of 50% slurry SulfoLink coupling resin. The mixture was rotated for 15 min at RT and then incubated for 30 min at RT. To measure the coupling efficiency another 10 µl was taken (T1).

Ellman's Reagent was used to validate the coupling efficiency by 20 µl to each 10 µl aliquot (T0 and T1). Additionally, 400 µl of 1x PBS was added and the mixture was incubated for 15 min at RT. Before measuring, another 600 µl of 1x PBS was added and the absorbance was taken at 412 nm. The phosphopeptide-coupled SulfoLink resin was washed twice with coupling buffer (3 beds volumes/wash). Resin was incubated with 1 ml of coupling buffer containing 50 mM L-cysteine with rotation for 15 min, and the beads were then allowed to rest at RT for 30 min. The resin was washed twice with 1 M NaCl and once with 1x PBS buffer (6 beds volumes/wash). The pool of IgG from Protein A-Sepharose step was incubated with the phosphopeptide-coupled SulfoLink resin for 1 h with rotation at RT. The resin was packed in a disposable plastic chromatography column and washed with 12 ml of sample buffer (0.1 mM sodium phosphate buffer pH 6, 5 mM EDTA). Elution was performed with 0.2 mM Glycine buffer pH 2.5 and collection was at 0.5 ml (up to 5 ml) into 50 µl 1 M Tris-HCL pH 7.5. The fractions were run on SDS-PAGE to verify the fractions-containing antibody. The fractions were then pooled and dialyzed in 1x PBS buffer and 0.05% sodium azide was added.

2.9 Western blotting and immunoprecipitation

An equal protein concertation of 15 µg or total cell lysate (TCL) volume of 40 µl was used for Western blotting and the loading also was monitored by Ponceau red staining. Protein samples and protein ladder (Bio-Rad, United States or FroggaBio, Canada) were separated by 15% SDS-PAGE gel that is carried out with Bio-Rad Mini-PROTEAN II electrophoresis system and transferred to 0.45 µm Polyvinylidene difluoride (PVDF) membrane (Millipore) by semi-dry transfer system (Bio-Rad). PVDF membrane was blocked by 5% non-fat milk for at RT 1 h, then the membrane was incubated with the primary antibody ON at 4°C with shaking with the following concentration: anti-H2BpT119 (1 µg/ml), anti-Flag (1/1000, Sigma, Germany), anti-H3pT3 (1/2000, GeneTex, United States), anti-H2B (1/1000, GeneTex, United States). The membrane was then washed with 1 x TBS-0.05% Tween generally three times each with 10 min incubation. A horseradish peroxidase-coupled secondary antibody (Jackson ImmunoResearch, United States) was used at 1/5000 for 1 h. After washing with PBS-T three times, signals were revealed by the enhanced chemiluminescence (ECL) solution (0.1 M Tris pH 8.5, 0.2 mM coumaric acid, 1.25 mM luminol, and 3% H_2O_2) and chemidoc imaging system (Bio-Rad). Membrane stripping was performed according to the harsh stripping procedure (Abcam, United Kingdom).

H2B tagged with 3xFlag-2xStrep was immunoprecipitated by using Strep-Tactin Sepharose resin (IBA, Belgium). Strep-Tactin 50% slurry beads were washed three times with 20 mM Hepes pH 7.9 washing buffer supplemented with 10% glycerol, 150 mM KCl, 0.1% Tween 20, and 1 mM DTT. Beads were spun at low speed (8000 x g for 3 min at 4°C) to remove the washing buffer. Equal amounts of protein or TCL volume was diluted by adding an equal volume of beads washing buffer. The diluted sample was then incubated with the beads ON with rotation at 4°C. Thereafter, the beads were spun down to remove lysates and washed three times with the washing buffer. Prior proceeding to Western blot, the interacting proteins were separated by SDS-PAGE loading buffer and heating at 95°C for 5 min. H2B tagged with single Flag IP was performed in a similar way to

the Strep-Tactin IP, but with the following washing buffer (0.1 M Hepes pH 7.5, 10% glycerol, 1.5 mM EDTA, and 150 mM KCl) and anti-Flag M2 magnetic beads (Sigma).

2.10 Histone purification and fractionation

The cells were lysed and neutralized as described above before proceeding to purification steps (active motive kit (*271*), catalog No. 40025, United States) (*270, 272*). Briefly, the spin column was equilibrated with the equilibration buffer provided with the kit. The sample was added to the column and spun at 50 x g for 3 min at 4°C and flowthrough was removed. Histones were eluted three times to collect all chromatin extract and fractions were monitored by Coomassie blue staining on 17% SDS-PAGE gel. Eluates were treated with 4% perchloric acid (Fisher) overnight at 4°C to precipitate the histones. The precipitates were spun out at maximum speed at 4°C for 1 h. Histone pellets were washed twice with ice-cold acetone (Fisher) and spun out at maximum speed for 15 min at 4°C. The pellets were then air dried at RT for 10-20 min.

Histones were then re-suspended in HPLC-grade water (Fisher) containing 0.4 M urea (Sigma). Protein concentration was quantified by measuring the absorbance by nanodrop at 230 nm, considering the 0.42 OD of 1/10 diluted core histones indicates 1 mg/ml. Histone fractionation was performed by histone purification kit (active motif). Briefly, 1.5 ml of slurry purification resin was loaded and packed in the column. Thereafter, resin was washed first with sterilized distilled water and second with the equilibration buffer and spun at 50 x g for 3 min at 4°C. Histones were extracted as mentioned above, gradually loaded on the column and eluted with H2A/H2B buffer, then with H3/H4 buffer. Purity of the histone fraction was monitored by Coomassie blue staining on 17% SDS-PAGE gel.

2.11 Immunofluorescence and chromosome spreading

Cells were cultured on coverslips and arrested at mitosis as described previously. For cell fixation, media was removed, and cells were washed once with 1x PBS and fixed with PTEMF buffer (20 mM pipes pH 6.8, 0.2% Triton X-100, 1 mM MgCl2, 10 mM EGTA, 4% formaldehyde) for 10 min at RT. The fixative was aspirated, and cells were washed three times with 1 x PBS and blocked by 3% BSA in 1 x PBS for 30 min at RT. For immunofluorescence (IF) staining, cells were incubated with primary antibody ON at 4°C in a humidified chamber with the following dilutions in 3% BSA in 1x PBS: anti-H2BpT119 (1/1000), anti-Flag (1/500, Sigma), anti-CREST (1/1000, ImmunoVision, United States), anti-Sgo1 (1/1000), anti-CENP-C (1/1000, MBL International), and anti-Aurora B (1/500, BD Transduction Laboratories). Cells were washed three times with 1 x PBS 0.2% Triton X100 and incubated with series of Dylight secondary antibodies (1/1000, Fisher or Jackson ImmunoResearch) and Hoechst 33342 (1 µg/ml, Sigma) for 1 h. Cells were washed three time with 1 x PBS 0.2% Triton X-100 and one time with pure sterilized water, then permanently fixed on a slide with mounting media.

For mitotic spread, cells were arrested in mitosis with 5 µM S-trityl-L-cysteine (STLC) for 16 h. Before fixation, cells were washed one time with 1x PBS, then cells were swollen for 30 min at 37°C in a hypotonic buffer (10 mM Tris-HCl pH 7.4, 10 mM NaCl, 5 mM MgCl2, and 0.5 µM okadaic acid) to swell the mitotic cells. After removing the hypotonic buffer, cells were washed one time with 1x PBS and fixed by PTMEF for 10 min at RT and then washed three times with 1 x PBS. The cells blocked with 3% BSA and 0.2 M glycine for 30 min at RT. Cells were stained as described above, but with 1/100 dilution of anti-H2BpT119.

2.12 Microscopy

Immunofluorescence images were obtained by confocal microscopy on an inverted Olympus IX80 microscope equipped with an Orca Flash 4.0 camera (Hamamatsu) and a WaveFX-Borealin-SC Yokogawa spinning disc (Quorum Technologies). Image acquisitions were performed by Metamorph software

(Molecular Devices) to obtain several optical sections in an identical exposure time for each channel at each specific wavelength. The optical sections were projected into a single image using ImageJ software (http://rsb.info.nih.gov). Projected images were processed and cropped in ImageJ in an identical scale. Signals quantifications were measured by using ImageJ. The data and statistical significance were analyzed by GraphPad Prism version 6 (La Jolla, CA, USA).

2.13 Glu-C digestion

HeLa S3 cells were arrested at interphase or mitosis (-/+5-IT) and core histones were purified as described above. Digestion was performed by using 20 µg purified histones in the following digestive reaction solution: 1 µg Endoproteinase GluC sequencing-grade (Promega) that was reconstituted in 100 mM ammonium bicarbonate, 5 mM DTT, 10 mM Tris-HCl pH 7.7, and 9.4 µl HPLC-grade water. Reaction was incubated at 37°C ON with agitation and stopped by adding 0.5% formic acid and heating at 95°C for 10 minutes. Digests were dried by SpeedVac for 90 min at 35°C and reconstituted in 20 µl of 0.1% formic acid before being subjected to mass spectrometry.

2.14 Stage-tip purification

Peptide fragments of Glu-C digestions were purified on 3M Empore C18 extraction disks (Fisher) as described in (*273*) with some modifications. C18 disks was punched by a 17G flat-tipped syringe and the disks were ejected twice into pipette tip (EPTIPS BOX W/5X96TIPS 10 µL, Fisher). Purification columns were conditioned by adding 30 µL methanol and centrifuged at 1452 x g for 3 min at RT. The column was equilibrated with sample buffer (3% ACN, 1% TFA, and 0.5% acetic acid in HPLC-grad water). Peptide digests were acidified to pH ≤2.5 with sample buffer. The acidified peptide digests were loaded on the C18 columns by centrifugation at 1452 x g for 3 min at RT. The columns were washed with sample buffer and peptides were eluted from the C18 disk using the elution buffer (0.5% acetic acid, 80% ACN in HPLC-grad water). Prior to mass spectrometry injection, the samples were subjected to SpeedVac to dry down as described before.

2.15 Mass spectrometry analysis

Mass spectrometry (MS) was performed by the Proteomics platform of the CHUL (CHUQc-UL research center CHUL, Quebec). Reconstituted peptide digests were injected and separated by LC-MS/MS on an Orbitrap-Fusion mass spectrometer (Fisher). Samples were eluted on a C18 3µ Pepmap (50 cm x 75 µm separation column, Fisher) in 90 min gradients at 300 nL/min. Mass spectra were obtained by utilizing data-dependent acquisition mode and XCalibur software (Version 4.1.50, Fisher). Acquisition of full scan mass spectra (350 to 1800 m/z) were obtained in the Orbitrap with 120 000 resolutions. MS scan was performed in a top speed mode by acquiring fragmentation spectra of the most intense ions in 3 sec total cycle time.

2.16 MS database searching and analysis

Proteome Discoverer 2.2 software (Fisher) was used to create the MGF peak list files. Mascot (version 2.5.1, Matrix Science, London, UK) was used to analyze MGF sample files. Mascot analysis was set up to find contaminant and complete proteomes (92988 entries, Uniprot HomoSapiens). Assuming the digestive enzyme was Glu-C. Mascot searches was performed with 0.60 Da fragment ion mass tolerance and 10.0 PPM parent ion tolerance. In Mascot search, cysteine carbamidomethylation (CAM) was a fixed modification. While, asparagine and glutamine deamidation and methionine oxidation were variable modifications. Post-translational modification (PTM) sought included threonine, serine, and tyrosine (STY) phosphorylation and lysine (K) acetylation and ubiquitination. MS/MS based peptide, protein, and PTM identifications was validated by Scaffold Proteome Software (version_4.8.4, Inc., Portland, OR). Proteins that contained similar peptides that were not differentiated in MS/MS analysis itself were considered to satisfy the parsimony principles. For PTM search, the false discovery rate in Scaffold was set up 0% for peptide and 20% for protein.

Chapter 3

3 Results

3.1 In vitro validation of H2BT119 phosphorylation by Haspin

H2B phosphorylation by Haspin was validated by in vitro kinase assays. This has been done with different materials including peptides and recombinant proteins. To do this, GST-Haspin kinase domain (wild-type (WT)) was produced in bacteria and purified by glutathione beads as described in the material and method chapter. Another version of GST-Haspin that is mutated in a specific amino acid in the active site was produced and purified. This version is mutated at the aspartic acid 687 (D687) into alanine to generate catalytically inactive GST-Haspin (kinase-dead (KD)) that can be used as a negative control.

To validate Haspin-dependent phosphorylation of H2BT119, a Haspin kinase assay was performed with short peptides immobilized (spots) on a nitrocellulose membrane. These peptides include sequence covering T119 in H2B C-terminus (-GTKAV**T**$_{119}$KFTSS-) and alongside with another version containing the mutant (H2BT119A). Also, the membrane contains peptides covering T3 in H3 N-terminus (-AR**T**$_{3}$KQTARKST-) and the mutant (T3A). In addition to that, another peptide version covering T3 in H3 N-terminus was designed. In the latter, few amino acids (lowercase) placed before T3 (-agaAR**T**$_{3}$KQTAR-) and three residues in the H3 N-terminus were deleted (-KST-) from the designed peptide. This altered version of H3 N-terminus was made to compare Haspin specificity and the phosphorylation signal in the kinase assay. More particularly, this altered version was designed to demonstrate whether Haspin phosphorylates residues other than H3T3 and also to compare the level of the phosphorylation with the original version of H3 versus H2B.

The membrane containing these peptide spots was incubated with GST-Haspin WT in presence of radiolabeled [^{32}P]ATP. Haspin kinase assay on the

peptide array shows H2BT119 phosphorylation since the radioactivity observed on the membrane is due to the incorporation of the radiolabeled phosphate (Figure 3-1 A). In the mutant T119A spot, the signal was less than that of the wild type (WT) spot on the membrane, indicating phosphorylation of other residues than T119 (Figure 3-1 A). In comparison, incorporation of radiolabeled phosphate is significantly higher in the peptide spots of H3 N-terminus (Figure 3-1 B). Thus, Haspin most likely has a greater affinity towards H3 over H2B. Interestingly, the mutant of the original version of H3 N-terminus still was showing radioactivity signal and that completely disappeared in the second modified version (Figure 3-1 B). Haspin can phosphorylate either the serine or the threonine, which both were not included in the additional altered version of H3 peptide, but at low level. Importantly, this serine residue is equivalent of S10 in H3, which is an Aurora B target sites during mitosis (*209*). In contrast, Haspin kinase assays with recombinant histones are showing strong radioactivity signals with all the WT and the mutants of H2B (T119A) and H3 (T3A) (Figure 3-1 C). These data suggest Haspin-dependent phosphorylation of H2BT119 in vitro.

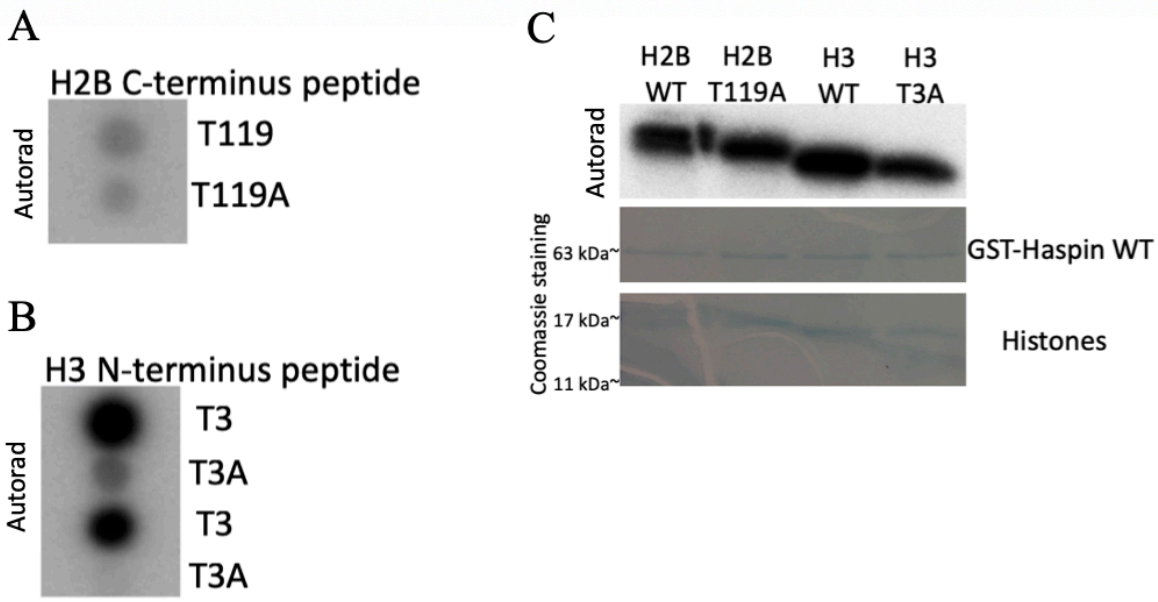

Figure 3-1: In vitro kinase assay to validate H2B phosphorylation by Haspin kinase through radioactivity-based assay. A. Synthetic peptides corresponding to the H2B C-terminus were synthesized directly on cellulose membranes, and were incubated with recombinant GST-Haspin (WT) for 3 h in the presence of radiolabeled [^{32}P]ATP. The phosphorylation was verified by incorporation of radiolabeled phosphate. **B.** Peptide spots of H3 N-terminus were treated as explained in (**A**). **C.** Recombinant H2B (WT or T119A) or H3 (WT or T3A) was incubated with recombinant GST-Haspin (WT) for 30 min in the presence of radiolabeled [^{32}P]ATP; then the reaction was terminated by adding SDS-PAGE sample buffer and boiling at 95°C. The reaction was then subjected to SDP-PAGE, and the phosphorylation was verified by incorporation of the radiolabeled phosphate. Protein loading was monitored by Coomassie blue staining. WT, Wild type; Autorad, Autoradiograph.

A rabbit polyclonal phospho-specific antibody against H2BpT119 was produced and then purified by protein A resin followed by phosphopeptide affinity chromatography. This antibody was used to confirm in a GST-Haspin kinase assay the phosphorylation of H2B at T119. The membrane containing peptide spots covering H2B C-terminus was incubated wit GST-Haspin in presence of regular ATP to validate phosphate incorporation by the phospho-specific antibody instead of the radioactivity. The antibody recognizes and interacts with pT119 on the peptide that was decreased with the mutant version (Figure 3-2 A). The results thus indicate that the anti-H2BpT119 can recognize non-specifically other phosphorylation in H2B other than T119 itself, in agreement with the presence of other phosphorylated residues detected in the kinase assay with the radiolabeled ATP-based assay.

In addition, the phospho-specific antibody against H2BpT119 recognizes phosphorylation sites in recombinant H2B following the kinase assay (Figure 3-2 B). The WT H2B shows upshift in the membrane after Haspin-dependent phosphorylation. Although the antibody recognizes and interacts with phospho-site in the mutant H2BT119A, the upshift was not observed (Figure 3-2 B). In the negative control conditions, in which a KD GST-Haspin was used, no signal was observed with the H2BpT119 antibody (Figure 3-2 B). This therefore indicates that the H2BpT119 antibody only recognizes and interacts with phospho-sites, but not with non-phosphorylated H2B.

This antibody was also used to validate H2BT119 phosphorylation in vivo during mitosis. Since there is significant homology between the H2B C-terminus and H3 N-terminus around the targeted residues of interest (T119 and T3, respectively), it is important to examine whether the H2BpT119 antibody interacts with H3pT3. Following a kinase assay with WT Haspin and recombinant H3 and blotting with the H2BpT119 antibody, signals were observed with both H3 WT and mutant T3A (Figure 3-2 C). However, these signals were lower than the signals observed with recombinant H2B (Figure 3-2 C). Similarly, no signal was observed

in the KD GST-Haspin (Figure 3-2 C). In addition to that, no upshift was observed in the phosphorylated WT H3 (Figure 3-2 C).

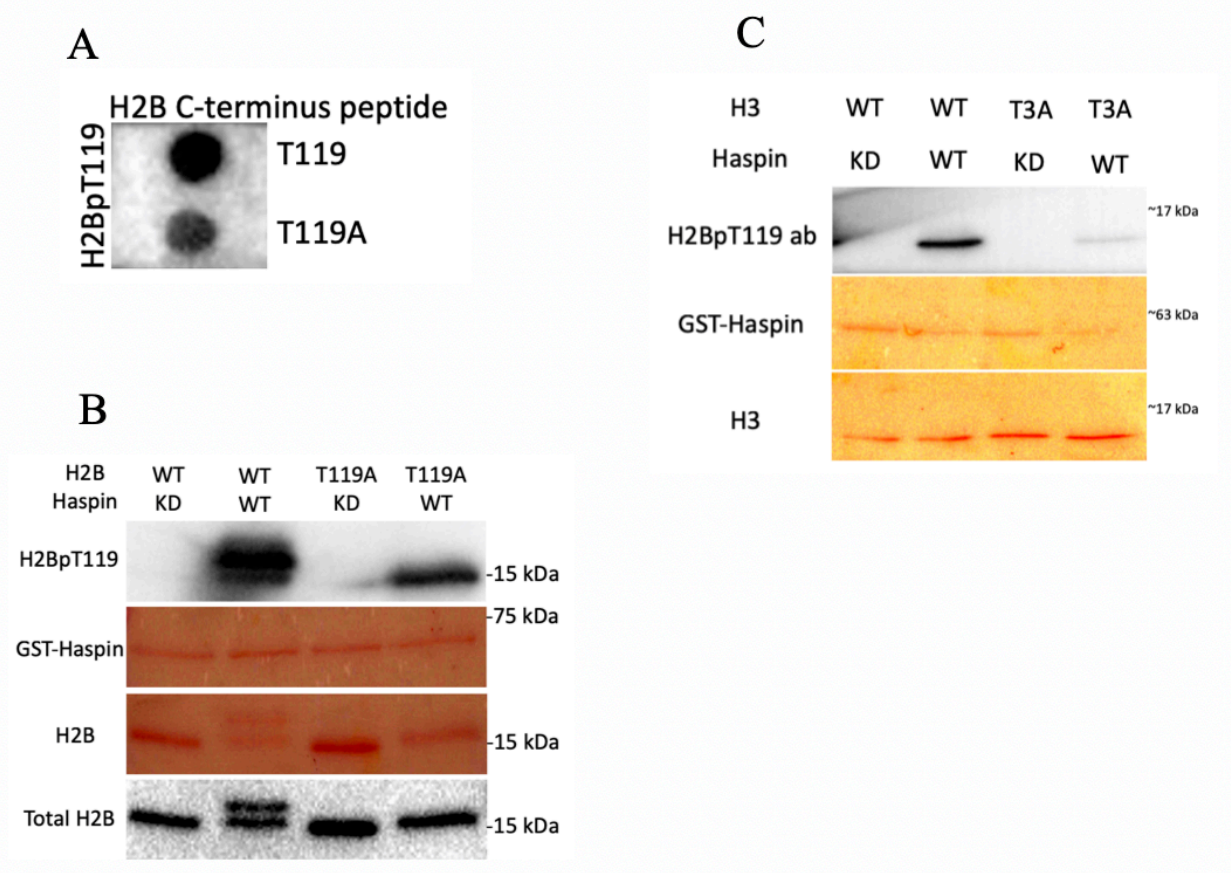

Figure 3-2: In vitro kinase assay to validate H2B phosphorylation by Haspin kinase by a Western blot-based assay. A. Synthetic peptides corresponding to the H2B C-terminus generated as in Figure 3-1 were incubated with recombinant GST-Haspin (WT) for 3 h in the presence of regular ATP. The phosphorylation was verified by immunoblotting with H2BpT119 antibody. **B.** Recombinant H2B (WT or T119A) was incubated with recombinant GST-Haspin (WT or KD) for 30 min in the presence of ATP; then the reaction was terminated by adding SDS-PAGE sample buffer and boiling at 95°C. The reaction was then subjected to Western blotting and signals were revealed by antibodies as indicated. **C.** Recombinant H3 (WT or T3A) was incubated with recombinant GST-Haspin (WT or KD) for 30 min in the presence of ATP; then the reaction was terminated by adding SDS-PAGE sample buffer and boiling at 95°C. The reaction was then subjected to Western blotting, and signals were revealed by antibodies as indicated. Ponceau red staining monitored protein loading. WT, Wild type; KD, Kinase dead.

The recombinant histones used in the previous kinase assay were native. These histones (WT or mutants) together with H2A and H4 were subjected to folding conditions to generate histones octamer (by Amélie Fradet-Turcotte's team). The octamers were first purified by gel filtration chromatography and then wrapped by DNA (147-bp 601 Widom positioning sequence) to produce nucleosome particles. These products were incubated with WT GST-Haspin in presence of radiolabeled [^{32}P]ATP. Signal of incorporated radiolabeled phosphate was observed only in the WT nucleosome and nucleosome containing H2BT119A mutant (Figure 3-3). No signal was observed in the nucleosomes containing either H3T3A mutant or double mutants (T119A and T3A) (Figure 3-3). Thus, despite kinase assays with two different concentrations of GST Haspin kinase (30 ng and 300 ng), no signal on nucleosomes containing H3T3A mutants were detected (Figure 3-3). Mutation of threonine-3 to alanine of H3 leads to no incorporation of the radiolabeled phosphate in the nucleosome.

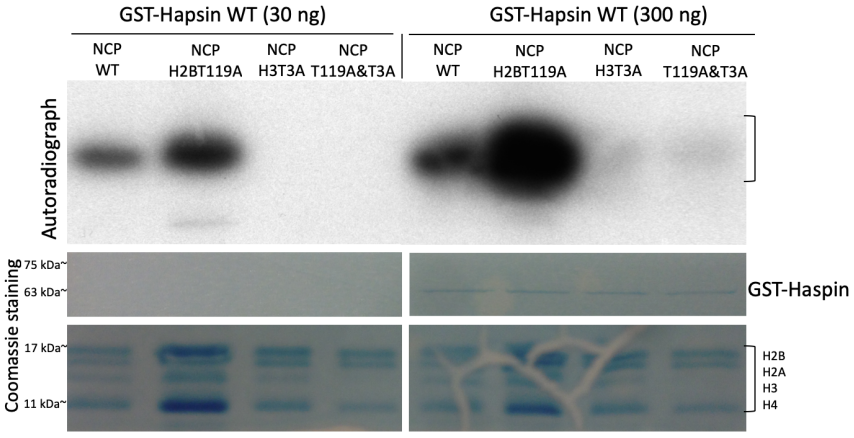

Figure 3-3: In vitro kinase assay of nucleosome particles and GST-Haspin. Nucleosome (NCP) particles, containing either all WT histones, H2BT119A, H3T3A, or both mutants, were incubated with recombinant GST-Haspin (WT or KD) for 30 min in the presence of radiolabeled [^{32}P]ATP; then the reaction was terminated by adding SDS-PAGE sample buffer and boiling at 95°C. Phosphorylation was verified by incorporation of the radiolabeled phosphate. WT, Wild type; KD, Kinase dead.

In conclusion, recombinant GST-Haspin kinase domain can phosphorylate H2BT119 and H3T3 in vitro, as well other sites. H2BpT119 antibody can specifically recognize H2BpT119 produced in vitro on H2B as well as on peptides tails. The H2BT119A mutant showed that other Haspin-dependent phosphorylation sites on H2B could be recognized non-specifically, albeit at lower level, as well as H3 phosphorylated by Haspin in vitro, also at a lower level. In vitro phosphorylation of T119 on recombinant H2B by Haspin leads to a slower migrating form on gel/SDS PAGE. Phosphorylation of recombinant nucleosomes by Haspin in vitro indicates that H3T3 is the major substrate site.

3.2 In vivo analysis of H2BpT119 signal during mitosis

Haspin is a mitotic kinase that outside of mitosis is poorly active. During the G2/M transition and mitotic entry, several phosphorylation events promote Haspin kinase activation (*254*). In this project, the goal is to study Haspin-dependent phosphorylation of H2B at T119. Thus, the following experiments were dedicated to exploring the signal of H2BpT119 during mitosis. To do this, HeLa S3 cells were used to conduct the in vivo investigation. Cells were cultured and then arrested at mitosis by nocodazole. To compare the level of H2BpT119 in mitosis with other cell cycle stages, thymidine blockage was used as a negative control. Treating the cells with thymidine induces cell cycle arrest in interphase, more specifically at G1/S, because of inhibition of DNA synthesis.

Acid-extracted histones by acid from HeLa S3 cells treated with nocodazole or thymidine were subjected to Western blotting. The anti-H2BpT119 detected signal in Western blot of HeLa S3 cells lysate that were arrested in mitosis, but not in interphase-blocked cells (Figure 3-4 A). The anti-H3pT3 was used as positive control. Similar signals were observed in mitotic cell extracts, but not in cells in interphase (Figure 3-4 A). Following the blotting with the phospho-specific antibodies, without a stripping, the membrane was used for total H2B blotting to validate the equal loading of the protein. H2B level was equal in all the conditions and in the mitotic cell extract an upshift was observed (Figure 3-4 A). The size of

this upshift is located at the same size of the bands that were detected with the anti-H2BpT119 and anti-H3pT3 (Figure 3-4 A). This therefore makes the recognition of the H2BpT119 signal very hard and the anti-H2BpT119 may cross-react with the H3pT3 signal, considering that there is cross-reactivity detected in the in vitro kinase assay.

The major Haspin substrate is H3T3, which has been observed by the immunofluorescence (IF) microscopy to start from prophase until early anaphase (*245*). Similarly, in this project, the H2BpT119 signal was explored by IF microscopy in HeLa S3 cells throughout the cell cycle phases. This was done by staining the cells with the anti-H2BpT119 and other markers, including CREST, Sgo, and Aurora B. The signal was observed starting from prophase until metaphase. The H2BpT119 signal completely disappears in anaphase (Figure 3-4 B). By magnifying the signal, H2BpT119 appears on the chromosomes and in co-localization with the kinetochore marker (CREST) in the centromere region (Figure 3-4 B).

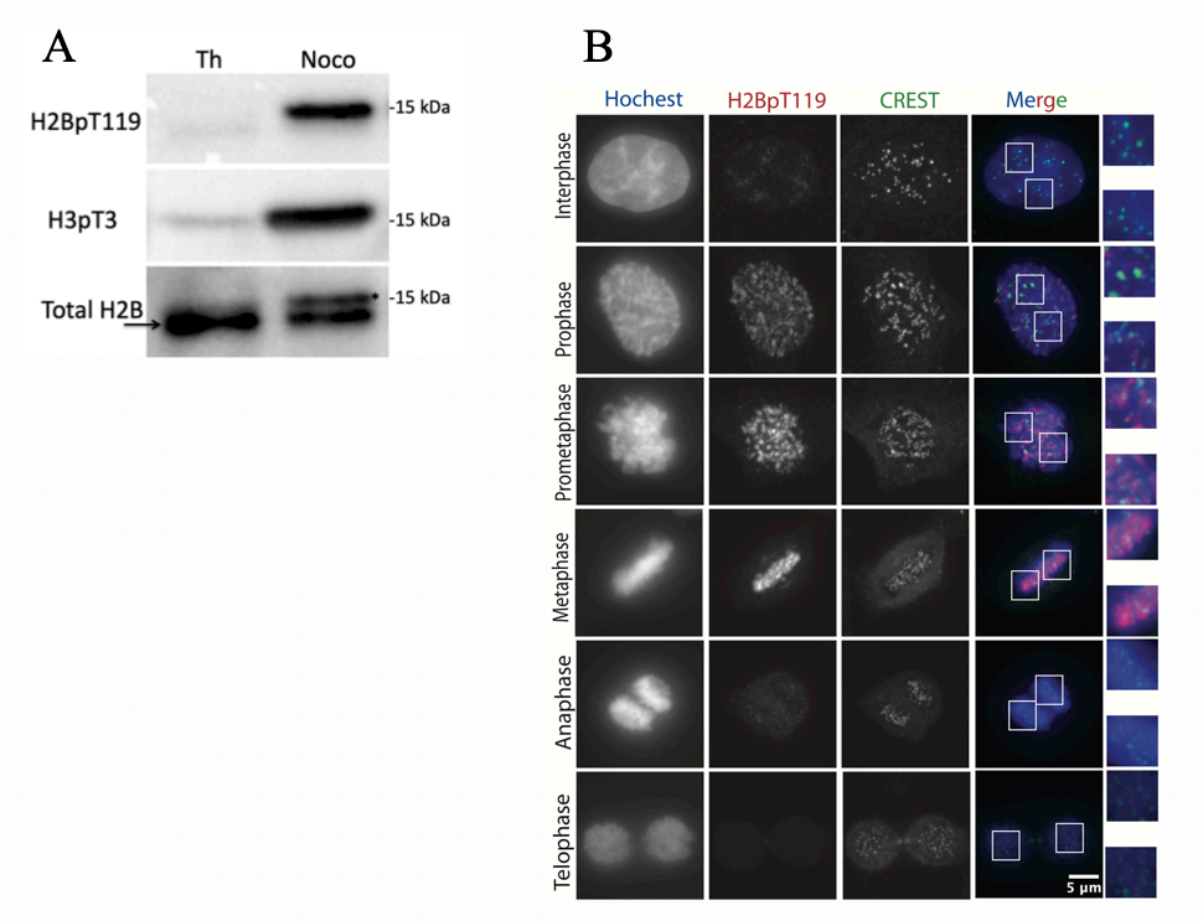

Figure 3-4: Exploring H2BpT119 signal during mitosis. A. HeLa S3 cells were treated with thymidine (Th) for 16 h to arrest the cells at interphase or with nocodazole (Noco) for 16 h to arrest the cells at mitosis. Total cell lysates (TCLs), histones extract by acid, were used for immunoblotting with specific antibodies as indicated. Total H2B blot is not stripped from H2BpT119 and H3pT3 antibodies and asterisk indicates phospho-specific antibodies signals. **B.** HeLa S3 cells were fixed and stained with Hoechst for DNA imaging (blue), CREST antibodies were used to mark the kinetochore (green), and anti-H2BpT119 (red). Scale bars, 5 µm.

The detected signal of H2BpT119 with the anti-H2BpT119 was also quantified during the different mitotic phases in HeLa S3 cells. H2BpT119 signal increases from prophase until it reaches the peak in metaphase (Figure 3-5). Other mitotic centromeric proteins were quantified, including Sgo1 and Aurora B, which both are well known to increase at the centromere region during mitosis. Sgo1

level at the centromere increases from prophase until metaphase before its levels drop in anaphase (Figure 3-5 A and C). This indeed represents the profile of H2ApT120, which is the histone mark that recruits Sgo1. While, Aurora B level increases in prophase and persists in increasing until metaphase, creating a profile similar to the H2BpT119 level (Figure 3-5 B and D).

In fact, Aurora B is recruited through Haspin-dependent phosphorylation of H3pT3, thus it has similar fluctuations as it moves with H3pT3 across the chromosome during the mitotic progression. Haspin is recruited at both the arm and the centromere during early mitosis through an interaction with the cohesion. However, PLK1-dependent removal of the cohesion in the chromosome arm promotes Haspin targeting to the centromere at the beginning of prometaphase. This in turns induces H3pT3 level to increase at the centromere and to reach the maximum level in metaphase, during which cohesion only remains at the centromere until anaphase.

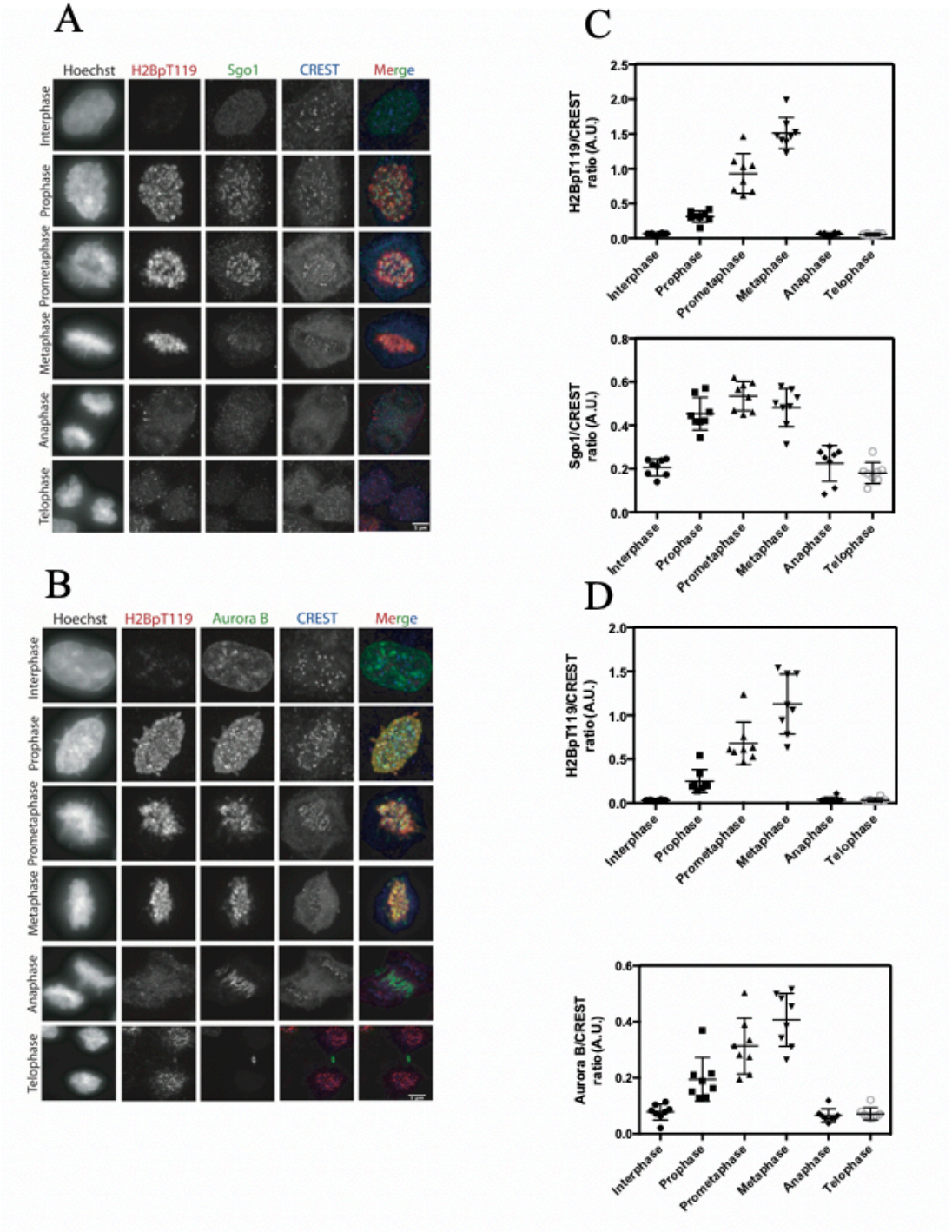

Figure 3-5: H2BpT119 signal quantification with anti-H2BpT119 during the cell cycle. A. and **B.** HeLa S3 cells were fixed and stained with Hoechst for DNA, CREST for kinetochore recognition (blue), anti-H2BpT119 (red), and Sgo1 or Aurora B (green). **C.** and **D.** H2BpT119 (upper), Sgo1, or Aurora B (lower) signal quantification from the IFs shown in (A and B). N=10 kinetochores from 8 different cells. Scale bars, 5 μm.

Chromosome spread staining was performed on mitotic HeLa S3 cells to clearly visualize the H2BpT119 signal in the mitotic cell with a very high resolution. Spreading produces enlarged chromosomes that are well separated with a clear morphology, which can be achieved by treating the cells with a hypotonic buffer. H2BpT119 signal was analyzed in chromosome spread obtained from prometaphase cells that were arrested at this stage by STLC. This drug is an inhibitor of the kinesin EG5 and thus spindle bipolarization; thus, it arrests cells at early mitosis and upon its removal cells can exit mitosis. In contrast, nocodazole irreversibly inhibits microtubule polymerization. Both drugs were used for mitotic spreading and they gave the same results at the end.

H2BpT119 signal localizes at the inner centromere between sister kinetochores, which were co-stained with CENP-C (Figure 3-6 A). Also, H2BpT119 signal was quantified across the centromere region and it appears to peak between CENP-C signals, confirming the observed localization at the inner centromere (Figure 3-6 B). This H2BpT119 signal localization is similar to one reported on H3pT3, because Haspin localizes at the centromere region. In contrast, H2ApT120 signal appears on the sister kinetochores, because this is mark of Bub1 catalytic activity, which is recruited at the outer kinetochore, relatively far from the inner centromere. No signal was observed on the chromosome arm (Figure 3-6 A), in agreement with the previous observed signal and quantification in the non-spreading cells staining. However, it is still very hard to distinguish whether the detected signal by the anti-H2BpT119 in the IF is for H2BpT119 or is cross-reactivity with the H3pT3 phosphorylation site. Since the anti-H2BpT119 interacts with the H3pT3 in the in vitro kinase assay, although at a lower level.

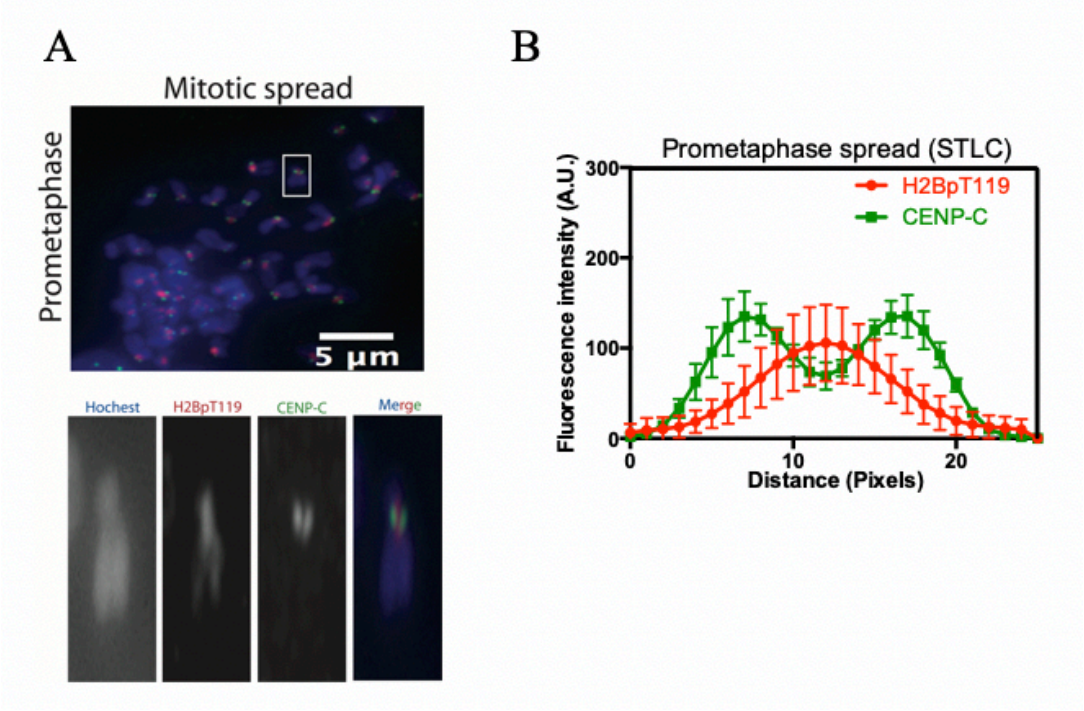

Figure 3-6: H2BpT119 signal quantification with anti-H2BpT119 at the centromere region. A. HeLa S3 cells were arrested at mitosis by STLC; before fixation, cells were swollen in a hypotonic buffer to generate the mitotic spreads and then subjected to staining of DNA by Hoechst (blue), CENP-C antibodies to mark the kinetochores (green), and anti-H2BpT119 (red). **B.** Signal quantification of H2BpT119 level at the centromere in the mitotic spread; n = 26 centromeres; Error bars, SD from three independent cells. CENP-C, Centromere protein. Scale bars, 5 µm.

To examine whether Haspin is the mitotic kinase that is catalyzing H2BpT119 in vivo. HeLa S3 cells were arrested at mitosis by nocodazole and MG-132, which is a proteasome inhibitor, thus preventing mitotic proteins degradation and promoting mitotic arrest. HeLa S3 cells were treated with the Haspin inhibitor (5-IT), plus another condition treated by DMSO as control. The acid extracted histones were subjected to Western blotting and probing with anti-H2BpT119. The signal of H2BpT119 was completely lost following the treatment with the 5-IT, as was the H3pT3 signal (Figure 3-7 A). The band size of the observed H2BpT119 is similar to that of H3pT3 (Figure 3-7 A). To avoid the confusion that could arise from

striping and re-blotting the Western blot membrane following blotting with the anti-H2BpT119, the samples of extracted histones were run again to perform total anti-H2B blotting on a new membrane. Importantly, no H2B upshift was observed in mitotic histone extract of both the control and 5-IT-treated sample (Figure 3-7 A). Therefore, the previously observed H2B upshift (Figure 3-4 A) might be the non-stripped anti-H2BpT119 signal instead of being an anti-H2B signal. Also, through IF microscopy, H2BpT119 signal completely disappeared in the mitotic HeLa S3 cells treated with 5-IT (Figure 3-7 A). The centromeric H2BpT119 signal was quantified in both the control and 5-IT-treated cells, indicating that the 5-IT treatment leads to the loss of the phosphorylation (Figure 3-7 B and C).

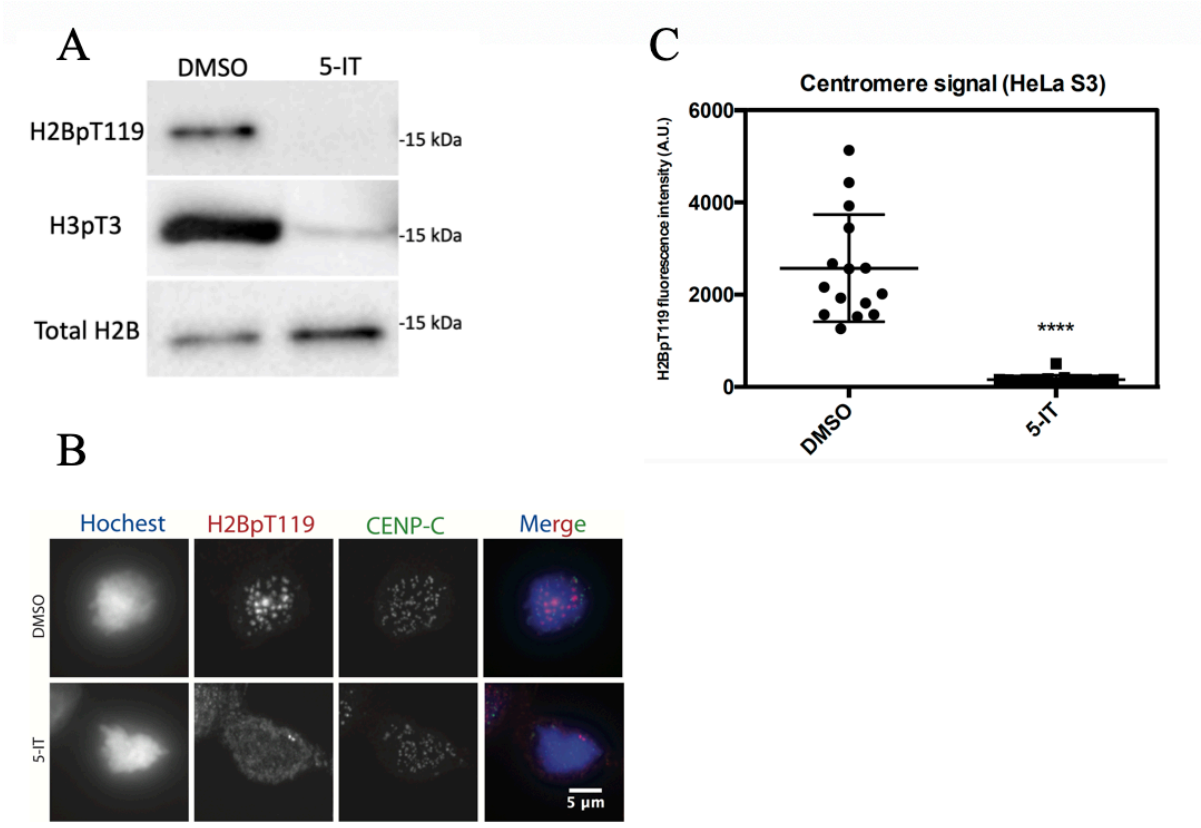

Figure 3-7: Effect of Haspin inhibition on H2BpT119 signal during mitosis in HeLa S3 cells. A. HeLa S3 cells were arrested at mitosis by nocodazole and MG-132 and then treated with 5-IT (5-Iodotubercidin) or DMSO as control. Total cell lysates were subjected to immunoblotting as shown. **B.** HeLa S3 cells were treated as mentioned in (A); then fixed and used for immunofluorescence staining. **C.** H2BpT119 signal quantification from the experiment shown in (B). Unpaired t-test ****P<0.0001. CENP-C, Centromere protein C. Scale bars, 5 µm.

The validation of H2BpT119 signal during mitosis and in response to Haspin inhibition by 5-IT, was also done in another cell type that is chromosomally stable compared to HeLa S3 cells. The retinal pigment epithelium1 (RPE1) cells were used to confirm the observations obtained with HeLa S3 cell. RPE1 cells were cultured and arrested at mitosis as described above for HeLa S3 cell, then treated with DMSO or 5-IT. Observations obtained with RPE1 cells were similar to those obtained with HeLa S3 cells following the 5-IT whether in Western blot or IF (Figure

3-8). These results obtained with the anti-H2BpT119 suggest Haspin-dependent phosphorylation of H2B in vivo during mitosis. Despite, all evidence regarding the anti-H2BpT119 mitotic signal, it still remains very important to confirm its specificity taking into consideration the nonspecific antibody recognition of the other phosphorylation sites, namely H3T3.

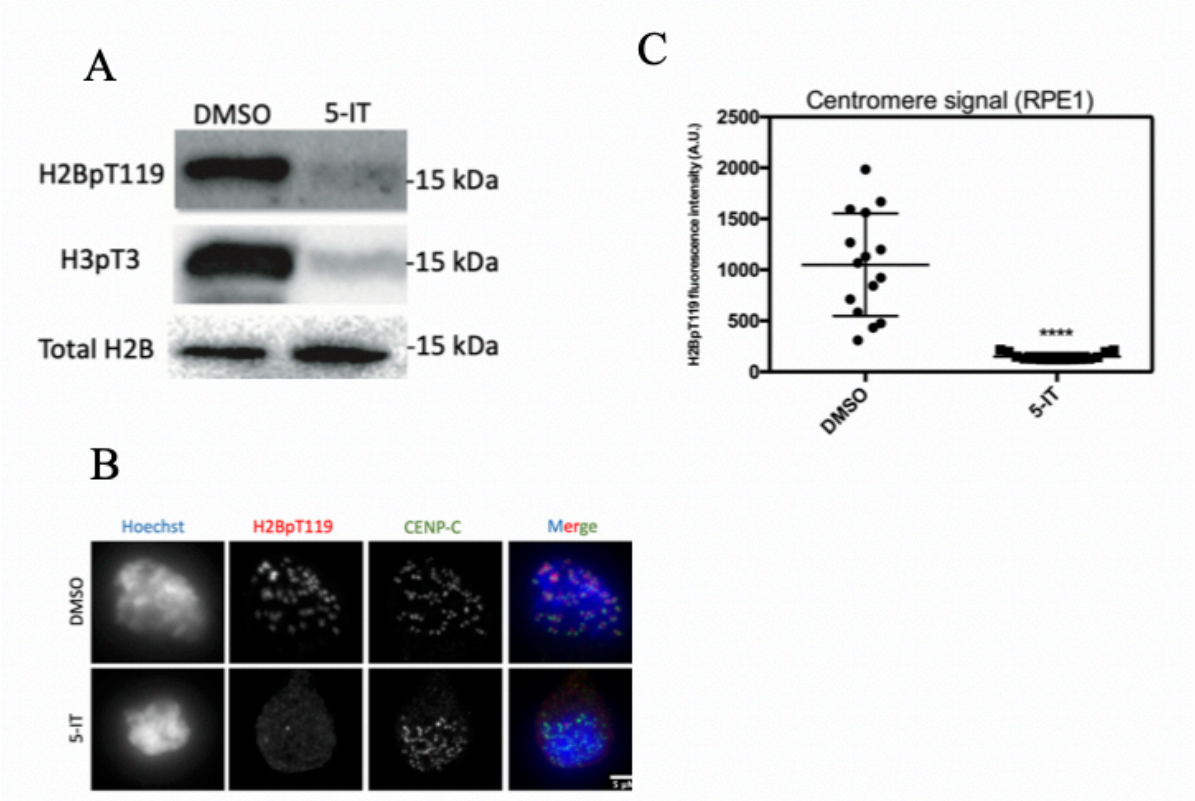

Figure 3-8: Effect of Haspin inhibition on H2BpT119 signal during mitosis in retinal pigment epithelium1 (RPE1) cell. A. RPE1 cells were arrested at mitosis by nocodazole and MG-132 and then treated with 5-IT or DMSO as a control. Total cell lysates were subjected to immunoblotting as shown. **B.** RPE1 cells were treated as mentioned in (A); then fixed and used for immunofluorescence staining. **C.** H2BpT119 signal quantification from the experiment shown in (B), unpaired t-test ****P<0.0001. Hoechst for DNA (blue), CENP-C for kinetochore recognition (green), and anti-H2BpT119 (red). Scale bars, 5 μm.

3.3 Attempts to validate the specificity of the H2BpT119 signal detected in vivo

The major problem with the mitotic signal detected with the anti-H2BpT119 is the band size on the blot seems to be that the observed signal is on H3 not H2B. It is such a major challenge to verify H2BpT119 signal due to several reasons. H2BT119 knockout by any mean of genome editing seems to be difficult, because of presence of many H2B genes variants (*205, 274, 275*). As well as, knockdown

by RNAi may also be difficult and even unfavorable, because of the various variants that are ubiquitously expressed and also the essentiality of H2B (*205, 274, 275*). Adding another fact that H2B is in complex with the other histones, depleting H2B will certainly affect chromatin status (*207, 276*). Therefore, to circumvent these issues, the aim here is to verify mitotic H2BpT119 signal on exogenous H2B tagged with another protein or epitope to increase the molecular size to allow a conclusive recognition.

Initially, H2B tagged with mCherry or GFP, which both are widely used tagging systems and showed a feasible incorporation with the endogenous chromatin. Indeed, these tagging systems are widely used to monitor chromosome segregation during mitosis and to observe defective phenotypes particularly in metaphase and anaphase. HeLa TREx cells were transfected with pcDNA3 for H2B-mCherry (WT or T119A) transient expression. Also, HeLa S3 stably expressing H2B-GFP were used side by side with the transiently expressed H2B-mCherry. The cells were arrested at mitosis by nocodazole and histones were extracted by acid. Total cell lysates were subject to Western blotting with the anti-H2BpT119 and the anti-mCherry. H2B Tagged with mCherry (H2B: 15 kDa and mCherry: 28.8 kDa, total protein size of 43.8 kDa) appears at the right size, which is detected by the anti-mCherry (Figure 3-9 A). The anti-H2BpT119 detects the endogenous phosphorylation signal around 15 kDa, which seems weaker in the HeLa TREx cells compared to the HeLa S3 (H2B-GFP expressing cells) (Figure 3-9 A). However, neither H2B-mCherry nor H2B-GFP, exhibited signals with the anti-H2BpT119 (Figure 3-9 A). It was assumed that the tag is relatively big and may affect either the exogenous H2B phosphorylation or the anti-H2BpT119 interaction with the phospho-site.

Thus, a small tagging system such as short epitopes (3xFlag-2xStrep) (*277*), which is around 5 kDa, was used. Also, the acid extraction of the histones was modified to increase the incubation time up to 3h, which was found to be more efficient. HeLa S3 cells were transfected with the 3xFlag-2xStrep-H2B plasmids

(WT or T119A) and arrested at mitosis by nocodazole, under two conditions -/+ 5-IT. Western blot analysis of histone extracts was performed to determine if the anti-H2BpT119 can detect any signal on the tagged WT H2B that would be lacking in the T119A mutant. Blotting with anti-Flag indicates that 3xFlag-2xStrep-H2B is located around 22 kDa (Figure 3-9 B). However, no signal on the 3xFlag-2xStrep-H2B was detected with the anti-H2BpT119 antibody in these extracts (Figure 3-9 B).

With increasing the incubation time during the extraction, the anti-H2BpT119 appears to recognize two bands that have not been seen with 30 min incubation time in the previous extracts. One band is located at H3 size and abolished with 5-IT treatment (Figure 3-9 B). Another band is located at H2B size and it was not affected by 5-IT. Although, a strep-tactin IP was performed to enrich the tagged-H2B, still no signal was detected with the anti-H2BpT119 on the tagged H2B (Figure 3-9 B). The membrane was also striped once to blot with total H2B, endogenous H2B and the upshift was noted, but the 3xFlag-2xStrep-H2B was not detected (Figure 3-9 B). In addition, by Ponceau red staining only endogenous histones were observed in the total cell lysates (histones extract), but not after the IP step. Moreover, 3xFlag-2xStrep-H2B was not detected by Ponceau staining. No signal was detected on tagged H2B making conclusions impossible, likely due to a low level of expression compared to endogenous total H2B.

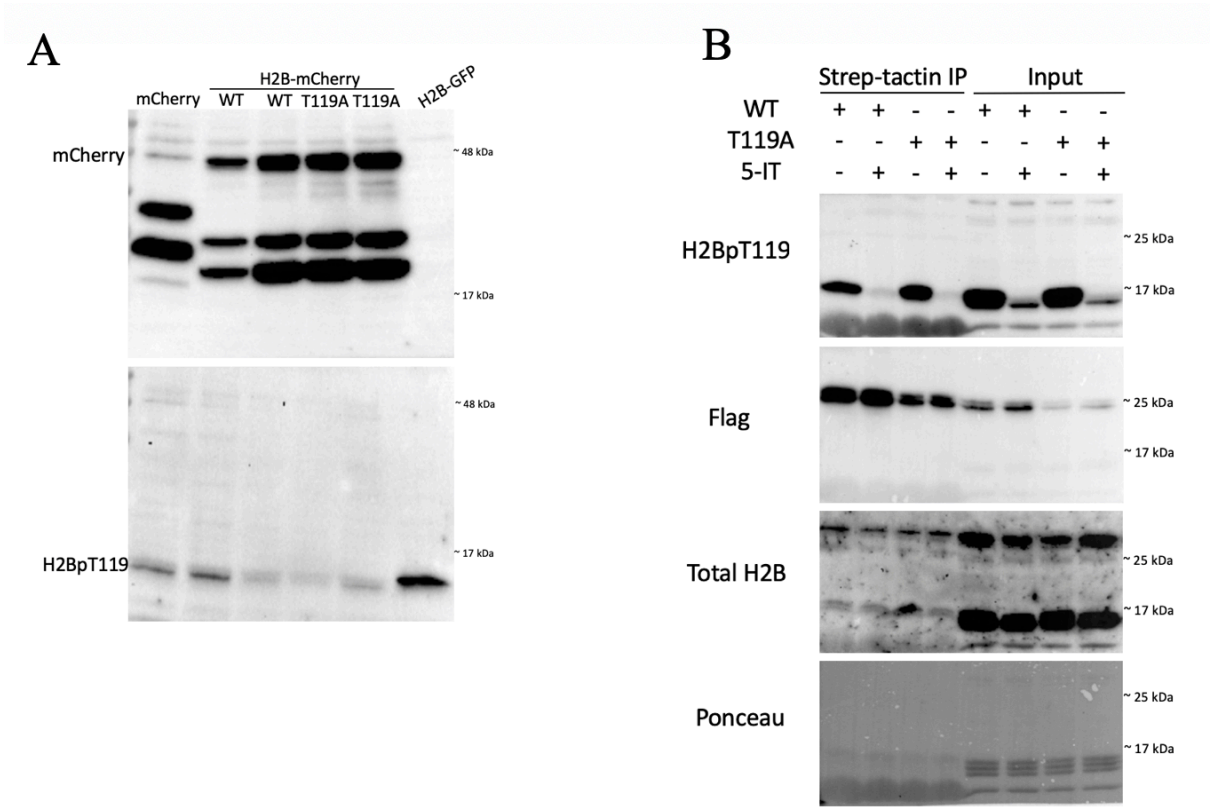

Figure 3-9: Detection of H2BpT119 signal on tagged H2B during mitosis. A. HeLa TREx cells were transfected with mCherry, H2B-mCherry WT, or H2B-mCherry T119A plasmid. The following day, transfected cells were arrested at mitosis by nocodazole for 16 h, and then lysates (histone acid extracted) were subjected to immunoblotting. The last lane contains mitotic cell lysate of HeLa S3 cells that stably expresses H2B-GFP. **B.** HeLa S3 cells were transfected with 3xFlag-2xStrep-H2B WT or 3xFlag-2xStrep-H2BT119A plasmid and arrested at mitosis for 16h. A fraction of TCLs was used for strep-tactin IP, then both TCL and IP eluates were subjected to immunoblotting as shown.

Another smaller epitope (1xFlag), which is widely used in studying histone PTMs was also used to in an attempt to confirm the H2BpT119 signal during mitosis (*278-281*). HeLa S3 cells were transfected with the 1xFlag-H2B plasmid (WT) and arrested at mitosis by nocodazole, including two conditions -/+ 5-IT. Moreover, another dish of HeLa cells were transfected with an empty 1xFlag expression plasmid as a negative control. Histones were extracted by acid (3 h incubation time) and after neutralizing the samples to pH 8, Flag IPs were

performed to enrich the Flag-tagged H2B. Anti-Flag blotting indicates that Flag-tagged H2B migration was around 17 kDa (Figure 3-10 A). No signal was detected on the endogenous histones or Flag-H2B with the anti-H2BpT119 antibody in the IP samples (Figure 3-10 A). In the control sample of mitotic histone extracts, the anti-H2BpT119 however does detect a phospho-signal (Figure 3-10 A). Following successful stripping steps, the membrane was blotted with total H2B, revealed a faint band on the endogenous H2B and Flag-H2B of the IP samples, but a comparably stronger band in the histones extracted from the control sample (Figure 3-10 A). Similarly, Ponceau red staining showed stronger signals of the endogenous histones compared to the IP samples (Figure 3-10 A).

Further attempts to detect H2BpT119 signals in HeLa S3 cells stably expressing Flag-H2B either WT or T119A mutant were made. This is to see if the stable expression will enhance the incorporation of the exogenous Flag-H2B with the endogenous chromatin. The established cell lines are non-isogenic, thus gives possibility of the genomic integration of multiple copies of the exogenous Flag-H2B, which in turn may increase the possibility of detecting the H2BpT119 signal during mitosis. These stable cell lines were cultured and then arrested at mitosis (-/+5-IT). Also, the parental HeLa S3 cells were used side by side as additional negative controls for any signal that will be detected at the same molecular weight of Flag-H2B with the anti-H2BpT119. Histones were extracted by acid (3 h incubation time) and subjected to Western blotting. Anti-Flag detects the Flag-H2B around 17 kDa; although the Ponceau red staining failed to detect it (Figure 3-10 B). Again, with these histone extracts, the anti-H2BpT119 recognizes two bands at the H3 size and H2B size. The latter persists following the 5-IT treatment (Figure 3-10 B). However, no H2BpT119 signal was detected on tagged H2B making conclusions impossible, likely due to too low level of expression compared to endogenous total H2B.

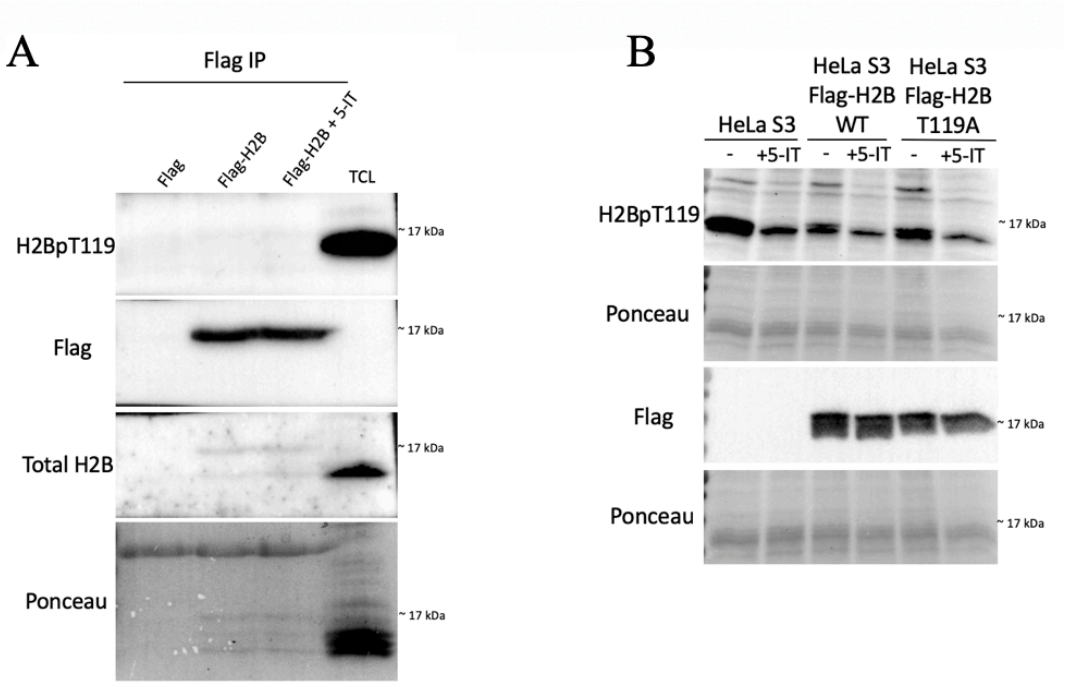

Figure 3-10: Detection of H2BpT119 signal on tagged H2B during mitosis. A. HeLa S3 cells were transfected with Flag, or Flag-H2B WT plasmid and arrested at mitosis as described before, then histones were extracted by acid and subjected to Flag IP. The last lane, it contains total cell lysate (TCL) of mitotic HeLa S3 cells that was lysed by acid to extract the histones. **B.** Parental HeLa S3 cell and HeLa S3 cells stably expresses Flag-H2B WT or Flag-H2BT119A were arrested at mitosis as described before, then histones were extracted by acid and subjected to immunoblotting with the antibodies as indicated.

In the regard of phospho-H2B upshift and co-migration with H3, the intention was to separate H2B from H3 to reach a clear conclusion. This can be also achieved by step-wise elution with salt in ion exchange chromatography, as well as by affinity chromatography (chromatin IP). To do so, HeLa S3 cells were arrested at mitosis by nocodazole and histones were extracted by acid. Extracted histones were loaded on the chromatography resin, and H2B-H2A was eluted by virtue of a low salt buffer, before H3-H4 elution with a high salt buffer. Eluates were subjected to SDS-PAGE and Coomassie blue staining to validate the purity. Indeed, the colorimetric staining shows that H2B-H2A was isolated from H3-H4. These eluates were also subjected to Western blotting for anti-H2BpT119 probing. The antibody

detects a stronger signal on the tetramer (total extract) and weaker signals on dimer fraction for mitotic H2BpT119 (Figure 3-11 B).

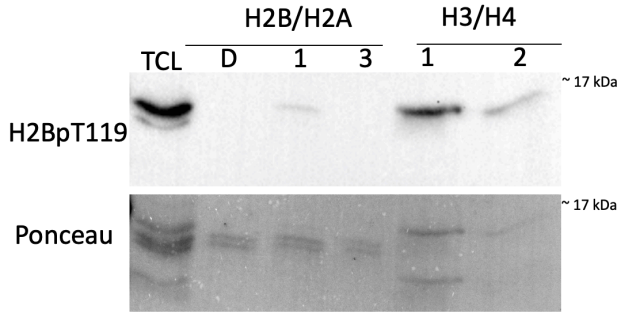

Figure 3-11: Validation of H2BpT119 antibody interaction with mitotic H2B and Haspin-dependent phosphorylation of H2BT119. HeLa S3 cells were arrested at mitosis by nocodazole for 16 h, then H2B/H2A were separated from H3/H4 through column purification and step-wise salt elution. Double purified fractions of H2B-H2A are indicated as D in the figure. Eluted fractions were used for immunoblotting as shown.

To validate H2BpT119 mitotic signals using another method, mass spectrometry was used as an independent approach. Three conditions of HeLa S3 cells were used, including interphase and mitosis -/+5-IT. Thymidine blockage was used to arrest the cells at interphase, while nocodazole was used for mitotic arrest. Histones were extracted by acid and purified by chromatography as described in the material and method chapter. Protein digestion was done by Glu-C endoproteinase, which catalyzes the cleavage at the C-terminus of either aspartic acid or glutamic acid residues in the protein. Glu-C should cleave (*) glutamic acid residue at 113 (or 114 in case counting the first methionine) in H2B (-**E**$_{113/114}$*GTKAV**T**$_{119/120}$KYTSSK-). This thus will cover specifically H2B C-terminus around the T119. 8 high confidence peptides spectra covering T119 were obtained in the mass spectrometry analysis of interphase digests, but none exhibited phosphorylation (Table 3-1). This should be expected, since the anti-H2BpT119 did not detect signal from histone extract of interphase cells in the Western blot

analysis. In the mitotic histone digests analysis, 7 high confidence peptides spectra were obtained covering T119, although none were phosphorylated (Table 3-2). Also, 5 high confidence peptides spectra in the mitotic samples treated with 5-IT, did not show phosphorylation (Table 3-3). The absence of detection of phosphopeptide in the mass spectrometry analysis could be due to the small number of spectra obtained, a low level of T119 phosphorylation compared to bulk H2B, the poor quality of the extracted samples and non-specific absorption of the histones samples on the purification resin.

Table 3-1: Histone H2B C-terminus peptides spectra in mass spectrometry analysis of Glu-C digest sample from interphase HeLa S3 cells.

Interphase	Sequence	Start-Stop	Peptide Identification Probability (%)	M/Z	Charge	pT119
	(E)GTKAVTKYTSSK(-)	115-126	100	424.2383	3	No
	(E)GTKAVTKYTSSK(-)	115-126	100	424.2383	3	No
	(E)GTKAVTKYTSSK(-)	115-126	100	635.8535	2	No
	(E)GTKAVTKYTSSK(-)	115-126	100	424.2384	3	No
	(E)GTKAVTKYTSSK(-)	115-126	20	424.2374	3	No
	(E)GTKAVTKYTSAK(-)	115-126	100	627.8533	2	No
	(E)GTKAVTKYTSAK(-)	115-126	100	627.8561	2	No
	(E)GTKAVTKYTSAK(-)	115-126	100	418.9067	3	No
	(E)GTKAVTKYTSAK(-)	115-126	99	418.9067	3	No
	(E)GTKAVTKYTSAK(-)	115-126	38	627.8560	2	No
	(E)GTKAVTKYTSAK(-)	115-126	25	418.9063	3	No

Table 3-2: Histone H2B C-terminus peptides spectra in mass spectrometry analysis of Glu-C digest sample from mitotic HeLa S3 cells.

Mitosis	Sequence	Start-Stop	Peptide Identification Probability (%)	M/Z	Charge	pT119
	(E)GTKAVTKYTSSK(-)	115-126	100	424.2372	3	No
	(E)GTKAVTKYTSSK(-)	115-126	100	635.8542	2	No
	(E)GTKAVTKYTSSK(-)	115-126	100	424.2385	3	No
	(E)GTKAVTKYTSAK(-)	115-126	100	418.9053	3	No
	(E)GTKAVTKYTSAK(-)	115-126	100	418.9065	3	No
	(E)GTKAVTKYTSAK(-)	115-126	100	627.8558	2	No
	(E)GTKAVTKYTSAK(-)	115-126	100	627.8564	2	No
	(E)GTKAVTKYTSAK(-)	115-126	74	418.9067	3	No

Table 3-3: Histone H2B C-terminus peptides spectra in mass spectrometry analysis of Glu-C digest sample from mitotic HeLa S3 cells treated with 5-IT.

Mitosis+5-IT	Sequence	Start-Stop	Peptide Identification Probability (%)	M/Z	Charge	pT119
	(E)GTKAVTKYTSSK(-)	115-126	100	635.8523	2	No
	(E)GTKAVTKYTSSK(-)	115-126	100	635.8536	2	No
	(E)GTKAVTKYTSSK(-)	115-126	86	424.2382	3	No
	(E)GTKAVTKYTSAK(-)	115-126	100	627.8556	2	No
	(E)GTKAVTKYTSAK(-)	115-126	100	627.8563	2	No
	(E)GTKAVTKYTSAK(-)	115-126	100	418.9067	3	No

Chapter 4

4 Discussion

The goal of this project was to investigate H2B phosphorylation at threonine 119 by Haspin kinase activity during mitosis. To reach this goal in an in vitro validation, the required materials were generated, including GST-Haspin, peptides, histones, and nucleosomes. GST-Haspin kinase domain was produced and purified to conduct the kinase assay. Also, another inactive version of GST-Haspin kinase domain (kinase dead) was generated to be used in the negative control condition in order to ensure the specificity of the phosphorylation reaction. Moreover, peptides covering H2B C-terminus tail (T119) and H3 N-terminus tail (T3) were generated to be used as substrates, in addition to their non-phosphorylatable versions (T119A and T3A).

Alternatively, recombinant histones H2B, H3, and their respective mutants (H2BT119A and H3T3A) were produced, purified, and used as Haspin substrates. Haspin in vitro kinase-radioactivity based assay with the peptides or the recombinant histones indicates that Haspin can phosphorylate H2BT119 (Figure 3-1). Also, signals were observed even with mutant peptide versions and mutant histones. Thus, Haspin can phosphorylate other sites in H2B other than T119. It was also possible to compare Haspin affinity toward H2BT119 and H3T3, showing the latter to be more phosphorylated in the kinase assay in the peptide tails (Figure 3-1).

To study H2B phosphorylation in vivo during mitosis, an anti-H2BpT119 was produced and purified. The antibody was tested for its capacity to recognize the phospho-site on H2B and to validate its specificity. Following Haspin kinase assay with either peptide tail or recombinant histone, the samples were subjected to Western blotting analysis with the anti-H2BpT119. The results indicate that the anti-H2BpT119 can specifically recognize phosphorylation in H2B (Figure 3-2). Also, the antibody can recognize other phosphorylation sites in H2B as the signal

persists in the mutant versions (Figure 3-2). The detected signals with the WT GST-Haspin conditions were not observed with the kinase dead conditions, indicating that the anti-H2BpT119 interacts with only phosphorylated H2B. Opposite to the results of this project, a previous study has shown that Haspin could not phosphorylate H2B in the in vitro kinase assay (*245*).

H2B incubated with Haspin in the in vitro kinase assay demonstrated an electrophoretic upshift (slower migration) on the gel/membrane. In addition to that, the anti-H2BpT119 non-specifically recognizes H3pT3 (Figure 3-2 C), thus a potential cross-reactivity might occur in the Western blot of mitotic cell lysate. In the kinase assay with NCP particle, H3pT3 appears to be the major substrate of Haspin (Figure 3-3). However, signals detected correspond to H3 based on mutants. However, T119A NCPs were more abundant in the assay, it was therefore difficult to judge the exact contribution of each nucleosome type accurately and whether individual histones were stoichiometrically represented. Thus, NCPs migration on native gel might be needed to show that the nucleosomes used were intact and functional. Importantly, recent study has showed that Haspin can phosphorylate H2AT127 in mouse oocytes (*282*). Moreover, Haspin was found to phosphorylate H3T11 in addition to H3T3 in *Arabidopsis thaliana* in vitro (*283*). Taken together, it is highly possible that other substrates for Haspin could exist in addition to H3pT3.

The anti-H2BpT119 was used to investigate H2B phosphorylation at the T119 during mitosis in human cells. This has been done in two cell types, including HeLa S3 cells and RPE1 cells. Cells were arrested specifically at mitosis and histones were extracted by acid. Western blot analyses of total H2B with the anti-H2BpT119 suggests Haspin-dependent phosphorylation of H2BT119 and H2B upshift in vivo (Figure 3-4 A). As well as, IF analysis of H2BpT119 signal shows that this mark appears restricted in mitosis, from prophase to metaphase. Moreover, H2BpT119 signal localizes at the inner centromere (Figure 3-6 A and B).

A previous study also has shown H2BpT119 signal during mitosis (*284*). Accordingly, an anti-H2BpT119 was generated and tested to verify its interaction with the peptides covering H2B C-terminus. Two peptides versions were used including phospho-T119 peptide and non-phospho-T119 peptide of the H2B C-terminus. After ensuring the antibody interaction with the phospho-site of H2BT119, the antibody was used to stain mitotic HeLa cells to visualize H2BpT119 signal under IF microscope. In mitotic HeLa cells, H2BpT119 was observed at the centromere in metaphase. This observation is similar to the one presented here in this project. However, the main limitation of the microscope observations is the impossibility of verifying the specificity of the detected signal with the anti-H2BpT119. To clarify, by Western blotting, it was possible to notice the anti-H2BpT119 cross-reactivity with H3pT3 due to the possibility of validating the molecular size of the detected band on the membrane. However, the microscopy only provides information on the H2BpT119 signal localization on the chromosome.

To investigate the specificity of the anti-H2BpT119, tagged H2B was used in several forms in both transient and stable expression in different cell types. The systems used include transient expression of tagged H2B (H2B-mCherry, 3xFlag-2xStrep-H2B, or 1xFlag-H2B). The stable expression cell line systems were used to generate H2B-GFP and 1xFlag-H2B. Cells were arrested at mitosis by nocodazole and a histone acid extraction protocol was used to isolate histones for Western blot analysis. However, the attempts of tagging H2B with epitopes in order to detect the phospho-signal in a distinct manner from the endogenous histones all ultimately failed (Figure 3-9 and Figure 3-10).

This could be related to the possibility of the very low expression of the transgene compared to the amount of endogenous H2B, although the stable expression of the tagged H2B was established to reach the maximum optimal level. Moreover, the newly deposited histone may differ in regard of PTMs comparing to the recycled old (parental) histones (*285, 286*). For instance, it has

been found that H3pT3 level is significantly higher in the old H3 than in the newly synthesized H3 (*285*).

Moreover, mass spectrometry analysis was used as an independent approach to validate Haspin-dependent phosphorylation of H2B during mitosis. Histones from interphase or mitosis (-/+5-IT) HeLa S3 cells were extracted by acid and purified by chromatography. Furthermore, Glu-C was used as a digestive enzyme to specifically cleave the C-terminus of H2B to cover T119. Indeed, peptides spectra covering T119 of H2B were obtained by the mass spectrometry analysis, but with no phosphorylation was detected under any condition (Tables 3-1, 3-2, and 3-3).

It is possible that the sample preparation of histone digests was not sufficient enough to enrich the H2BpT119 peptides due to the level of this mark in vivo. Indeed, it may be difficult to detect some PTMs by mass spectrometry for reasons such as the level of the PTM and type of methods of detection (*287*). Moreover, presence of other modifications beside the H2BpT119 could make the recognition of the modifications in the peptides by mass spectrometry very difficult due to the complication of resolving the peptide spectra (*288, 289*). Thus, it remains to be proven whether H2BpT119 exists in mitosis.

In a previous study, a quantitative large-scale mass spectrometry analysis of HeLa S3 cells was performed to identify mitotic PTMs (*290*). In that study, H2BpT119 signal was found during cell cycle. Accordingly, stable isotope labeling by amino acids in cell culture (SILAC) was used to perform a quantitative mass spectrometry. Here, cells were grown in the presence of different lysine and arginine isotopes, which can be distinguished in the mass spectrometer due to differences in the mass to charge ratio of the spectra. Despite having used trypsin as an enzyme to digest the proteins, the C-terminal tail of H2B covering pT119 was identified. H2BpT119 signal was excluded from the identified mitotic PTMs due to low abundance and poor significance.

In another mass spectrometry study, using trypsin for digestion, H2BpT119 signal was detected in asynchronous cells (*291*). However, digests were subject to phosphopeptide enrichment step by immobilized metal ion affinity chromatography (IMAC) (*292*). Such step appears to be necessary to detect H2BpT119 signal specifically during mitosis.

General conclusion and perspectives

In conclusion, it was very hard to detect a bona fide H2BpT119 signal with the anti-H2BpT119 in vivo during mitosis. This complexity is apparently brought on the Haspin-dependent upshift of H2B migration, that co-migrates with H3, making analysis of mitotic histone extract by Western blot very difficult. In addition to that, the potential cross-reactivity of the anti-H2BpT119 antibody with H3pT3 further complicates matters. These observations were also seen in the vitro kinase assay with purified histones and nucleosomes. To overcome these obstacles, tagged H2B was used to detect H2BpT119 mitotic signal specifically. However, it was also difficult to observe signal on the exogenous tagged H2B due to the low level of the expression and most likely the low level of H2BpT119 signal in vivo during mitosis.

For H2BpT119 signal validation by Western blot, acid extraction methods (*269, 270, 272*) that were used in this project may not have been the best way to recover modified histones. Mainly because of the principle of acid extraction, which is based on the highly positive charged content of histones. Thus, any histone modification (acetylation/phosphorylation) that reduces the positive charge will decrease the recovery of those specific histones. In that regard, other histone extraction strategies could lead to a better outcome. An obvious, experiment to be performed to clearly answer the question of H2BpT119 signal during mitosis would involve extracting the native chromatin from cell line expressing tagged H2B.

The native chromatin is physiological and better reflects the modification state of histones in vivo. Two conditions must be included WT tagged H2B and the T119A mutant to validate the specificity of the anti-H2BpT119 antibody. Moreover, purification of mitotic native chromatin by an IP step and validation of the fraction quality on SDS-PAGE gel are necessary. In the Western blot analysis with the anti-H2BpT119; a better migration is required to separate the tagged H2B from H3 to clear the cross-reactivity in case using the 1xFlag-H2B stable cell lines. According to Western blot experiments that were performed in this project, a better migration could be achieved by using 15% or 17% separating gel in the SDS-PAGE

preparation.

Similarly, such preparation of the native chromatin can be used to extract an enriched histone sample for mass spectrometry analysis. Furthermore, in the regard of the low level of the mitotic H2BpT119 signal, a phosphopeptide enrichment step must be applied following protein digestion. As mentioned above in the discussion, this step has been used in a previous study, in which H2BpT119 was detect in asynchronous cells (*291*). Thus, cell arrest at mitosis by nocodazole, native chromatin preparation, and phosphopeptide enrichment are likely all necessary steps to maximize the chances of H2BpT119 signal detection during mitosis by mass spectrometry. The advantage of mass spectrometry analysis is the broad identification of PTMs. Thus, performing the suggested steps will help a better investigation not just for H2BpT119, but also for identification of other novel mitotic PTMs.

Haspin in the in vitro kinase assay was found to phosphorylate other sites in H2B and H3. In the mutant versions, H2BT119A and H3T3A, signals were observed following the kinase assay. These observations were obtained with either the radioactivity-based assay or with the anti-H2BpT119. Indeed, H2BT19 in the N-terminal tail seems to be Haspin target site. To easily identify these phosphorylated sites, histones phosphorylated by Haspin can be subjected to mass spectrometry analysis. Histone samples extracted from mitotic cells (-/+ 5-IT) can be also analyzed by mass spectrometry as described above to validate Haspin-dependent phosphorylation of these residues in vivo. Moreover, protein crystallization technique or bioinformatics prediction tool can be used to validate Haspin accessibility to the T119 in H2B or other sites.

Another strategy, generating peptide arrays for histone tail domains with the corresponding serine or threonine mutant. These arrays can be incubated with Haspin or other mitotic kinases such as Aurora B, PLK1, or CDK1 to identify some novel phospho-sites. Further, mass spectrometry analysis will be an asset to verify

the phosphorylation in vivo, in addition to generation of phospho-specific antibodies. Importantly, not all of the mitotic histone PTMs has been completely explored. Recently, it has been found that CDK1 phosphorylates serine 6 in the H2B N-terminal tail during mitosis (*293*).

Histone PTMs contribute to vital cellular processes, including proliferation, differentiation and repair (*207, 209*). One key mechanism of the PTM function is through recruiting a protein or a complex of proteins, which is called effector (or reader) (*207*). The interacting protein reads and translates the histone mark into a biological signal or effect. Therefore, identifying the reader may be necessary to understand the complete mechanism and function of a particular histone modification. Peptide pull-down is one of the most commonly used and credible methods for identifying histone modification readers (*294*). The major principal of the method relies on using a short peptide sequence representing the target histone tail domain carrying the specific modification of interest. This peptide must be biotinylated to allow its coupling with avidin, which is a tetrameric biotin-binding protein. The biotinylated peptide is incubated with avidin beads to generate the peptide-coupled beads that will be later incubated with the cellular extract. Associated proteins can then be identified by mass spectrometry. Such an assay can be used to identify the reader of H2BpT119 or a novel PTM.

Haspin mitotic substrates are still an important topic to study to better understand the regulatory mechanisms of chromosome segregation. Previous studies have revealed a detailed mechanism for Haspin function through H3pT3 during mitosis in human and xenopus cells (*252, 253*). Other studies have found that Haspin mitotic function is also through H3pT3 in yeast cells (*223, 295*). This thus indicates that the H3pT3 signaling pathway is evolutionarily conserved from yeast to humans. Importantly, Haspin mitotic function is not restricted to H3pT3 as it was discovered that Haspin could protect cohesion by phosphorylating WAPL protein (*250*). Moreover, advance proteomic analysis has identified several mitotic substrates for Haspin, but unfortunately none of these has been adequately

studied yet (*267*). Finally, the results of this project suggest that Haspin can also target H2B; this may suggest the discovery of a novel Haspin-dependent mitotic signaling pathway.

References

1. B. Alberts *et al.*, *Molecular biology of the cell*. (Garland Science, Taylor and Francis Group, New York, NY, ed. Sixth edition., 2015), pp. xxxiv, 1342, 1334, 1353, 1341 pages.
2. D. Lloyd, Biochemistry of the cell cycle. *Biochem J* **242**, 313-321 (1987).
3. A. N. Kousholt, T. Menzel, C. S. Sorensen, Pathways for genome integrity in G2 phase of the cell cycle. *Biomolecules* **2**, 579-607 (2012).
4. E. M. BB. Larsen, MK. Rhodes, JJ. Wiens, Inordinate Fondness Multiplied and Redistributed: the Number of Species on Earth and the New Pie of Life. *The Quarterly Review of Biology* **92**, (2017).
5. J. D. Wang, P. A. Levin, Metabolism, cell growth and the bacterial cell cycle. *Nat Rev Microbiol* **7**, 822-827 (2009).
6. D. M. Bryant, K. E. Mostov, From cells to organs: building polarized tissue. *Nat Rev Mol Cell Biol* **9**, 887-901 (2008).
7. K. P. Krafts, Tissue repair: The hidden drama. *Organogenesis* **6**, 225-233 (2010).
8. A. C. Chien, N. S. Hill, P. A. Levin, Cell size control in bacteria. *Curr Biol* **22**, R340-349 (2012).
9. I. M. Cheeseman, A. Desai, Molecular architecture of the kinetochore-microtubule interface. *Nat Rev Mol Cell Biol* **9**, 33-46 (2008).
10. D. A. Foster, P. Yellen, L. Xu, M. Saqcena, Regulation of G1 Cell Cycle Progression: Distinguishing the Restriction Point from a Nutrient-Sensing Cell Growth Checkpoint(s). *Genes Cancer* **1**, 1124-1131 (2010).
11. J. L. J Bartek, Pathways governing G1/S transition and their response to DNA damage. *FEBS Lett.* **490**, (2001).
12. K. J. Barnum, M. J. O'Connell, Cell cycle regulation by checkpoints. *Methods Mol Biol* **1170**, 29-40 (2014).
13. A. Ho, S. F. Dowdy, Regulation of G(1) cell-cycle progression by oncogenes and tumor suppressor genes. *Curr Opin Genet Dev* **12**, 47-52 (2002).
14. S. Lim, P. Kaldis, Cdks, cyclins and CKIs: roles beyond cell cycle regulation. *Development* **140**, 3079-3093 (2013).
15. O. Larsson, A. Zetterberg, W. Engstrom, Cell-cycle-specific induction of quiescence achieved by limited inhibition of protein synthesis: counteractive effect of addition of purified growth factors. *J Cell Sci* **73**, 375-387 (1985).
16. A. Maes *et al.*, The therapeutic potential of cell cycle targeting in multiple myeloma. *Oncotarget* **8**, 90501-90520 (2017).
17. L. H. Hartwell, J. Culotti, J. R. Pringle, B. J. Reid, Genetic control of the cell division cycle in yeast. *Science* **183**, 46-51 (1974).
18. B. Recolin, S. van der Laan, N. Tsanov, D. Maiorano, Molecular mechanisms of DNA replication checkpoint activation. *Genes (Basel)* **5**, 147-175 (2014).
19. R. A. Sclafani, T. M. Holzen, Cell cycle regulation of DNA replication. *Annu Rev Genet* **41**, 237-280 (2007).

20. D. Y. Takeda, A. Dutta, DNA replication and progression through S phase. *Oncogene* **24**, 2827-2843 (2005).
21. J. L. Bandura, B. R. Calvi, Duplication of the genome in normal and cancer cell cycles. *Cancer Biol Ther* **1**, 8-13 (2002).
22. E. Johansson, N. Dixon, Replicative DNA polymerases. *Cold Spring Harb Perspect Biol* **5**, (2013).
23. H. Masai, M. Foiani, in *Advances in Experimental Medicine and Biology,*. (Imprint: Springer, 2017), pp. 1 online resource (XII, 581 p. 594 illus., 587 illus. in color.).
24. R. Bailey, S. Priego Moreno, A. Gambus, Termination of DNA replication forks: "Breaking up is hard to do". *Nucleus* **6**, 187-196 (2015).
25. A. M. Narasimha *et al.*, Cyclin D activates the Rb tumor suppressor by mono-phosphorylation. *Elife* **3**, (2014).
26. D. O. Morgan, *The cell cycle : principles of control*. Primers in biology (New Science Press Ltd in association with Oxford University Press, London, 2007), pp. xxvii, 297 p.
27. A. Beucher *et al.*, ATM and Artemis promote homologous recombination of radiation-induced DNA double-strand breaks in G2. *EMBO J* **28**, 3413-3427 (2009).
28. H. H. Y. Chang, N. R. Pannunzio, N. Adachi, M. R. Lieber, Non-homologous DNA end joining and alternative pathways to double-strand break repair. *Nat Rev Mol Cell Biol* **18**, 495-506 (2017).
29. M. Jasin, R. Rothstein, Repair of strand breaks by homologous recombination. *Cold Spring Harb Perspect Biol* **5**, a012740 (2013).
30. Y. Kee, A. D. D'Andrea, Expanded roles of the Fanconi anemia pathway in preserving genomic stability. *Genes Dev* **24**, 1680-1694 (2010).
31. J. M. Enserink, R. D. Kolodner, An overview of Cdk1-controlled targets and processes. *Cell Div* **5**, 11 (2010).
32. Y. Huang, R. M. Sramkoski, J. W. Jacobberger, The kinetics of G2 and M transitions regulated by B cyclins. *PLoS One* **8**, e80861 (2013).
33. A. Lindqvist, V. Rodriguez-Bravo, R. H. Medema, The decision to enter mitosis: feedback and redundancy in the mitotic entry network. *J Cell Biol* **185**, 193-202 (2009).
34. N. Rhind, P. Russell, Signaling pathways that regulate cell division. *Cold Spring Harb Perspect Biol* **4**, (2012).
35. E. A. Nigg, Mitotic kinases as regulators of cell division and its checkpoints. *Nat Rev Mol Cell Biol* **2**, 21-32 (2001).
36. V. Lafarga *et al.*, TIAR marks nuclear G2/M transition granules and restricts CDK1 activity under replication stress. *EMBO Rep* **20**, (2019).
37. J. P. Chow, R. Y. Poon, The CDK1 inhibitory kinase MYT1 in DNA damage checkpoint recovery. *Oncogene* **32**, 4778-4788 (2013).
38. L. T. Vassilev, Cell cycle synchronization at the G2/M phase border by reversible inhibition of CDK1. *Cell Cycle* **5**, 2555-2556 (2006).
39. K. Luger, Nucleosomes: Structure and Function. *ENCYCLOPEDIA OF LIFE SCIENCES*, (2001).

40. H. J. Szerlong, J. C. Hansen, Nucleosome distribution and linker DNA: connecting nuclear function to dynamic chromatin structure. *Biochem Cell Biol* **89**, 24-34 (2011).
41. S. El Kennani, M. Crespo, J. Govin, D. Pflieger, Proteomic Analysis of Histone Variants and Their PTMs: Strategies and Pitfalls. *Proteomes* **6**, (2018).
42. A. Musacchio, E. D. Salmon, The spindle-assembly checkpoint in space and time. *Nat Rev Mol Cell Biol* **8**, 379-393 (2007).
43. S. Colaco, D. Modi, Genetics of the human Y chromosome and its association with male infertility. *Reprod Biol Endocrinol* **16**, 14 (2018).
44. W. Antonin, H. Neumann, Chromosome condensation and decondensation during mitosis. *Curr Opin Cell Biol* **40**, 15-22 (2016).
45. K. Nagasaka, M. J. Hossain, M. J. Roberti, J. Ellenberg, T. Hirota, Sister chromatid resolution is an intrinsic part of chromosome organization in prophase. *Nat Cell Biol* **18**, 692-699 (2016).
46. R. Ladurner *et al.*, Sororin actively maintains sister chromatid cohesion. *EMBO J* **35**, 635-653 (2016).
47. R. V. Skibbens, M. Maradeo, L. Eastman, Fork it over: the cohesion establishment factor Ctf7p and DNA replication. *J Cell Sci* **120**, 2471-2477 (2007).
48. J. M. Peters, A. Tedeschi, J. Schmitz, The cohesin complex and its roles in chromosome biology. *Genes Dev* **22**, 3089-3114 (2008).
49. K. Ishiguro, Y. Watanabe, Chromosome cohesion in mitosis and meiosis. *J Cell Sci* **120**, 367-369 (2007).
50. M. Yanagida, Clearing the way for mitosis: is cohesin a target? *Nat Rev Mol Cell Biol* **10**, 489-496 (2009).
51. N. Zhang, A. K. Panigrahi, Q. Mao, D. Pati, Interaction of Sororin protein with polo-like kinase 1 mediates resolution of chromosomal arm cohesion. *J Biol Chem* **286**, 41826-41837 (2011).
52. S. Hauf *et al.*, Dissociation of cohesin from chromosome arms and loss of arm cohesion during early mitosis depends on phosphorylation of SA2. *PLoS Biol* **3**, e69 (2005).
53. T. S. Kitajima *et al.*, Shugoshin collaborates with protein phosphatase 2A to protect cohesin. *Nature* **441**, 46-52 (2006).
54. D. L. Bauer, R. Marie, K. H. Rasmussen, A. Kristensen, K. U. Mir, DNA catenation maintains structure of human metaphase chromosomes. *Nucleic Acids Res* **40**, 11428-11434 (2012).
55. M. Antoniou-Kourounioti, M. L. Mimmack, A. C. G. Porter, C. J. Farr, The Impact of the C-Terminal Region on the Interaction of Topoisomerase II Alpha with Mitotic Chromatin. *Int J Mol Sci* **20**, (2019).
56. S. E. Hughes, R. S. Hawley, Topoisomerase II is required for the proper separation of heterochromatic regions during Drosophila melanogaster female meiosis. *PLoS Genet* **10**, e1004650 (2014).
57. A. W. Murray, J. W. Szostak, Chromosome segregation in mitosis and meiosis. *Annu Rev Cell Biol* **1**, 289-315 (1985).

58. T. Chen, Y. Sun, P. Ji, S. Kopetz, W. Zhang, Topoisomerase IIalpha in chromosome instability and personalized cancer therapy. *Oncogene* **34**, 4019-4031 (2015).
59. C. S. Downes, A. M. Mullinger, R. T. Johnson, Inhibitors of DNA topoisomerase II prevent chromatid separation in mammalian cells but do not prevent exit from mitosis. *Proc Natl Acad Sci U S A* **88**, 8895-8899 (1991).
60. Y. Zhai, P. J. Kronebusch, P. M. Simon, G. G. Borisy, Microtubule dynamics at the G2/M transition: abrupt breakdown of cytoplasmic microtubules at nuclear envelope breakdown and implications for spindle morphogenesis. *J Cell Biol* **135**, 201-214 (1996).
61. M. Kirschner, T. Mitchison, Beyond self-assembly: from microtubules to morphogenesis. *Cell* **45**, 329-342 (1986).
62. S. Petry, Mechanisms of Mitotic Spindle Assembly. *Annu Rev Biochem* **85**, 659-683 (2016).
63. S. L. Jaspersen, M. Winey, The budding yeast spindle pole body: structure, duplication, and function. *Annu Rev Cell Dev Biol* **20**, 1-28 (2004).
64. S. L. Kline-Smith, C. E. Walczak, Mitotic spindle assembly and chromosome segregation: refocusing on microtubule dynamics. *Mol Cell* **15**, 317-327 (2004).
65. Y. H. Chi, Z. J. Chen, K. T. Jeang, The nuclear envelopathies and human diseases. *J Biomed Sci* **16**, 96 (2009).
66. S. Sazer, Nuclear envelope: nuclear pore complexity. *Curr Biol* **15**, R23-26 (2005).
67. F. R. Putkey *et al.*, Unstable kinetochore-microtubule capture and chromosomal instability following deletion of CENP-E. *Dev Cell* **3**, 351-365 (2002).
68. Y. Yamagishi, T. Sakuno, Y. Goto, Y. Watanabe, Kinetochore composition and its function: lessons from yeasts. *FEMS Microbiol Rev* **38**, 185-200 (2014).
69. I. M. Cheeseman, The kinetochore. *Cold Spring Harb Perspect Biol* **6**, a015826 (2014).
70. S. Cao, K. Zhou, Z. Zhang, K. Luger, A. F. Straight, Constitutive centromere-associated network contacts confer differential stability on CENP-A nucleosomes in vitro and in the cell. *Mol Biol Cell* **29**, 751-762 (2018).
71. K. Bloom, E. Yeh, Tension management in the kinetochore. *Curr Biol* **20**, R1040-1048 (2010).
72. J. K. Monda, I. M. Cheeseman, The kinetochore-microtubule interface at a glance. *J Cell Sci* **131**, (2018).
73. D. Varma, E. D. Salmon, The KMN protein network--chief conductors of the kinetochore orchestra. *J Cell Sci* **125**, 5927-5936 (2012).
74. Y. W. Chan, A. A. Jeyaprakash, E. A. Nigg, A. Santamaria, Aurora B controls kinetochore-microtubule attachments by inhibiting Ska complex-KMN network interaction. *J Cell Biol* **196**, 563-571 (2012).
75. T. U. Tanaka, Kinetochore-microtubule interactions: steps towards bi-orientation. *EMBO J* **29**, 4070-4082 (2010).
76. C. A. Cooke, B. Schaar, T. J. Yen, W. C. Earnshaw, Localization of CENP-E in the fibrous corona and outer plate of mammalian kinetochores from prometaphase through anaphase. *Chromosoma* **106**, 446-455 (1997).

77. V. Magidson *et al.*, Adaptive changes in the kinetochore architecture facilitate proper spindle assembly. *Nat Cell Biol* **17**, 1134-1144 (2015).
78. Y. Luo, E. Ahmad, S. T. Liu, MAD1: Kinetochore Receptors and Catalytic Mechanisms. *Front Cell Dev Biol* **6**, 51 (2018).
79. G. Itoh *et al.*, Author Correction: Lateral attachment of kinetochores to microtubules is enriched in prometaphase rosette and facilitates chromosome alignment and bi-orientation establishment. *Sci Rep* **8**, 7003 (2018).
80. X. Wan *et al.*, Protein architecture of the human kinetochore microtubule attachment site. *Cell* **137**, 672-684 (2009).
81. D. M. Kern, J. K. Monda, K. C. Su, E. M. Wilson-Kubalek, I. M. Cheeseman, Astrin-SKAP complex reconstitution reveals its kinetochore interaction with microtubule-bound Ndc80. *Elife* **6**, (2017).
82. R. L. Shrestha, V. M. Draviam, Lateral to end-on conversion of chromosome-microtubule attachment requires kinesins CENP-E and MCAK. *Curr Biol* **23**, 1514-1526 (2013).
83. C. Ditchfield *et al.*, Aurora B couples chromosome alignment with anaphase by targeting BubR1, Mad2, and Cenp-E to kinetochores. *J Cell Biol* **161**, 267-280 (2003).
84. R. L. Shrestha *et al.*, Aurora-B kinase pathway controls the lateral to end-on conversion of kinetochore-microtubule attachments in human cells. *Nat Commun* **8**, 150 (2017).
85. T. Zhu *et al.*, Phosphorylation of microtubule-binding protein Hec1 by mitotic kinase Aurora B specifies spindle checkpoint kinase Mps1 signaling at the kinetochore. *J Biol Chem* **288**, 36149-36159 (2013).
86. M. Kalantzaki *et al.*, Kinetochore-microtubule error correction is driven by differentially regulated interaction modes. *Nat Cell Biol* **17**, 530 (2015).
87. J. P. Welburn *et al.*, Aurora B phosphorylates spatially distinct targets to differentially regulate the kinetochore-microtubule interface. *Mol Cell* **38**, 383-392 (2010).
88. F. A. Barr, U. Gruneberg, Cytokinesis: placing and making the final cut. *Cell* **131**, 847-860 (2007).
89. I. Nasa, A. N. Kettenbach, Coordination of Protein Kinase and Phosphoprotein Phosphatase Activities in Mitosis. *Front Cell Dev Biol* **6**, 30 (2018).
90. C. Acquaviva, J. Pines, The anaphase-promoting complex/cyclosome: APC/C. *J Cell Sci* **119**, 2401-2404 (2006).
91. E. Manchado, M. Eguren, M. Malumbres, The anaphase-promoting complex/cyclosome (APC/C): cell-cycle-dependent and -independent functions. *Biochem Soc Trans* **38**, 65-71 (2010).
92. A. M. Page, P. Hieter, The anaphase-promoting complex: new subunits and regulators. *Annu Rev Biochem* **68**, 583-609 (1999).
93. J. D. Reimann *et al.*, Emi1 is a mitotic regulator that interacts with Cdc20 and inhibits the anaphase promoting complex. *Cell* **105**, 645-655 (2001).
94. R. Grosskortenhaus, F. Sprenger, Rca1 inhibits APC-Cdh1(Fzr) and is required to prevent cyclin degradation in G2. *Dev Cell* **2**, 29-40 (2002).
95. H. C. Vodermaier, APC/C and SCF: controlling each other and the cell cycle. *Curr Biol* **14**, R787-796 (2004).

96. A. D. Rudner, A. W. Murray, Phosphorylation by Cdc28 activates the Cdc20-dependent activity of the anaphase-promoting complex. *J Cell Biol* **149**, 1377-1390 (2000).
97. H. Ohkura, Meiosis: an overview of key differences from mitosis. *Cold Spring Harb Perspect Biol* **7**, (2015).
98. Y. Hirose *et al.*, Chiasmata promote monopolar attachment of sister chromatids and their co-segregation toward the proper pole during meiosis I. *PLoS Genet* **7**, e1001329 (2011).
99. D. P. Melters, L. V. Paliulis, I. F. Korf, S. W. Chan, Holocentric chromosomes: convergent evolution, meiotic adaptations, and genomic analysis. *Chromosome Res* **20**, 579-593 (2012).
100. Y. Watanabe, P. Nurse, Cohesin Rec8 is required for reductional chromosome segregation at meiosis. *Nature* **400**, 461-464 (1999).
101. N. R. Kudo *et al.*, Role of cleavage by separase of the Rec8 kleisin subunit of cohesin during mammalian meiosis I. *J Cell Sci* **122**, 2686-2698 (2009).
102. M. Malumbres, M. Barbacid, Cell cycle, CDKs and cancer: a changing paradigm. *Nat Rev Cancer* **9**, 153-166 (2009).
103. V. L. Katis *et al.*, Spo13 facilitates monopolin recruitment to kinetochores and regulates maintenance of centromeric cohesion during yeast meiosis. *Curr Biol* **14**, 2183-2196 (2004).
104. A. Toth *et al.*, Functional genomics identifies monopolin: a kinetochore protein required for segregation of homologs during meiosis i. *Cell* **103**, 1155-1168 (2000).
105. S. Yokobayashi, Y. Watanabe, The kinetochore protein Moa1 enables cohesion-mediated monopolar attachment at meiosis I. *Cell* **123**, 803-817 (2005).
106. J. Kim *et al.*, Author Correction: Meikin is a conserved regulator of meiosis-I-specific kinetochore function. *Nature* **563**, E23 (2018).
107. T. Hassold, H. Hall, P. Hunt, The origin of human aneuploidy: where we have been, where we are going. *Hum Mol Genet* **16 Spec No. 2**, R203-208 (2007).
108. T. Chiang, R. M. Schultz, M. A. Lampson, Meiotic origins of maternal age-related aneuploidy. *Biol Reprod* **86**, 1-7 (2012).
109. M. S. Levine, A. J. Holland, The impact of mitotic errors on cell proliferation and tumorigenesis. *Genes Dev* **32**, 620-638 (2018).
110. L. Pikor, K. Thu, E. Vucic, W. Lam, The detection and implication of genome instability in cancer. *Cancer Metastasis Rev* **32**, 341-352 (2013).
111. N. K. Chunduri, Z. Storchova, The diverse consequences of aneuploidy. *Nat Cell Biol* **21**, 54-62 (2019).
112. S. L. Thompson, S. F. Bakhoum, D. A. Compton, Mechanisms of chromosomal instability. *Curr Biol* **20**, R285-295 (2010).
113. S. L. Thompson, D. A. Compton, Proliferation of aneuploid human cells is limited by a p53-dependent mechanism. *J Cell Biol* **188**, 369-381 (2010).
114. G. J. Gorbsky, Kinetochores, microtubules and the metaphase checkpoint. *Trends Cell Biol* **5**, 143-148 (1995).
115. P. Silva *et al.*, Monitoring the fidelity of mitotic chromosome segregation by the spindle assembly checkpoint. *Cell Prolif* **44**, 391-400 (2011).

116. P. T. Stukenberg, D. J. Burke, Connecting the microtubule attachment status of each kinetochore to cell cycle arrest through the spindle assembly checkpoint. *Chromosoma* **124**, 463-480 (2015).
117. J. Kuhn, S. Dumont, Spindle assembly checkpoint satisfaction occurs via end-on but not lateral attachments under tension. *J Cell Biol* **216**, 1533-1542 (2017).
118. H. Lee, How chromosome mis-segregation leads to cancer: lessons from BubR1 mouse models. *Mol Cells* **37**, 713-718 (2014).
119. A. A. Guerrero, A. C. Martinez, K. H. van Wely, Merotelic attachments and non-homologous end joining are the basis of chromosomal instability. *Cell Div* **5**, 13 (2010).
120. M. A. Hoyt, L. Totis, B. T. Roberts, S. cerevisiae genes required for cell cycle arrest in response to loss of microtubule function. *Cell* **66**, 507-517 (1991).
121. R. Li, A. W. Murray, Feedback control of mitosis in budding yeast. *Cell* **66**, 519-531 (1991).
122. A. Musacchio, The Molecular Biology of Spindle Assembly Checkpoint Signaling Dynamics. *Curr Biol* **25**, R1002-1018 (2015).
123. M. C. Caillaud *et al.*, Spindle assembly checkpoint protein dynamics reveal conserved and unsuspected roles in plant cell division. *PLoS One* **4**, e6757 (2009).
124. S. T. Liu, H. Zhang, The mitotic checkpoint complex (MCC): looking back and forth after 15 years. *AIMS Mol Sci* **3**, 597-634 (2016).
125. A. Musacchio, A. Ciliberto, The spindle-assembly checkpoint and the beauty of self-destruction. *Nat Struct Mol Biol* **19**, 1059-1061 (2012).
126. A. C. Faesen *et al.*, Basis of catalytic assembly of the mitotic checkpoint complex. *Nature* **542**, 498-502 (2017).
127. G. Fang, H. Yu, M. W. Kirschner, The checkpoint protein MAD2 and the mitotic regulator CDC20 form a ternary complex with the anaphase-promoting complex to control anaphase initiation. *Genes Dev* **12**, 1871-1883 (1998).
128. A. De Antoni *et al.*, The Mad1/Mad2 complex as a template for Mad2 activation in the spindle assembly checkpoint. *Curr Biol* **15**, 214-225 (2005).
129. A. R. Tipton, M. Tipton, T. Yen, S. T. Liu, Closed MAD2 (C-MAD2) is selectively incorporated into the mitotic checkpoint complex (MCC). *Cell Cycle* **10**, 3740-3750 (2011).
130. M. Mapelli, L. Massimiliano, S. Santaguida, A. Musacchio, The Mad2 conformational dimer: structure and implications for the spindle assembly checkpoint. *Cell* **131**, 730-743 (2007).
131. V. Silio, A. D. McAinsh, J. B. Millar, KNL1-Bubs and RZZ Provide Two Separable Pathways for Checkpoint Activation at Human Kinetochores. *Dev Cell* **35**, 600-613 (2015).
132. M. Yang *et al.*, Insights into mad2 regulation in the spindle checkpoint revealed by the crystal structure of the symmetric mad2 dimer. *PLoS Biol* **6**, e50 (2008).
133. A. M. V. West, E. A. Komives, K. D. Corbett, Conformational dynamics of the Hop1 HORMA domain reveal a common mechanism with the spindle checkpoint protein Mad2. *Nucleic Acids Res* **46**, 279-292 (2018).
134. S. C. Rosenberg, K. D. Corbett, The multifaceted roles of the HORMA domain in cellular signaling. *J Cell Biol* **211**, 745-755 (2015).

135. F. G. Westhorpe, A. Tighe, P. Lara-Gonzalez, S. S. Taylor, p31comet-mediated extraction of Mad2 from the MCC promotes efficient mitotic exit. *J Cell Sci* **124**, 3905-3916 (2011).
136. Q. Ye *et al.*, TRIP13 is a protein-remodeling AAA+ ATPase that catalyzes MAD2 conformation switching. *Elife* **4**, (2015).
137. K. Uzunova *et al.*, APC15 mediates CDC20 autoubiquitylation by APC/C(MCC) and disassembly of the mitotic checkpoint complex. *Nat Struct Mol Biol* **19**, 1116-1123 (2012).
138. G. Varetti, C. Guida, S. Santaguida, E. Chiroli, A. Musacchio, Homeostatic control of mitotic arrest. *Mol Cell* **44**, 710-720 (2011).
139. A. Kulukian, J. S. Han, D. W. Cleveland, Unattached kinetochores catalyze production of an anaphase inhibitor that requires a Mad2 template to prime Cdc20 for BubR1 binding. *Dev Cell* **16**, 105-117 (2009).
140. G. K. Chan, S. T. Liu, T. J. Yen, Kinetochore structure and function. *Trends Cell Biol* **15**, 589-598 (2005).
141. P. Lara-Gonzalez, F. G. Westhorpe, S. S. Taylor, The spindle assembly checkpoint. *Curr Biol* **22**, R966-980 (2012).
142. A. DeAntoni, V. Sala, A. Musacchio, Explaining the oligomerization properties of the spindle assembly checkpoint protein Mad2. *Philos Trans R Soc Lond B Biol Sci* **360**, 637-647, discussion 447-638 (2005).
143. V. Sudakin, G. K. Chan, T. J. Yen, Checkpoint inhibition of the APC/C in HeLa cells is mediated by a complex of BUBR1, BUB3, CDC20, and MAD2. *J Cell Biol* **154**, 925-936 (2001).
144. A. Eskat *et al.*, Step-wise assembly, maturation and dynamic behavior of the human CENP-P/O/R/Q/U kinetochore sub-complex. *PLoS One* **7**, e44717 (2012).
145. L. A. Harasymiw, D. Tank, M. McClellan, N. Panigrahy, M. K. Gardner, Centromere mechanical maturation during mammalian cell mitosis. *Nat Commun* **10**, 1761 (2019).
146. C. Sacristan, G. J. Kops, Joined at the hip: kinetochores, microtubules, and spindle assembly checkpoint signaling. *Trends Cell Biol* **25**, 21-28 (2015).
147. J. Maciejowski *et al.*, Mps1 directs the assembly of Cdc20 inhibitory complexes during interphase and mitosis to control M phase timing and spindle checkpoint signaling. *J Cell Biol* **190**, 89-100 (2010).
148. P. Meraldi, V. M. Draviam, P. K. Sorger, Timing and checkpoints in the regulation of mitotic progression. *Dev Cell* **7**, 45-60 (2004).
149. M. J. Emanuele *et al.*, Aurora B kinase and protein phosphatase 1 have opposing roles in modulating kinetochore assembly. *J Cell Biol* **181**, 241-254 (2008).
150. Z. Ji, H. Gao, L. Jia, B. Li, H. Yu, A sequential multi-target Mps1 phosphorylation cascade promotes spindle checkpoint signaling. *Elife* **6**, (2017).
151. Y. Yamagishi, C. H. Yang, Y. Tanno, Y. Watanabe, MPS1/Mph1 phosphorylates the kinetochore protein KNL1/Spc7 to recruit SAC components. *Nat Cell Biol* **14**, 746-752 (2012).
152. L. A. Shepperd *et al.*, Phosphodependent recruitment of Bub1 and Bub3 to Spc7/KNL1 by Mph1 kinase maintains the spindle checkpoint. *Curr Biol* **22**, 891-899 (2012).

153. M. D. Gurden, S. J. Anderhub, A. Faisal, S. Linardopoulos, Aurora B prevents premature removal of spindle assembly checkpoint proteins from the kinetochore: A key role for Aurora B in mitosis. *Oncotarget* **9**, 19525-19542 (2018).
154. B. B. Gadea, J. V. Ruderman, Aurora kinase inhibitor ZM447439 blocks chromosome-induced spindle assembly, the completion of chromosome condensation, and the establishment of the spindle integrity checkpoint in Xenopus egg extracts. *Mol Biol Cell* **16**, 1305-1318 (2005).
155. S. Santaguida, A. Tighe, A. M. D'Alise, S. S. Taylor, A. Musacchio, Dissecting the role of MPS1 in chromosome biorientation and the spindle checkpoint through the small molecule inhibitor reversine. *J Cell Biol* **190**, 73-87 (2010).
156. A. T. Saurin, M. S. van der Waal, R. H. Medema, S. M. Lens, G. J. Kops, Aurora B potentiates Mps1 activation to ensure rapid checkpoint establishment at the onset of mitosis. *Nat Commun* **2**, 316 (2011).
157. S. D'Arcy, O. R. Davies, T. L. Blundell, V. M. Bolanos-Garcia, Defining the molecular basis of BubR1 kinetochore interactions and APC/C-CDC20 inhibition. *J Biol Chem* **285**, 14764-14776 (2010).
158. X. Wang *et al.*, The mitotic checkpoint protein hBUB3 and the mRNA export factor hRAE1 interact with GLE2p-binding sequence (GLEBS)-containing proteins. *J Biol Chem* **276**, 26559-26567 (2001).
159. P. Lara-Gonzalez, M. I. Scott, M. Diez, O. Sen, S. S. Taylor, BubR1 blocks substrate recruitment to the APC/C in a KEN-box-dependent manner. *J Cell Sci* **124**, 4332-4345 (2011).
160. K. Overlack *et al.*, BubR1 Promotes Bub3-Dependent APC/C Inhibition during Spindle Assembly Checkpoint Signaling. *Curr Biol* **27**, 2915-2927 e2917 (2017).
161. V. Krenn, A. Musacchio, The Aurora B Kinase in Chromosome Bi-Orientation and Spindle Checkpoint Signaling. *Front Oncol* **5**, 225 (2015).
162. B. Lesage, J. Qian, M. Bollen, Spindle checkpoint silencing: PP1 tips the balance. *Curr Biol* **21**, R898-903 (2011).
163. D. Liu *et al.*, Regulated targeting of protein phosphatase 1 to the outer kinetochore by KNL1 opposes Aurora B kinase. *J Cell Biol* **188**, 809-820 (2010).
164. G. Vallardi, A. T. Saurin, Mitotic kinases and phosphatases cooperate to shape the right response. *Cell Cycle* **14**, 795-796 (2015).
165. W. Nijenhuis, G. Vallardi, A. Teixeira, G. J. Kops, A. T. Saurin, Negative feedback at kinetochores underlies a responsive spindle checkpoint signal. *Nat Cell Biol* **16**, 1257-1264 (2014).
166. S. Sivakumar *et al.*, The human SKA complex drives the metaphase-anaphase cell cycle transition by recruiting protein phosphatase 1 to kinetochores. *Elife* **5**, (2016).
167. M. Yang *et al.*, p31comet blocks Mad2 activation through structural mimicry. *Cell* **131**, 744-755 (2007).
168. E. Eytan *et al.*, Disassembly of mitotic checkpoint complexes by the joint action of the AAA-ATPase TRIP13 and p31(comet). *Proc Natl Acad Sci U S A* **111**, 12019-12024 (2014).

169. C. Rizzardi *et al.*, MAD2 expression in oral squamous cell carcinoma and its relationship to tumor grade and proliferation. *Anticancer Res* **34**, 7021-7027 (2014).
170. A. Maciejczyk *et al.*, Elevated BUBR1 expression is associated with poor survival in early breast cancer patients: 15-year follow-up analysis. *J Histochem Cytochem* **61**, 330-339 (2013).
171. M. Hu *et al.*, Abnormal expression of the mitotic checkpoint protein BubR1 contributes to the anti-microtubule drug resistance of esophageal squamous cell carcinoma cells. *Oncol Rep* **29**, 185-192 (2013).
172. H. Grabsch *et al.*, Overexpression of the mitotic checkpoint genes BUB1, BUBR1, and BUB3 in gastric cancer--association with tumour cell proliferation. *J Pathol* **200**, 16-22 (2003).
173. B. Yuan *et al.*, Increased expression of mitotic checkpoint genes in breast cancer cells with chromosomal instability. *Clin Cancer Res* **12**, 405-410 (2006).
174. Correction: Significance of MAD2 Expression to Mitotic Checkpoint Control in Ovarian Cancer Cells. *Cancer Res* **78**, 4800 (2018).
175. P. Chieffi, Aurora B: A new promising therapeutic target in cancer. *Intractable Rare Dis Res* **7**, 141-144 (2018).
176. B. A. Pinsky, C. Kung, K. M. Shokat, S. Biggins, The Ipl1-Aurora protein kinase activates the spindle checkpoint by creating unattached kinetochores. *Nat Cell Biol* **8**, 78-83 (2006).
177. D. Cimini *et al.*, Merotelic kinetochore orientation is a major mechanism of aneuploidy in mitotic mammalian tissue cells. *J Cell Biol* **153**, 517-527 (2001).
178. D. Cimini, B. Moree, J. C. Canman, E. D. Salmon, Merotelic kinetochore orientation occurs frequently during early mitosis in mammalian tissue cells and error correction is achieved by two different mechanisms. *J Cell Sci* **116**, 4213-4225 (2003).
179. S. L. Thompson, D. A. Compton, Chromosome missegregation in human cells arises through specific types of kinetochore-microtubule attachment errors. *Proc Natl Acad Sci U S A* **108**, 17974-17978 (2011).
180. J. D. Bishop, J. M. Schumacher, Phosphorylation of the carboxyl terminus of inner centromere protein (INCENP) by the Aurora B Kinase stimulates Aurora B kinase activity. *J Biol Chem* **277**, 27577-27580 (2002).
181. K. Tanaka, Regulatory mechanisms of kinetochore-microtubule interaction in mitosis. *Cell Mol Life Sci* **70**, 559-579 (2013).
182. D. Liu, G. Vader, M. J. Vromans, M. A. Lampson, S. M. Lens, Sensing chromosome bi-orientation by spatial separation of aurora B kinase from kinetochore substrates. *Science* **323**, 1350-1353 (2009).
183. T. U. Tanaka, Bi-orienting chromosomes: acrobatics on the mitotic spindle. *Chromosoma* **117**, 521-533 (2008).
184. B. Nicklas, How Cells Get the Right Chromosomes. *Science* **275**, (1997).
185. J. Gregan, S. Polakova, L. Zhang, I. M. Tolic-Norrelykke, D. Cimini, Merotelic kinetochore attachment: causes and effects. *Trends Cell Biol* **21**, 374-381 (2011).
186. B. G. Fuller *et al.*, Midzone activation of aurora B in anaphase produces an intracellular phosphorylation gradient. *Nature* **453**, 1132-1136 (2008).

187. G. J. Guimaraes, Y. Dong, B. F. McEwen, J. G. Deluca, Kinetochore-microtubule attachment relies on the disordered N-terminal tail domain of Hec1. *Curr Biol* **18**, 1778-1784 (2008).
188. L. J. Sundin, G. J. Guimaraes, J. G. Deluca, The NDC80 complex proteins Nuf2 and Hec1 make distinct contributions to kinetochore-microtubule attachment in mitosis. *Mol Biol Cell* **22**, 759-768 (2011).
189. S. A. Miller, M. L. Johnson, P. T. Stukenberg, Kinetochore attachments require an interaction between unstructured tails on microtubules and Ndc80(Hec1). *Curr Biol* **18**, 1785-1791 (2008).
190. J. G. DeLuca *et al.*, Kinetochore microtubule dynamics and attachment stability are regulated by Hec1. *Cell* **127**, 969-982 (2006).
191. I. M. Cheeseman, J. S. Chappie, E. M. Wilson-Kubalek, A. Desai, The conserved KMN network constitutes the core microtubule-binding site of the kinetochore. *Cell* **127**, 983-997 (2006).
192. M. A. Lampson, I. M. Cheeseman, Sensing centromere tension: Aurora B and the regulation of kinetochore function. *Trends Cell Biol* **21**, 133-140 (2011).
193. P. D. Andrews *et al.*, Aurora B regulates MCAK at the mitotic centromere. *Dev Cell* **6**, 253-268 (2004).
194. W. Lan *et al.*, Aurora B phosphorylates centromeric MCAK and regulates its localization and microtubule depolymerization activity. *Curr Biol* **14**, 273-286 (2004).
195. X. Zhang, W. Lan, S. C. Ems-McClung, P. T. Stukenberg, C. E. Walczak, Aurora B phosphorylates multiple sites on mitotic centromere-associated kinesin to spatially and temporally regulate its function. *Mol Biol Cell* **18**, 3264-3276 (2007).
196. A. L. Knowlton, V. V. Vorozhko, W. Lan, G. J. Gorbsky, P. T. Stukenberg, ICIS and Aurora B coregulate the microtubule depolymerase Kif2a. *Curr Biol* **19**, 758-763 (2009).
197. S. Kim, H. Yu, Multiple assembly mechanisms anchor the KMN spindle checkpoint platform at human mitotic kinetochores. *J Cell Biol* **208**, 181-196 (2015).
198. Y. Yang *et al.*, Phosphorylation of HsMis13 by Aurora B kinase is essential for assembly of functional kinetochore. *J Biol Chem* **283**, 26726-26736 (2008).
199. X. Zhou *et al.*, Phosphorylation of CENP-C by Aurora B facilitates kinetochore attachment error correction in mitosis. *Proc Natl Acad Sci U S A* **114**, E10667-E10676 (2017).
200. C. S. Campbell, A. Desai, Tension sensing by Aurora B kinase is independent of survivin-based centromere localization. *Nature* **497**, 118-121 (2013).
201. T. J. Maresca, E. D. Salmon, Intrakinetochore stretch is associated with changes in kinetochore phosphorylation and spindle assembly checkpoint activity. *J Cell Biol* **184**, 373-381 (2009).
202. S. Li, Implication of posttranslational histone modifications in nucleotide excision repair. *Int J Mol Sci* **13**, 12461-12486 (2012).
203. T. J. Kang, S. Yuzawa, H. Suga, Expression of histone H3 tails with combinatorial lysine modifications under the reprogrammed genetic code for the investigation on epigenetic markers. *Chem Biol* **15**, 1166-1174 (2008).

204. D. Corujo, M. Buschbeck, Post-Translational Modifications of H2A Histone Variants and Their Role in Cancer. *Cancers (Basel)* **10**, (2018).
205. R. C. Molden, N. V. Bhanu, G. LeRoy, A. M. Arnaudo, B. A. Garcia, Multi-faceted quantitative proteomics analysis of histone H2B isoforms and their modifications. *Epigenetics Chromatin* **8**, 15 (2015).
206. J. C. Hansen *et al.*, The 10-nm chromatin fiber and its relationship to interphase chromosome organization. *Biochem Soc Trans* **46**, 67-76 (2018).
207. J. R. Tollervey, V. V. Lunyak, Epigenetics: judge, jury and executioner of stem cell fate. *Epigenetics* **7**, 823-840 (2012).
208. W. Li, Y. Ye, Polyubiquitin chains: functions, structures, and mechanisms. *Cell Mol Life Sci* **65**, 2397-2406 (2008).
209. F. Wang, J. M. Higgins, Histone modifications and mitosis: countermarks, landmarks, and bookmarks. *Trends Cell Biol* **23**, 175-184 (2013).
210. J. Y. Kaimori *et al.*, Histone H4 lysine 20 acetylation is associated with gene repression in human cells. *Sci Rep* **6**, 24318 (2016).
211. K. Overlack *et al.*, A molecular basis for the differential roles of Bub1 and BubR1 in the spindle assembly checkpoint. *Elife* **4**, e05269 (2015).
212. V. M. Bolanos-Garcia, J. Nilsson, T. L. Blundell, The architecture of the BubR1 tetratricopeptide tandem repeat defines a protein motif underlying mitotic checkpoint-kinetochore communication. *Bioarchitecture* **2**, 23-27 (2012).
213. V. Krenn, A. Wehenkel, X. Li, S. Santaguida, A. Musacchio, Structural analysis reveals features of the spindle checkpoint kinase Bub1-kinetochore subunit Knl1 interaction. *J Cell Biol* **196**, 451-467 (2012).
214. V. M. Bolanos-Garcia, T. L. Blundell, BUB1 and BUBR1: multifaceted kinases of the cell cycle. *Trends Biochem Sci* **36**, 141-150 (2011).
215. M. Vleugel *et al.*, Dissecting the roles of human BUB1 in the spindle assembly checkpoint. *J Cell Sci* **128**, 2975-2982 (2015).
216. C. Klebig, D. Korinth, P. Meraldi, Bub1 regulates chromosome segregation in a kinetochore-independent manner. *J Cell Biol* **185**, 841-858 (2009).
217. W. Qi, H. Yu, KEN-box-dependent degradation of the Bub1 spindle checkpoint kinase by the anaphase-promoting complex/cyclosome. *J Biol Chem* **282**, 3672-3679 (2007).
218. V. L. Johnson, M. I. Scott, S. V. Holt, D. Hussein, S. S. Taylor, Bub1 is required for kinetochore localization of BubR1, Cenp-E, Cenp-F and Mad2, and chromosome congression. *J Cell Sci* **117**, 1577-1589 (2004).
219. C. D. Warren *et al.*, Distinct chromosome segregation roles for spindle checkpoint proteins. *Mol Biol Cell* **13**, 3029-3041 (2002).
220. S. Yamaguchi, A. Decottignies, P. Nurse, Function of Cdc2p-dependent Bub1p phosphorylation and Bub1p kinase activity in the mitotic and meiotic spindle checkpoint. *EMBO J* **22**, 1075-1087 (2003).
221. A. P. Baron *et al.*, Probing the catalytic functions of Bub1 kinase using the small molecule inhibitors BAY-320 and BAY-524. *Elife* **5**, (2016).
222. S. A. Kawashima, Y. Yamagishi, T. Honda, K. Ishiguro, Y. Watanabe, Phosphorylation of H2A by Bub1 prevents chromosomal instability through localizing shugoshin. *Science* **327**, 172-177 (2010).

223. Y. Yamagishi, T. Honda, Y. Tanno, Y. Watanabe, Two histone marks establish the inner centromere and chromosome bi-orientation. *Science* **330**, 239-243 (2010).
224. T. S. Kitajima, S. A. Kawashima, Y. Watanabe, The conserved kinetochore protein shugoshin protects centromeric cohesion during meiosis. *Nature* **427**, 510-517 (2004).
225. A. L. Marston, W. H. Tham, H. Shah, A. Amon, A genome-wide screen identifies genes required for centromeric cohesion. *Science* **303**, 1367-1370 (2004).
226. V. L. Katis, M. Galova, K. P. Rabitsch, J. Gregan, K. Nasmyth, Maintenance of cohesin at centromeres after meiosis I in budding yeast requires a kinetochore-associated protein related to MEI-S332. *Curr Biol* **14**, 560-572 (2004).
227. K. P. Rabitsch *et al.*, Two fission yeast homologs of Drosophila Mei-S332 are required for chromosome segregation during meiosis I and II. *Curr Biol* **14**, 287-301 (2004).
228. Z. Tang, Y. Sun, S. E. Harley, H. Zou, H. Yu, Human Bub1 protects centromeric sister-chromatid cohesion through Shugoshin during mitosis. *Proc Natl Acad Sci U S A* **101**, 18012-18017 (2004).
229. T. S. Kitajima, S. Hauf, M. Ohsugi, T. Yamamoto, Y. Watanabe, Human Bub1 defines the persistent cohesion site along the mitotic chromosome by affecting Shugoshin localization. *Curr Biol* **15**, 353-359 (2005).
230. B. E. McGuinness, T. Hirota, N. R. Kudo, J. M. Peters, K. Nasmyth, Shugoshin prevents dissociation of cohesin from centromeres during mitosis in vertebrate cells. *PLoS Biol* **3**, e86 (2005).
231. K. Shintomi, T. Hirano, Releasing cohesin from chromosome arms in early mitosis: opposing actions of Wapl-Pds5 and Sgo1. *Genes Dev* **23**, 2224-2236 (2009).
232. M. Nakajima *et al.*, The complete removal of cohesin from chromosome arms depends on separase. *J Cell Sci* **120**, 4188-4196 (2007).
233. H. Liu, S. Rankin, H. Yu, Phosphorylation-enabled binding of SGO1-PP2A to cohesin protects sororin and centromeric cohesion during mitosis. *Nat Cell Biol* **15**, 40-49 (2013).
234. M. E. Bekier, T. Mazur, M. S. Rashid, W. R. Taylor, Borealin dimerization mediates optimal CPC checkpoint function by enhancing localization to centromeres and kinetochores. *Nat Commun* **6**, 6775 (2015).
235. H. Tanaka *et al.*, Isolation and characterization of cDNA clones specifically expressed in testicular germ cells. *FEBS Lett* **355**, 4-10 (1994).
236. H. Tanaka *et al.*, Identification and characterization of a haploid germ cell-specific nuclear protein kinase (Haspin) in spermatid nuclei and its effects on somatic cells. *J Biol Chem* **274**, 17049-17057 (1999).
237. L. B. Klickstein, Production of a subtracted cDNA library. *Curr Protoc Mol Biol* **Chapter 25**, Unit 25B 21 (2001).
238. F. Villa *et al.*, Crystal structure of the catalytic domain of Haspin, an atypical kinase implicated in chromatin organization. *Proc Natl Acad Sci U S A* **106**, 20204-20209 (2009).
239. J. Eswaran *et al.*, Structure and functional characterization of the atypical human kinase haspin. *Proc Natl Acad Sci U S A* **106**, 20198-20203 (2009).

240. J. M. Higgins, The Haspin gene: location in an intron of the integrin alphaE gene, associated transcription of an integrin alphaE-derived RNA and expression in diploid as well as haploid cells. *Gene* **267**, 55-69 (2001).
241. J. M. Higgins, Haspin-like proteins: a new family of evolutionarily conserved putative eukaryotic protein kinases. *Protein Sci* **10**, 1677-1684 (2001).
242. J. M. Higgins, Structure, function and evolution of haspin and haspin-related proteins, a distinctive group of eukaryotic protein kinases. *Cell Mol Life Sci* **60**, 446-462 (2003).
243. A. Nespoli *et al.*, Alk1 and Alk2 are two new cell cycle-regulated haspin-like proteins in budding yeast. *Cell Cycle* **5**, 1464-1471 (2006).
244. J. M. Higgins, Haspin: a newly discovered regulator of mitotic chromosome behavior. *Chromosoma* **119**, 137-147 (2010).
245. J. Dai, S. Sultan, S. S. Taylor, J. M. Higgins, The kinase haspin is required for mitotic histone H3 Thr 3 phosphorylation and normal metaphase chromosome alignment. *Genes Dev* **19**, 472-488 (2005).
246. F. Wang *et al.*, Haspin inhibitors reveal centromeric functions of Aurora B in chromosome segregation. *J Cell Biol* **199**, 251-268 (2012).
247. J. Dai, B. A. Sullivan, J. M. Higgins, Regulation of mitotic chromosome cohesion by Haspin and Aurora B. *Dev Cell* **11**, 741-750 (2006).
248. K. L. McKinley, I. M. Cheeseman, Large-Scale Analysis of CRISPR/Cas9 Cell-Cycle Knockouts Reveals the Diversity of p53-Dependent Responses to Cell-Cycle Defects. *Dev Cell* **40**, 405-420 e402 (2017).
249. L. Zhou *et al.*, The N-Terminal Non-Kinase-Domain-Mediated Binding of Haspin to Pds5B Protects Centromeric Cohesion in Mitosis. *Curr Biol* **27**, 992-1004 (2017).
250. C. Liang *et al.*, A kinase-dependent role for Haspin in antagonizing Wapl and protecting mitotic centromere cohesion. *EMBO Rep* **19**, 43-56 (2018).
251. M. M. Yoshida, L. Ting, S. P. Gygi, Y. Azuma, SUMOylation of DNA topoisomerase IIalpha regulates histone H3 kinase Haspin and H3 phosphorylation in mitosis. *J Cell Biol* **213**, 665-678 (2016).
252. C. Ghenoiu, M. S. Wheelock, H. Funabiki, Autoinhibition and Polo-dependent multisite phosphorylation restrict activity of the histone H3 kinase Haspin to mitosis. *Mol Cell* **52**, 734-745 (2013).
253. L. Zhou, X. Tian, C. Zhu, F. Wang, J. M. Higgins, Polo-like kinase-1 triggers histone phosphorylation by Haspin in mitosis. *EMBO Rep* **15**, 273-281 (2014).
254. T. Moutinho-Santos, H. Maiato, Plk1 puts a (Has)pin on the mitotic histone code. *EMBO Rep* **15**, 203-204 (2014).
255. A. A. Jeyaprakash, C. Basquin, U. Jayachandran, E. Conti, Structural basis for the recognition of phosphorylated histone h3 by the survivin subunit of the chromosomal passenger complex. *Structure* **19**, 1625-1634 (2011).
256. E. Niedzialkowska *et al.*, Molecular basis for phosphospecific recognition of histone H3 tails by Survivin paralogues at inner centromeres. *Mol Biol Cell* **23**, 1457-1466 (2012).
257. A. A. Jeyaprakash *et al.*, Structure of a Survivin-Borealin-INCENP core complex reveals how chromosomal passengers travel together. *Cell* **131**, 271-285 (2007).

258. R. Honda, R. Korner, E. A. Nigg, Exploring the functional interactions between Aurora B, INCENP, and survivin in mitosis. *Mol Biol Cell* **14**, 3325-3341 (2003).
259. J. Haase, M. K. Bonner, H. Halas, A. E. Kelly, Distinct Roles of the Chromosomal Passenger Complex in the Detection of and Response to Errors in Kinetochore-Microtubule Attachment. *Dev Cell* **42**, 640-654 e645 (2017).
260. A. De Antoni, S. Maffini, S. Knapp, A. Musacchio, S. Santaguida, A small-molecule inhibitor of Haspin alters the kinetochore functions of Aurora B. *J Cell Biol* **199**, 269-284 (2012).
261. F. Wang *et al.*, Histone H3 Thr-3 phosphorylation by Haspin positions Aurora B at centromeres in mitosis. *Science* **330**, 231-235 (2010).
262. C. van de Werken *et al.*, Chromosome segregation regulation in human zygotes: altered mitotic histone phosphorylation dynamics underlying centromeric targeting of the chromosomal passenger complex. *Hum Reprod* **30**, 2275-2291 (2015).
263. R. S. Nozawa *et al.*, Human POGZ modulates dissociation of HP1alpha from mitotic chromosome arms through Aurora B activation. *Nat Cell Biol* **12**, 719-727 (2010).
264. J. G. Ruppert *et al.*, HP1alpha targets the chromosomal passenger complex for activation at heterochromatin before mitotic entry. *EMBO J* **37**, (2018).
265. T. Tsukahara, Y. Tanno, Y. Watanabe, Phosphorylation of the CPC by Cdk1 promotes chromosome bi-orientation. *Nature* **467**, 719-723 (2010).
266. J. Qian, M. Beullens, B. Lesage, M. Bollen, Aurora B defines its own chromosomal targeting by opposing the recruitment of the phosphatase scaffold Repo-Man. *Curr Biol* **23**, 1136-1143 (2013).
267. A. Maiolica *et al.*, Modulation of the chromatin phosphoproteome by the Haspin protein kinase. *Mol Cell Proteomics* **13**, 1724-1740 (2014).
268. H. Liu, J. H. Naismith, An efficient one-step site-directed deletion, insertion, single and multiple-site plasmid mutagenesis protocol. *BMC Biotechnol* **8**, 91 (2008).
269. A. Motif, Histone Purification Mini Kit. (2014).
270. P. Rodriguez-Collazo, S. H. Leuba, J. Zlatanova, Robust methods for purification of histones from cultured mammalian cells with the preservation of their native modifications. *Nucleic Acids Res* **37**, e81 (2009).
271. A. Motif, Histone Purification Kit. (2014).
272. S. H. L. Pedro Rodriguez-Collazo, Jordanka Zlafanova Method of Extracting Chromatin Fractions From Intact Cells (US20080241845A1). *United States*, (2008).
273. J. Rappsilber, M. Mann, Y. Ishihama, Protocol for micro-purification, enrichment, pre-fractionation and storage of peptides for proteomics using StageTips. *Nat Protoc* **2**, 1896-1906 (2007).
274. W. F. Marzluff, P. Gongidi, K. R. Woods, J. Jin, L. J. Maltais, The human and mouse replication-dependent histone genes. *Genomics* **80**, 487-498 (2002).
275. I. Maze, K. M. Noh, A. A. Soshnev, C. D. Allis, Every amino acid matters: essential contributions of histone variants to mammalian development and disease. *Nat Rev Genet* **15**, 259-271 (2014).

276. R. Sperling, M. Bustin, Histone dimers: a fundamental unit in histone assembly. *Nucleic Acids Res* **3**, 1263-1275 (1976).
277. M. Dalvai *et al.*, A Scalable Genome-Editing-Based Approach for Mapping Multiprotein Complexes in Human Cells. *Cell Rep* **13**, 621-633 (2015).
278. L. Wu, B. M. Zee, Y. Wang, B. A. Garcia, Y. Dou, The RING finger protein MSL2 in the MOF complex is an E3 ubiquitin ligase for H2B K34 and is involved in crosstalk with H3 K4 and K79 methylation. *Mol Cell* **43**, 132-144 (2011).
279. Z. C. Yu, Y. F. Huang, S. Y. Shieh, Requirement for human Mps1/TTK in oxidative DNA damage repair and cell survival through MDM2 phosphorylation. *Nucleic Acids Res* **44**, 1133-1150 (2016).
280. J. Gagnon *et al.*, Undetectable histone O-GlcNAcylation in mammalian cells. *Epigenetics* **10**, 677-691 (2015).
281. L. Moyal *et al.*, Requirement of ATM-dependent monoubiquitylation of histone H2B for timely repair of DNA double-strand breaks. *Mol Cell* **41**, 529-542 (2011).
282. M. Hada *et al.*, TH2A is phosphorylated at meiotic centromere by Haspin. *Chromosoma* **126**, 769-780 (2017).
283. D. Kurihara, S. Matsunaga, T. Omura, T. Higashiyama, K. Fukui, Identification and characterization of plant Haspin kinase as a histone H3 threonine kinase. *BMC Plant Biol* **11**, 73 (2011).
284. W. M. Baarends *et al.*, Increased phosphorylation and dimethylation of XY body histones in the Hr6b-knockout mouse is associated with derepression of the X chromosome. *J Cell Sci* **120**, 1841-1851 (2007).
285. N. Reveron-Gomez *et al.*, Accurate Recycling of Parental Histones Reproduces the Histone Modification Landscape during DNA Replication. *Mol Cell* **72**, 239-249 e235 (2018).
286. J. Xie *et al.*, Histone H3 Threonine Phosphorylation Regulates Asymmetric Histone Inheritance in the Drosophila Male Germline. *Cell* **163**, 920-933 (2015).
287. P. Mertins *et al.*, Integrated proteomic analysis of post-translational modifications by serial enrichment. *Nat Methods* **10**, 634-637 (2013).
288. J. S. Cottrell, Protein identification using MS/MS data. *J Proteomics* **74**, 1842-1851 (2011).
289. C. Baumgartner, T. Rejtar, M. Kullolli, L. M. Akella, B. L. Karger, SeMoP: a new computational strategy for the unrestricted search for modified peptides using LC-MS/MS data. *J Proteome Res* **7**, 4199-4208 (2008).
290. J. V. Olsen *et al.*, Quantitative phosphoproteomics reveals widespread full phosphorylation site occupancy during mitosis. *Sci Signal* **3**, ra3 (2010).
291. T. Shiromizu *et al.*, Identification of missing proteins in the neXtProt database and unregistered phosphopeptides in the PhosphoSitePlus database as part of the Chromosome-centric Human Proteome Project. *J Proteome Res* **12**, 2414-2421 (2013).
292. T. E. Thingholm, M. R. Larsen, Phosphopeptide Enrichment by Immobilized Metal Affinity Chromatography. *Methods Mol Biol* **1355**, 123-133 (2016).
293. M. Seibert *et al.*, CDK1-mediated phosphorylation at H2B serine 6 is required for mitotic chromosome segregation. *J Cell Biol* **218**, 1164-1181 (2019).

294. J. Wysocka, Identifying novel proteins recognizing histone modifications using peptide pull-down assay. *Methods* **40**, 339-343 (2006).
295. D. Panigada *et al.*, Yeast haspin kinase regulates polarity cues necessary for mitotic spindle positioning and is required to tolerate mitotic arrest. *Dev Cell* **26**, 483-495 (2013).